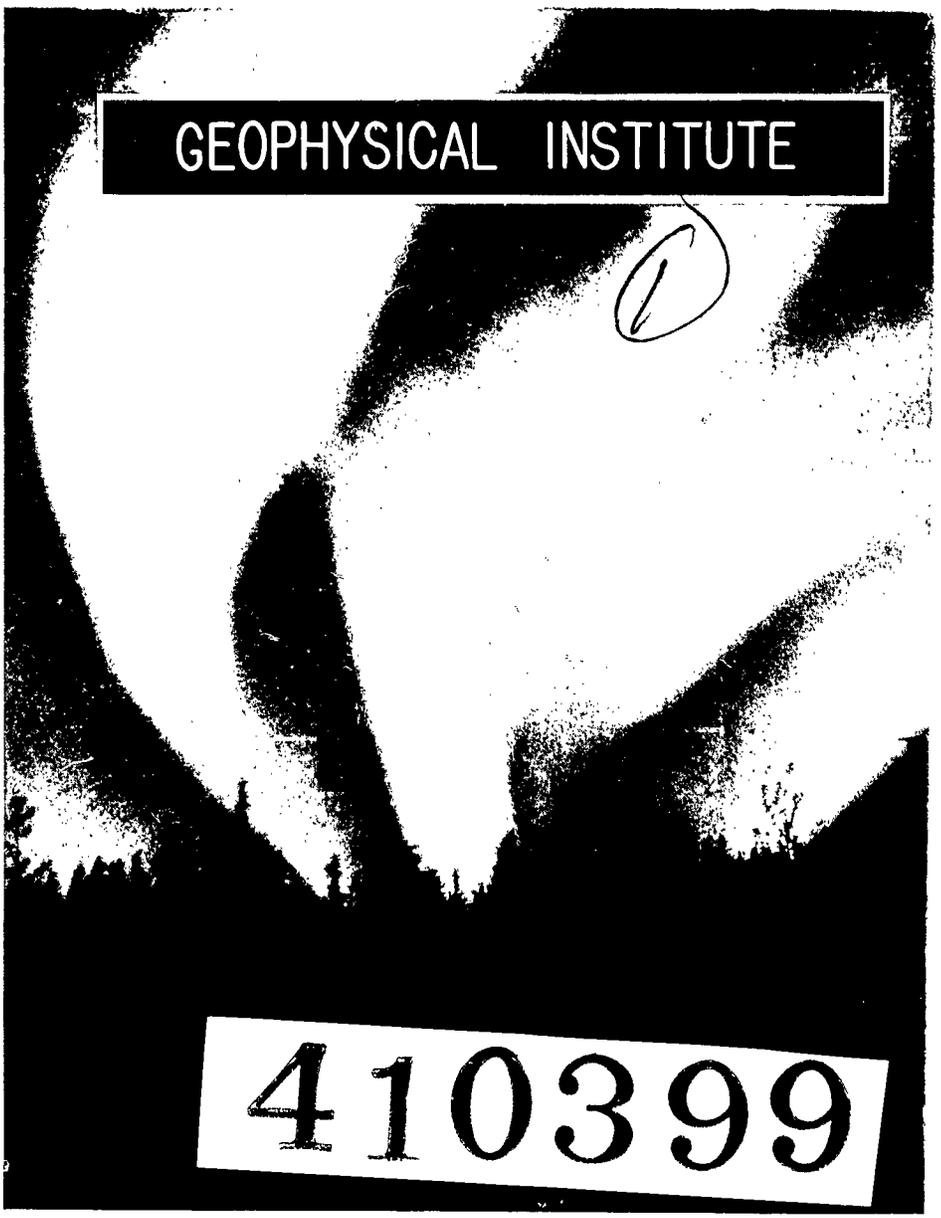

HYDROMAGNETIC INTERPRETATION OF SUDDEN COMMENCEMENTS OF GEOMAGNETIC STORMS

by

Charles R. Wilson

Contract No. AF 19(604)-7988
Project No. 8601
Task No. 860104

Scientific Report No. 3

MAY 1963

Air Force Cambridge Research Laboratories
Office of Aerospace Research

(19) (17) AFCRL-63-605

(4) 1450

(5) 359500

GEOPHYSICAL INSTITUTE

of the

UNIVERSITY OF ALASKA

(6) 7-9 nl

HYDROMAGNETIC INTERPRETATION OF SUDDEN COMMENCEMENTS OF GEOMAGNETIC STORMS

by

(10) by Charles R. Wilson

(12) 161p.
(13) NA
(20) U
(21) nil

(14) Scientific Report No. 3; 1st rev UAG-R135

(15) Contract No. AF 19(604)-7988

(16) Project 8601

(17) Task 860104

(11) May 1963

Prepared for

AIR FORCE CAMBRIDGE RESEARCH LABORATORIES
OFFICE OF AEROSPACE RESEARCH
UNITED STATES AIR FORCE
BEDFORD, MASSACHUSETTS

Report approved by:

C. T. Elvey
Director

Requests for additional copies by Agencies of the Department of Defense, their contractors and other government agencies should be directed to the:

DEFENSE DOCUMENTATION CENTER (DDC)
ARLINGTON HALL STATION
ARLINGTON 12, VIRGINIA

Department of Defense contractors must be established for DDC services or have their "need-to-know" certified by the cognizant military agency of their project or contract.

All other persons and organizations should apply to the:

U.S. DEPARTMENT OF COMMERCE
OFFICE OF TECHNICAL SERVICES
WASHINGTON 25, D.

ABSTRACT

A new hydromagnetic model for the sudden commencement (SC) of a magnetic storm is presented. The model is based on a new morphology of the SC field in which the polarization of the field is interpreted in terms of circularly polarized transverse and linearly polarized longitudinal hydromagnetic waves.

The longitudinal wave is the immediate consequence of the impact of a solar plasma cloud on the magnetosphere; whereas the transverse wave is produced by a coupling with the longitudinal shock wave in the magnetosphere. The triply refracting nature of the plasma in the magnetosphere results in the production of three hydromagnetic modes by the SC disturbance; namely, ordinary and extraordinary transverse waves with opposite directions of circular polarization which propagate to high latitudes in the morning and evening hemispheres respectively, and longitudinal waves which propagate to the earth in low latitudes.

ACKNOWLEDGMENTS

The research described in this thesis was carried out at the Geophysical Institute under the direction of Dr. Masahisa Sugiura to whom I am deeply grateful for having suggested the project and for his guidance during the analysis. I would also like to express my graditude to Dr. C. T. Elvey, Director of the Geophysical Institute and Vice President of Research and Advanced Study, University of Alaska for his interest and support of the sudden commencement program.

I am indebted to my colleagues at the Geophysical Institute, Keith Mather, S.-I. Akasofu and Benson Fogel for stimulating discussions concerning the SC analysis. I would especially like to thank Mrs. Sharon Dean for her excellent help in the task of data reduction, for the vector diagrams and power spectra. My thanks are extended to Dennis Ruff and Ed Gauss for help with the 1620 computer programs.

I am indebted to the World Data Center A--geomagnetism and to the directors of all the magnetic observatories listed in Table 3-2 for supplying the necessary magnetograms. I gratefully acknowledge the financial support of this project by Air Force Cambridge Research Laboratories under Contract No. AF 19(604)-7988.

TABLE OF CONTENTS

LIST OF TABLES

LIST OF ILLUSTRATIONS

CHAPTER I

INTRODUCTION

The results of a new analysis of sudden commencements of magnetic storms and an interpretation of them in terms of hydromagnetic perturbations are presented in this thesis. The data used in the analysis were taken from rapid-run magnetograms of sudden commencements* beginning with the I.G.Y. through September 1961 as recorded at magnetic observatories all over the world. The interpretation of an SC as the effect of the impact of solar gas on the geomagnetic field and the subsequent propagation to the earth of the resulting magnetic disturbance by hydromagnetic waves is based on a new method of describing the SC field over the earth by the total horizontal disturbance vector $\underset{\sim}{\Delta H}$. This departure from the representation of the SC field by an equivalent current system that has been attempted by several workers to a new portrayal by vector diagrams of the vector $\underset{\sim}{\Delta H}$ led immediately to the most salient but long ignored feature of the SC field, namely its polarization or the rotation of $\underset{\sim}{\Delta H}$ with time.

Figure 1-1 for SC's at Fredericksburg and College shows the variation with time of the horizontal component H in the upper half and the locus of the end point of the total horizontal disturbance vector $\underset{\sim}{\Delta H}$ in the lower half. The SC shown in Figure 1-1 for Fredericksburg would be classified as a typical SC because of its familiar shape of the variation of H. However, the vector diagram for $\underset{\sim}{\Delta H}$, in which the change in D is included as well as

---

*In what follows "storm sudden commencement" is denoted by SC. The symbol s.s.c. is designated to this term by the Committee #10 of the International Association of Geomagnetism and Aeronomy, but because of the repeated use of the term in this thesis, the shorter notation SC will be used.

that in H, clearly shows that the SC field vector rotates in azimuth by about 90° in 25 seconds; in the figure the points are 5 seconds apart. The SC for College in Figure 1-1 would be classified as an SC* according to the conventional classification. In this case, for the SC* at College, the corresponding vector diagram of $\underset{\sim}{\Delta H}$ shows an azimuth change of 270° in three minutes; the points are plotted with 30 second intervals.

The variation over the earth of the characteristics of the SC vector diagrams (e.g. polarization, shape and initial phase of $\underset{\sim}{\Delta H}$) suggests that the SC field could be interpreted as the result of two different types of hydromagnetic waves. Thus the SC in high latitudes is thought to be due principally to circularly polarized transverse hydromagnetic waves, while at low latitudes the SC is due principally to longitudinal hydromagnetic waves.

The behavior of the SC field over the earth is extremely complex and varies from one SC to the next. In low latitudes the disturbance vector of the SC field is almost horizontal and remains approximately in the magnetic meridian, while at moderate and high latitudes rotation of the disturbance vector with storm time produces large variations in both D and H and at very high latitudes large Z variations accompnay the SC field. The traditional description of SC's in terms of the behavior of H alone, although inadequate, will be used in this thesis for the classification of SC's for the sake of continuity with the previous works.

In standard magnetograms at low latitudes an SC is typically a sudden increase in the horizontal component H as shown for the SC at Fredericksburg in Figure 1-1. Chapman and Ferraro (1931, 1932, 1940) and Ferraro (1960) gave the first plausible theory to account for the rise in H in a typical low latitude SC in terms of the compression of the geomagnetic field by a

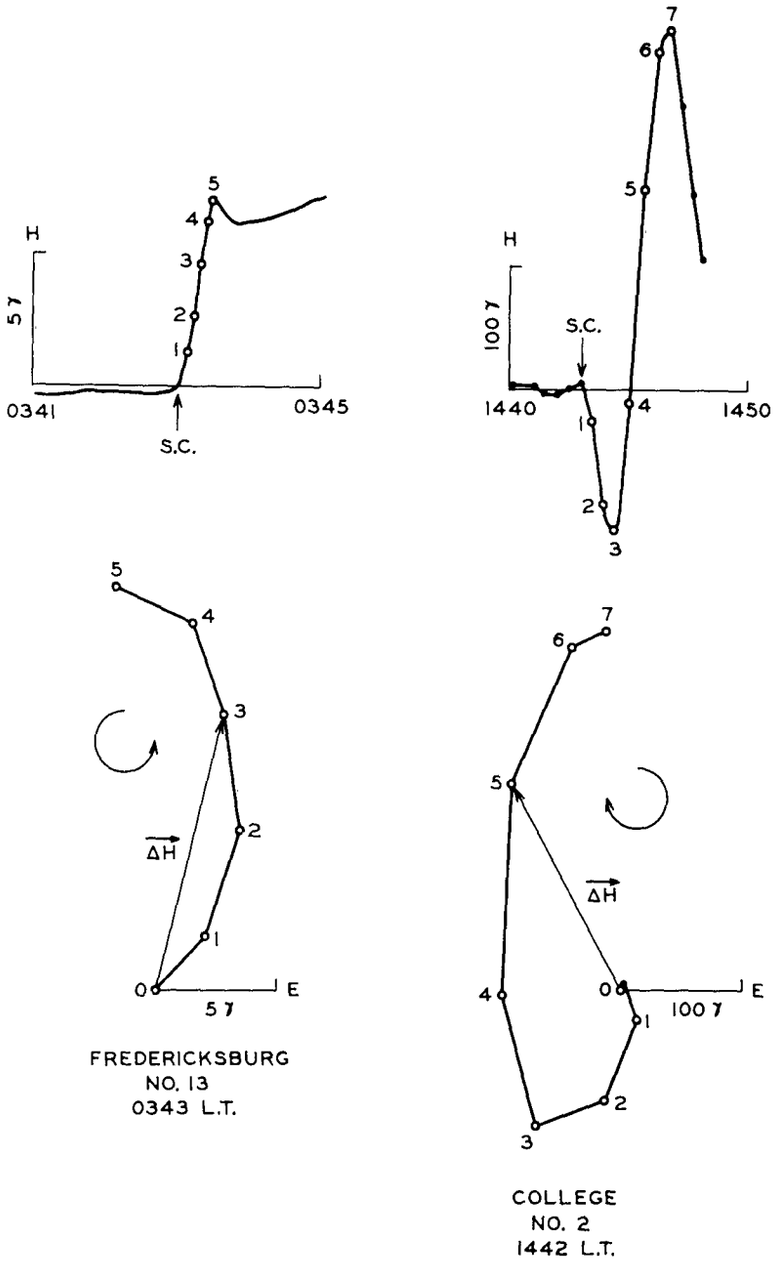

Fig. 1-1. H component of SC's and the corresponding vector diagrams.

cloud of solar gas. This theory is outlined below following the paper by Ferraro (1960).

When a neutral ionized stream of corpuscles emitted from the sun advances into the earth's magnetic field, which is assumed to extend to infinity, electric currents are induced in the stream surface. As a result of these induced currents the stream remains impervious to interpenetration by the earth's magnetic field. The action of the magnetic field on the induced currents is to retard the motion of the stream. Thus, a hollow, called the magnetic cavity, develops in the solar stream. Because the field lines cannot penetrate the stream they are compressed and crowded together in the hollow, thereby increasing the magnetic field in the hollow. This increase in the magnetic field is identified with the increase in H in a typical low latitude SC. The distance to the vertex of the hollow, along the sun-earth line, is shown by Chapman and Bartels (Geomagnetism, p. 859, 1940) to be inversely proportional to the sixth root of the kinetic energy density of the stream (E); while the magnetic perturbation at the earth due to the compression of the magnetic field is shown to be proportional to the square root of E.

Ferraro (1960), by equating the rate at which momentum is destroyed in the surface layers of the stream to the magnetic pressure of the tubes of force on the stream surface, derives an equation from which the rate at which the stream is retarded (as a function of the distance from the earth to the stream surface) can be determined. If V/V_o is the ratio of the stream velocity V at a distance R from the earth to the original velocity V_o of the stream, and if R_m is the distance at which the stream is stopped, then Ferraro (1960) finds that,

$$V/V_o \approx 1 - (R_m/R)^3 \qquad 1\text{-}1$$

where R_m is proportional to $(E)^{-1/6}$ as stated above. The value of V_o, of about 10^6 cm/sec, is determined from the delay time between solar flares and their associated earth magnetic storms. In Figure 1 in Ferraro's paper (1960), in which V/V_o is plotted for various values of number density of the stream, the rapid retardation of the stream over a few earth radii to a small fraction of its initial speed can be seen. Because the stream velocity is initially the order of 10^6 cm/sec the retardation and therefore the compression of the field and corresponding increase in H observed at the earth's surface as an SC take place in the order of one minute, if instantaneous propagation of the magnetic disturbance is assumed.

The above theory of the increase in H in a typical SC is universally accepted, with the exception of the fact that the velocity of the propagation of the compressional magnetic disturbance can no longer be considered to be that of light. This is because of a plasma in the magnetosphere (which was neglected by Chapman and Ferraro); the presence of the plasma makes the propagation of the disturbance hydromagnetic rather than electromagnetic, as has been pointed out by Dessler (1958), Piddington (1959) and Dessler and Parker (1959).

Although the impact on the geomagnetic field of the solar stream takes place only over the sunlit hemisphere, Parker (1958) has shown that this uneven distortion of the boundary of the field produces a nearly uniform perturbation field which is closely parallel to the geomagnetic axis. Thus even on the back side of the earth there is an increase in H during an SC due to the compression of the field by the solar stream.

In order to explain the difference between the observed SC rise time of from one to six minutes and the rapid one minute rise time predicted by the Chapman-Ferraro theory, the effect of the interplanetary gas was taken into account by Dessler (1958), Dessler, Francis and Parker (1960) and Ferraro (1960). Thus the magnetic perturbation is assumed by these authors to propagate through the magnetosphere at the speed of a compressional hydromagnetic wave in a conducting plasma pervaded by a magnetic field. Dessler et al. (1960) explained the long SC rise time in H in terms of the successive arrival of longitudinal hydromagnetic waves from the broad impact boundary at the surface of the magnetic cavity. Their numerical results can probably not be trusted because of their unjustifiable use of Fermat's principle as was discussed by von Kenschitzki and Stegelmann (1962); however, Parker (1962) states that this at least offers a qualitative explanation of the long rise times of SC's compared with the abruptness of the retardation of the solar stream.

As soon as one examines the SC field variations, other than the simple rise in H observed in low latitudes, it becomes obvious that a further explanation is called for. The geometrical shapes of SC's in H have been studied by Jackson (1952), Obayashi and Jacobs (1957), Matsushita (1957, 1960), Akasofu and Chapman (1960) and Abe (1959). Obayashi and Jacobs, and Matsushita investigated the local time dependence of occurrence of different types of SC's. On the basis of the morphology of SC's Vestine (1953) suggested that SC's are due mainly to electric currents flowing in the ionosphere. Dessler and Parker (1959) concluded that surface magnetic observations of SC's may be interpreted as ionospheric current systems and Piddington (1959) concludes that the currents responsible for all geomagnetic disturbances must flow below about 1000 km.

Many researchers have used morphological representations of the vector SC field in terms of currents concentrated in spherical sheets. Nagata and Abe (1955) constructed a current system for the reversed impulse in SC*'s and proposed that the currents are generated in the ionosphere in polar regions. To explain the average SC field, Obayaski and Jacobs (1957) divided the current system into two parts, Dst and DS, in the same manner as the disturbance field of magnetic storms is usually analyzed. Dst is a function of storm time t and geomagnetic latitude ϕ and is used to represent the axially symmetrical change in H, while DS is a function of local time as well as t and ϕ and represents the high latitude SC field variations. These current systems, when added in order to represent the SC field, show a parallel flow across the polar cap, centered on the geomagnetic pole, away from the 0900 hour meridian. Oguti (1956) stated that the DS part of the SC current system may rapidly rotate clockwise during an SC(-+). Watanabe (1961) concludes that SC's in high latitudes are caused by currents that flow in the ionosphere due to three electric dipoles which appear and disappear in succession near the geomagnetic pole with their moments directed toward 0300, 2100 and 1500 hours respectively. Sano (1962) separates the DS current system into two parts; DS_p for the preliminary reversed impulse and DS_m for the main positive impulse. He uses four SC's, two of the type SC(-+) and two SC(+-), and gives current diagrams of $DS_p + DS_m$ for each successive 30 seconds of the four SC's. From these current diagrams Sano shows how, if the foci of the current diagrams move toward the pole in a time equal to the rise time of the main impulse, the SC field can be accounted for by ionospheric currents.

Sano, Watanabe, Oguti, Obayashi and Jacobs all assume that the ionospheric currents are driven by dynamo action and that solar particles from the solar stream percipitate into the ionosphere from the "horns" of the stream front (at the focal points of the induced surface currents) causing the greatly increased conductivity that would be necessary.

Maeda (1959) concluded that dynamo action would not be sufficient to generate the DS currents. Akasofu and Chapman (1960) argue against dynamo action to produce the DS currents on the basis of the physically impossible rapid changes in the wind, such as rotation and reversal of direction, that would be needed to produce the DS currents envisioned by the above workers.

Vestine and Kern (1962) have proposed a mechanism based on the propagation down the lines of force of a polarization field to the ionosphere that would drive the currents there in order to explain the preliminary reversed impulse of an SC*. They ascribe the polarization field, $\underset{\sim}{E}_2 = \underset{\sim}{u} \times \underset{\sim}{B}_o$, to be due to the mass motion $\underset{\sim}{u}$ of the plasma in front of the solar stream surface and conclude that the duration of this polarization field will be equal to the time required for the solar stream to be stopped by the compression of the earth's field, or about 50 seconds.

Gold (1955) suggested that the SC of a magnetic storm is due to a shock wave, without mass transport, propagated from the sun. Singer (1957) attributed the SC to a shock wave developed when a high speed jet of gas is ejected by the sun. Singer supposed that when the shock wave arrives near the earth, it is focused by the geomagnetic field into the auroral zones and thus accounts for the large SC amplitudes observed there.

There are many features of the SC field at high latitudes such as SC oscillations, the directions of polarization of $\underset{\sim}{\Delta H}$ over the earth, the

variations in the Z component and the rotation of $\underset{\sim}{\Delta H}$ for stations very near the geomagnetic pole whose morphology cannot adequately be described by equivalent current systems in the ionosphere. Also, in spite of the many SC features that can be explained in terms of ionsopheric current systems, there is as yet no physically tenable theory for the origin of these current systems.

In this thesis a new model for SC's is proposed, as a result of the analysis of the SC field vector diagrams of the total horizontal disturbance vector, in terms of hydromagnetic waves that resolves the problem of high latitude SC's and is in agreement with the accepted morphology of the SC field. The model is particularly applicable to the fast pulsative and rotational changes observed in the SC field. Thus these changes can be immediately described on the base of oscillatory circularly polarized hydromagnetic waves or, more accurately expressed, by the pulsating or rotating currents induced to flow in the highly conductive ionosphere as the consequence of the Maxwell equation from Ampere's law, curl $\underset{\sim}{B} = 4\pi\underset{\sim}{J}$, by the impinging of hydromagnetic waves on the ionosphere from above.

The model for the interaction between the solar wind and the earth's magnetic field to generate the observed SC field is as follows. The two primary effects of the impact of the solar gas cloud on the surface of the magnetosphere are: 1) to cause a sudden compression of the magnetic field in the magnetic cavity; and 2) to twist the field lines by distortion of the frozen-in field as a result of the solar wind velocity normal to the meridian planes of the field lines in both the morning and evening hemispheres. The uniform increase in the magnetic field resulting from the compression of the field in the equatorial plane can be represented by a

perturbation vector parallel to the undistorted field lines; and the distortion of the field lines can be represented by a rotating magnetic vector that is transverse to the field line in the equatorial plane and whose initial position is antiparallel to the solar wind direction.

The sudden compression of the field propagates to low latitudes on the earth across the lines of force as a longitudinal hydromagnetic wave. Because of the curvature of the lines of force of the earth's field, this longitudinal hydromagnetic wave generates transverse hydromagnetic waves by coupling. These transverse hydromagnetic waves are transmitted to the earth essentially along the lines of magnetic force. The coupling is most effective in the outer regions of the magnetosphere where the magnetic field is weak; from these regions the transverse hydromagnetic waves propagate to the earth in high latitudes.

The distortion of the field lines is propagated along the field lines in the morning hemisphere as a transverse hydromagnetic wave in the ordinary mode while over the evening hemisphere this disturbance is propagated in the extraordinary mode.

The transverse hydromagnetic waves will be circularly polarized as a result of the triply refracting nature of the magnetospheric plasma. Thus if an SC magnetic perturbation observed at an observatory were due to the currents generated in the ionosphere by a pure transverse wave, then the polarization of the SC perturbation would be circular. On the other hand if the SC were due to a pure longitudinal wave its polarization would be linear.

Although the above picture is greatly idealized, and in reality the magnetic perturbation created by the impact of the solar plasma will

propagate in a more complex way, it does give the essential structure of the SC of a magnetic storm. In Figure 1-2 a schematic representation is given to show the distortion by the solar wind of the earth's field lines in the morning and evening meridian planes. The shock front distorts the end loops of the dipole field lines such that a clockwise rotation of the loop is produced on the morning side and a counterclockwise rotation of the field line loop is produced on the evening side. The propagation of this rotation of the field lines to the earth along the field lines produces the pattern of directions of polarization of SC's observed over the earth and is thus the basis of the belief that the above mechanism is valid.

In Chapter II, on magnetohydrodynamics, a summary of the basic ideas and equations which lead to hydromagnetic wave propagation is presented together with a discussion of their application to the problem of SC's. The various modes of hydromagnetic waves are discussed with the help of dispersion equations beginning with a simple Alfvén wave in an incompressible infinitely conducting plasma pervaded by a steady uniform magnetic field, and ending with a triply refracting compressible plasma with anisotropic conductivity in which the three hydromagnetic modes are anisotropically damped. From the discussion of the three hydromagnetic modes with respect to the propagation in the magnetosphere and ionosphere, it is concluded that only two of the modes are important for SC propagation.

In Chapter III, on polarization of SC's, all the vector diagrams that were analyzed are presented and discussed in terms of the effect of circularly polarized transverse hydromagnetic waves and longitudinal hydromagnetic waves. The ratio of the transverse to longitudinal components as a function of latitude and the distribution in local time of the direction

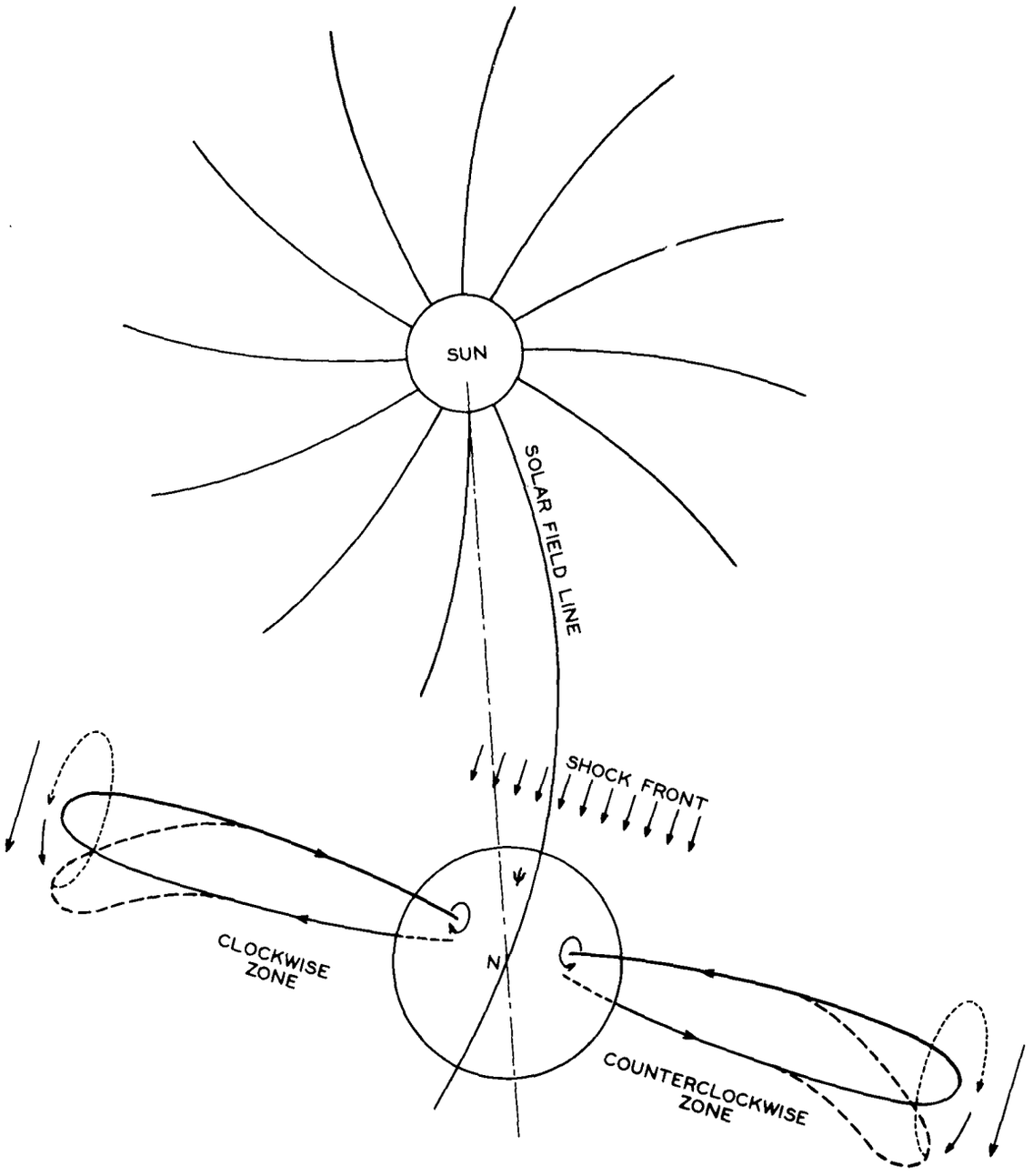

Fig. 1-2. Schematic picture of SC transverse hydromagnetic wave excitation.

of polarization of the transverse component are discussed. Polarization rules are obtained from the SC vector diagrams in terms of four quadrants of the earth's surface within each of which the polarization has the same sense of rotation.

In Chapter IV, on SC oscillations, pulsative phenomena which accompany SC's are described. Data are presented from a detailed analysis of SC oscillations at College giving the frequency spectra as well as other characteristics of the oscillations. A calculation of the period of SC oscillations is made on the basis of a resonance oscillation of the field lines and a gyrofrequency model for the ion density in the magnetosphere.

In Chapter V, on vector diagrams, a complete analysis is given of the effects of the amplitude, time dependence, polarization and phase of both transverse and longitudinal wave components on the resultant shape of the vector diagram. Vector diagrams are synthesized assuming various models for the transverse and longitudinal waves in order to relate the observed SC field to the proposed model. The phase of the ordinary wave is discussed in terms of a model that agrees with the SC observations. The occurrence frequencies of SC(-+) and SC(+-) as a function of local time and latitude as observed over the earth are shown to follow from the proposed model. The difficulties of determining rise time, frequency of the transverse component, ratio of the two components and the initial phase of the polarized component are discussed in terms of the synthesized vector diagrams.

CHAPTER II

HYDROMAGNETIC WAVES

In the theory of the sudden commencement and the initial phase of a magnetic storm proposed by Chapman and Ferraro (1931), the stream of solar plasma was assumed to advance in the earth's magnetic field which was represented by a dipole field extending to infinite distance. The existence of ionized gas surrounding the earth to large distances was then not known, and hence Chapman and Ferraro supposed that the solar plasma stream advances in the magnetic field in vacuum and that the magnetic field of the electric current induced in the front surface of the solar gas is transmitted to the earth with the speed of light.

The discovery that the earth's outer atmosphere contains a highly conducting plasma and that the earth's magnetic field is confined in a cavity carved in the steady solar wind necessitates a re-evaluation of the problem of the interaction with the earth's magnetic field of the solar corpuscular stream that causes a magnetic storm.

In the magnetosphere electromagnetic perturbations are in general coupled with gas motions. Hence the problem of the distortion of the earth's magnetic field by the impact of an enhanced solar wind and of the subsequent propagation of the impact effect to the earth must be formulated according to the laws of magnetohydrodynamics.

The equations revelant to the concept of frozen-in field, magnetic pressure and hydromagnetic waves are briefly reviewed below.

The electromagnetic fields in the fluid are given by Maxwell's equations with the displacement current $\frac{\partial D}{\partial t}$ neglected:

$$\text{curl } \underset{\sim}{B} = 4\pi \underset{\sim}{J} \qquad 2\text{-}1$$

$$\text{curl } \underset{\sim}{E} = -\frac{\partial \underset{\sim}{B}}{\partial t} \qquad 2\text{-}2$$

Equation 2-1 implies that:

$$\text{div } \underset{\sim}{J} = 0 \qquad 2\text{-}3$$

The current denstiy $\underset{\sim}{J}$ is given by Ohm's Law if we assume an isotropic conductivity σ and a neutral plasma:

$$\underset{\sim}{J} = \sigma[\underset{\sim}{E} + \underset{\sim}{v} \times \underset{\sim}{B}] \qquad 2\text{-}4$$

where $\underset{\sim}{v} \times \underset{\sim}{B}$ is the induced field due to the motion of the fluid with velocity $\underset{\sim}{v}$. The magnetic indiction $\underset{\sim}{B}$, the electric field intensity $\underset{\sim}{E}$, the current density $\underset{\sim}{J}$, and conductivity σ are expressed in electromagnetic units. The hydrodynamic equations are the equation of continuity:

$$\frac{\partial \rho}{\partial t} + \text{div}(\rho \underset{\sim}{v}) = 0 \qquad 2\text{-}5$$

and Euler's equation with forces including the gravity, magnetic force, and viscous forces:

$$\rho\left(\frac{\partial}{\partial t} + \underset{\sim}{v} \cdot \text{grad}\right)\underset{\sim}{v} = -\text{grad } p + \rho \underset{\sim}{g} + \underset{\sim}{J} \times \underset{\sim}{B} + \rho\nu\nabla^2 \underset{\sim}{v} \qquad 2\text{-}6$$

where ν is the kinematic viscosity.

If it is assumed that σ is uniform then the time dependence of the magnetic induction can be found from equations 2-1, 2-2, and 2-4 by eliminating $\underset{\sim}{E}$ and $\underset{\sim}{J}$ to give:

$$\frac{\partial \underset{\sim}{B}}{\partial t} = \text{curl } \underset{\sim}{v} \times \underset{\sim}{B} + \eta \nabla^2 \underset{\sim}{B} \qquad 2\text{-}7$$

where $\eta = 1/4\pi\sigma$ and is called the magnetic viscosity. From equation 2-7 it can be shown that, depending on the conductivity σ, the magnetic

field in a conducting fluid will behave in very different ways. Thus if $\underset{\sim}{v} = 0$ then equation 2-7 reduces to a diffusion equation in which the initial configuration of the magnetic field will decay in a diffusion time $\tau = 4\pi\sigma L^2$, where L is a length comparable to the dimensions of the system in which $\underset{\sim}{J}$ flows. When the conductivity σ is very large then in times short compared to the diffusion time τ the behavior of the field is described by:

$$\frac{\partial \underset{\sim}{B}}{\partial t} = \text{curl } (\underset{\sim}{v} \times \underset{\sim}{B}) \qquad 2\text{-}8$$

Equation 2-8 implies that the lines of magnetic force move with the fluid so that the total flux through a closed circuit moving with the fluid is conserved. This condition of "frozen-in" fields prevails whenever the ratio of the first to second terms in equation 2-7 is large. This ratio is of the order of Lv/η, and this latter quantity is called the magnetic Reynolds number.

Another concept of importance in discussing the behavior of the magnetic fields in a conducting fluid is that of magnetic pressure. By use of equation 2-1 and a vector identity the magnetic force $\underset{\sim}{J} \times \underset{\sim}{B}$ can be written as:

$$\underset{\sim}{J} \times \underset{\sim}{B} = - \text{grad } \frac{B^2}{8\pi} + \frac{1}{4\pi} \text{ div } (\underset{\sim}{B}\,\underset{\sim}{B}) \qquad 2\text{-}9$$

Equation 2-9 shows that the magnetic force is equivalent to a hydrostatic magnetic pressure $B^2/8\pi$ and a tension $\frac{1}{4\pi}$ div $(\underset{\sim}{B}\,\underset{\sim}{B})$ along the lines of force, where $(\underset{\sim}{B}\,\underset{\sim}{B})$ is a dyadic. When the magnetic field is frozen into the fluid then the total pressure $p + B^2/8\pi$ remains constant so any change in p will be compensated by an opposite change in $B^2/8\pi$. The

relative importance of $\underset{\sim}{B}$ in determining the motion of the fluid depends on the ratio S of the magnetic energy density $B^2/8\pi$ to the kinetic energy density $(1/2)\rho v^2$. If S is small the fluid motion is hardly affected by B; if S is large the motion is controled by $\underset{\sim}{B}$.

Alfvén (1950) explained a transverse hydromagnetic wave by an anology with a transverse wave on an elastic string using the concept of tension along the lines of magnetic force. The coupling between the magnetic field and the fluid motion which results in the propagation of hydromagnetic waves can be illustrated by the example of Alfvén waves in which both the motion of the fluid $\underset{\sim}{v}$ and the magnetic perturbation $\underset{\sim}{b}$ are transverse to a uniform magnetic field $\underset{\sim}{B}_o$ and hence to the direction of propagation of the wave. The physical picture is as follows. Taking the Z axis along $\underset{\sim}{B}_o$, an initial fluid motion $-\underset{\sim}{v}_x$ in the negative X direction produces an induced field $\underset{\sim}{v}_x \times \underset{\sim}{B}_o$ which because of the conductivity of the fluid causes a current $\underset{\sim}{J}_y$ to flow in the Y direction. This current couples with $\underset{\sim}{B}_o$ to produce a mechanical force $\underset{\sim}{J}_y \times \underset{\sim}{B}_o$ in the positive X direction which reverses the original motion of the fluid and sets up an oscillation. Thus a restoring force which is of electromagnetic origin is generated by the motion of the fluid itself. This restoring force (which can be thought of as due to the component normal to the line of force of the tension $\frac{1}{4\pi}$ div $(\underset{\sim}{\underset{\sim}{B}}\underset{\sim}{B})$) combines with the inertia of the fluid to give transverse wave propagation along the field lines at the Alfvén velocity $V_a = B_o/\sqrt{4\pi\rho}$.

The addition of the Hall current causes circular polarization of the normal Alfvén mode when a sinusoidal plane wave propagates in an incompressible fluid pervaded by a uniform magnetic field (Åström, 1950).

When the compressibility of the fluid is taken into account then an infinitely conducting fluid in a uniform magnetic field becomes triply

refracting. According to Kahalas (1960), the dispersion equation for a plane wave solution in this case is given by:

$$(\omega^2-k^2V_a{}^2\cos^2\theta)\left\{\omega^4-\omega^2k^2(V_a{}^2+U^2)+k^4V_a{}^2U^2\cos^2\theta\right\}=0 \qquad 2\text{-}10$$

where ω and k are the angular frequency and the propagation vector of the wave and V_a and U are the Alfvén and sound velocity respectively. The pure Alfvén mode phase velocity is found by setting the left hand bracket of equation 2-10 equal to zero, i.e., $V = \omega/k = V_a\cos\theta$. When the right hand bracket is set equal to zero and when it is assumed that $V_a >> U$ then the phase velocities of the two coupled magneto-acoustic modes are found to be $V_f = V_a$ for the so called fast mode which is a predominatly transverse magnetic wave, and $V_s = V_a\cos\theta$ for the slow mode which is a predominatly longitudinal sound wave.

Piddington (1954) derived wave equations for hydromagnetic waves in a moving anisotropically conducting medium in which Ohm's law is given by:

$$\underset{\sim}{J} = \sigma_o \underset{\sim}{E}_{\parallel} + \sigma_1 \underset{\sim}{E}_{\perp} + \sigma_2 \frac{\underset{\sim}{B} \times \underset{\sim}{E}}{B} \qquad 2\text{-}11$$

where σ_o, σ_1, and σ_2 are the parallel, perpendicular and Hall conductivities respectively. In the derivation of the wave equation he made the following assumptions: 1) a binary type gas in which only electron conduction is important, 2) weak magnetic perturbations, 3) σ_o, σ_1 and σ_2 are constant, 4) Maxwell's continuum equations could be used neglecting displacement current, 5) a steady magnetic field along the OZ axis of a right handed coordinate system, 6) plane wave solutions of the type $\exp i(\omega t - k\S)$ where k is along the $O\S$ axis which is in the XZ plane

and makes an angle of θ with OZ. With the above assumptions Piddington (1955) obtained a dispersion equation of the third degree in k^2 showing that in general three pairs of hydromagnetic waves may be present for any value of θ; each pair comprises two similar waves moving in opposite directions. The dispersion equation could only be factored for arbitrary θ to give separate modes for the case in which $V_a >> U$. He thus obtained the following dispersion equation:

$$\frac{\omega^2}{k^2} = V_a^2 \left\{ 1 - \frac{\sin^2\theta}{2} \mp \left(\frac{\sin^4\theta}{4} + \frac{\omega^2}{\Omega^2} \cos^2\theta \right)^{\frac{1}{2}} \right\} + i/\varepsilon_o \qquad 2\text{-}12$$

where $\Omega = \frac{B_o e}{M}$ is the gyromagnetic frequency of the heavy ions, and $\varepsilon_o = 4\pi\sigma_o/\omega$ and $V_a = B_o/\sqrt{4\pi\rho}$. When the wave frequency ω is small compared to the gyromagnetic frequency Ω of the heavy ions then ω^2/Ω^2 can be neglected. With this assumption equation 2-12 gives two pairs of transverse elliptically polarized waves, the O or ordinary wave and the E or extraordinary wave. Using the negative sign in equation 2-12 one obtains $V_o = V_a \cos\theta$ for the O wave velocity while the plus sign gives $V_E = V_a$ for the E wave velocity. Piddington shows that the E and O waves are elliptically polarized in a plane perpendicular to $\underset{\sim}{k}$. The direction of rotation of the O wave is counterclockwise when looking along the direction of the field; the sense of rotation of the E wave is opposite to this. The polarization of the two waves is given by R where $R = B_y/B_p$ where B_p is the maximum value of the perturbation in the XZ plane. $B_p = B_x/\cos\theta$ and $B_y/B_x = R/\cos\theta$ where R is given by:

$$R = \frac{i}{2} \left\{ \frac{\Omega \sin^2\theta}{\omega \cos\theta} \pm \left(\frac{\Omega^2 \sin^4\theta}{\omega^2 \cos^2\theta} + 4 \right)^{\frac{1}{2}} \right\} \qquad 2\text{-}13$$

For values of Ω/ω from 1 to 10^2 the polarization varies from plane for $\theta = 90°$ to circular for $\theta = 0$. For $\omega << \Omega$ the energy propagation is along the magnetic field direction for the O wave and along the direction of wave propagation $\underset{\sim}{k}$ for the E wave. Thus the O wave is guided along the field line while the E wave propagates spherically. The waves were shown to decay by a factor of 1/e in a distance 1/K where $K = \frac{\omega^2}{8\pi\sigma_o V_a{}^3}$ for E wave and $K = \frac{\omega^2}{8\pi\sigma_o V_a{}^3 \cos^3\theta}$ for the O wave. Thus the attenuation is least for the O wave when $\theta = 0$ and it will not propagate for $\theta = 90°$.

Piddington found that the third root of the dispersion equation gives a magneto-acoustic wave which propagates energy along 0§ and whose velocity is approximately U cos θ. This sound wave can only propagate if the ion collision frequency is very much greater than the wave frequency.

MacDonald (1961) discusses the propagation of hydromagnetic waves for the case in which $V_a >> U$ in terms of the following three modes: 1) the V mode which is the vorticity of the fluid about the lines of force and which propagates one dimensionally along the lines of force at the Alfvén velocity; 2) the pressure or P mode (slow or magneto-acoustic wave) which is the component of the fluid velocity along the lines of force that propagates at near the sound velocity almost one dimensionally; 3) the transverse or T mode (fast wave) which is the two dimensional divergence of the fluid velocity in the plane perpendicular to the lines of force together with the longitudinal component of the magnetic field that propagate almost spherically at the Alfvén velocity.

The applicability of the above treatments of hydromagnetic wave propagation to the problem of sudden commencements depends on the validity

for the magnetosphere of the approximations made in the derivations. If an SC disturbance produces all three modes, (i.e. Alfvén, fast and slow waves), then whether or not these three modes will propagate as three separate waves depe..ds on their coupling and on their subsequent attenuation. MacDonald (1961) states that in general the modes V, T and P will be coupled because of the effect of gravity. In the case where the magnetic and gravity fields are parallel, the vorticity mode is separable but gravity leads to anisotropic dispersion in the other modes. Lehnert (1956) shows that Hall current generated by one type of wave interacts with the other wave to produce coupling of the modes. The effects of density gradients and non-uniformity of the ambient field will also produce coupling.

Even if the three modes were not coupled their attenuation is anisotropic. Kahalas (1960) finds that the pure Alfvén and slow modes propagate with least damping in the direction of the magnetic field and that these modes are evanescent for propagation normal to the field. For the fast mode the damping is independent of direction and has a value equal to that of the minimum for the Alfvén mode. The characteristics of the propagation of the three modes depend on the relation of the angular frequency of the wave to the gyro and collision frequencies of the ions. Thus for any hydromagnetic propagation the wave frequency must be less than the positive ion gyromagnetic frequency, and for the slow mode the wave frequency must be very much less than the ion collision frequency.

Fejer (1959) states that Piddington's (1955) treatment is valid for wave frequency range $\omega_1 << \omega << \omega_2$ where $\omega_1 = \frac{\nu_i \delta}{2\rho}$ and $\omega_2 = \frac{\nu_i}{2}\left(\frac{\rho+\delta}{\rho}\right)$ where ν_i = collision frequency of ions with neutral particles, δ is density of charged matter and ρ is the density of the neutral matter.

Dungey (1954) estimates that the largest value of ω_1 is $\simeq 10^{-3}$/sec in the ionosphere corresponding to a period of $\simeq$ 3 hrs. Chapman (1956) gives an expression for ν_i that depends on ρ and δ and the molecular weight of the particles. Thus ω_2 can be expressed as $1.3 \times 10^{-9} M^{1/2} \left(\frac{\rho+\delta}{\rho}\right)^2$ where M is the molecular weight of the neutral and ionized particles. Using data from Piddington (1959) ω_2 is ~ 0.1/sec corresponding to a period of 10 seconds. The polarized components of sudden commencements have a period from about 30 to 300 seconds and are thus within the range of applicability of Piddington's (1955) analysis.

Parker (1962) sums up the situation by stating that because in the geomagnetic field $V_a >> U$ that the slow wave drops out and only the pure Alfvén wave which propagates along the field lines and the fast wave which propagates in all directions are left. Both waves propagate with the Alfvén velocity.

Various hydromagnetic waves have been proposed to explain the propagation of an SC to the earth. Dessler (1958) suggested that a longitudinal hydromagnetic wave would propagate the increase in the geomagnetic field at an SC due to the impact on the magnetosphere of a solar plasma cloud. Piddington (1959) proposed that an E (or fast) wave would be generated at the noon meridian at the edge of the magnetosphere which would propagate the observed SC increase in H to the earth. He also suggested, (Piddington, 1960), that disturbances due to the blowing back of the field lines by the solar wind at the morning meridian would propagate a "twist" wave or 0 wave along the field lines to high latitude to cause the increase in disturbance seen there.

MacDonald (1961) suggested that the vorticity mode was responsible for SC propagation. In the model proposed in the Introduction, the SC was said

to be caused by both longitudinal (fast wave) and transverse (Alfvén 0 and E) waves. The longitudinal mode causes the increase in H observed at moderate to low latitudes and the transverse mode causes the elliptical polarization of SC's observed in latitudes greater than 45°.

Because the atmosphere below the ionosphere is not conducting, the SC signal received at the earth's surface is not due to the hydromagnetic waves themselves but rather the result of their interaction with the ionosphere. Thus Dessler and Parker (1959) conclude that the SC impulse is due to ionospheric currents induced in the E layer by the arrival of hydromagnetic waves. Piddington (1959) has shown that geomagnetic disturbances in the region above 10^3 km propagate as hydromagnetic waves in the ion plasma alone and that below a transition level, whose height depends on the frequency of the disturbance, the propagation is by the diffusion of the disturbance magnetic field through the lower atmosphere to the earth.

Francis and Karplus (1960) have considered the propagation of hydromagnetic waves through the ionosphere for the case of vertically incident 0 and E waves at 45° geomagnetic latitude. They conclude that the ionosphere is essentially transparent for waves with periods greater than 2π seconds. The transit times from 550 km to 80 km altitude for both waves are figured on the basis of the delay time from $t = 0$ when all the harmonic components of the disturbance are in phase above the ionosphere until they are again all in phase below the ionosphere. These authors find that the 0 and E wave transit times are of the order of 1.5 seconds. Thus, in agreement with Piddington's (1959) result, the presence of the ionosphere does not screen the signal due to SC hydromagnetic waves because the period of SC hydromagnetic waves is much greater than 2π seconds. The above delay time of the propagation of the hydromagnetic signals through the ionosphere to the

altitude of 80 km, (below which the propagation is electromagnetic), is too small to be significant relative to the 3 minute propagation time of the SC disturbance given by Dessler et al. (1960).

Recently Dungey (1962) showed that the effect of the ionosphere may be larger than was found previously (1954) by himself and by Francis and Karplus (1960) when the incidence of the wave is oblique. The same effect has been found by Nashida (1962). Thus the effect of the ionosphere on the SC hydromagnetic is not as yet fully understood. In this thesis, the effect of the ionosphere is considered as secondary and is completely ignored.

Ultimately the type of waves which are responsible for the observed SC field are determined by two factors: first, which modes are generated by the impact of the enhanced solar wind on the magnetosphere; and second, whether these waves can propagate without attenuation to the earth. Parker (1962) gives the magnetic Reynolds number for the magnetosphere as $3 \times 10^6/\tau$ where τ is the characteristic time in seconds of the magnetic disturbance. For an SC τ is the order of a few minutes so for this disturbance the magnetic Reynolds number is large compared to unity indicating that the line lines of magnetic force are frozen into the plasma in the magnetosphere. Thus the concept of blowing back of the field lines by the pressure of the solar wind in the morning and evening hemispheres to produce transverse Alfvén waves as well as the concept of the compression of the field around the noon meridian to produce longitudinal waves are both physically valid.

CHAPTER III

POLARIZATION RULES

Because of the variation that occurs in D simultaneously with the changes in H during the SC of a magnetic storm, it is essential for a proper description of the SC field to study the total horizontal disturbance vector $\underset{\sim}{\Delta H}$*. During an SC the changes in the vertical component are usually small enough to be neglected except in the case where strong oscillations accompany the SC. Thus in the following discussions only the horizontal component $\underset{\sim}{\Delta H}$ of the total SC disturbance vector $\underset{\sim}{\Delta F}$ will be considered. The time scale of the SC variation is given by the rise time of the disturbance which varies from one to five minutes depending on the individual SC and the location of the magnetic observatory at which it is observed. It is necessary to use rapid-run magnetograms for the description of the SC field in order to be able to resolve the rapid variations in which the changes in H may be as much as hundreds of gammas per minute. During the International Geophysical Year rapid-run magnetograms have become available for about 40 magnetic observatories.

---

*The symbols used in the discussion of magnetic field variations are defined as follows. The total horizontal disturbance vector $\underset{\sim}{\Delta H}$ is the projection on the earth's surface of the total field disturbance vector $\underset{\sim}{\Delta F}$. The vector $\underset{\sim}{\Delta H}$ can be resolved into the following three pairs of orthogonal components; namely, ΔH and ΔDH, ΔX and ΔY, or finally $\Delta X'$ and $\Delta Y'$. The scalar ΔH is the variation in the horizontal component H measured with respect to the pre-SC value of H, while ΔD is the variation of the declination D with respect to the pre-SC value. When ΔD is measured in radians ΔDH gives the projection of $\underset{\sim}{\Delta H}$ on the direction normal to H. The pairs of components ΔX and ΔY and $\Delta X'$ and $\Delta Y'$ are the north and east forces referred to the geographic and dipole axes respectively.

The material for the following analysis of SC's was drawn from virtually all the rapid-run magnetograms at the IGY World Data Center A and concerns 93 SC's that occurred during the period beginning with the IGY and ending September 1961. In addition, data were collected from 38 magnetic observatories listed in Table 3-2 for 10 selected SC's that are evenly distributed over the Greenwich day. For the SC's listed in Table A-1 in the Appendix, ΔH and ΔD were scaled with respect to the pre-storm values of H and D at intervals of 5 to 30 seconds, depending on the nature of the SC. In order to construct a vector diagram of the locus of the end point of the total horizontal disturbance vector $\underset{\sim}{\Delta H}$, $\Delta X'$ and $\Delta Y'$ were calculated from ΔH and ΔD as follows:

$$\Delta X' = \Delta H \cos (D-\Psi) - \Delta DH \sin (D-\Psi) \qquad 3\text{-}1$$

$$\Delta Y' = \Delta H \sin (D-\Psi) + \Delta DH \cos (D-\Psi) \qquad 3\text{-}2$$

where Ψ is the angle between the geographic and geomagnetic north, from which $|\underset{\sim}{\Delta H}| = \sqrt{(\Delta X')^2 + (\Delta Y')^2}$ was found. Examples of two such vector diagrams are shown in Figure 1-1 for SC's at College and Fredericksburg. The path traced out on the horizontal plane by the disturbance vector $\underset{\sim}{\Delta H}$ as storm time increases as well as the instantaneous positions of $\underset{\sim}{\Delta H}$ at 15 seconds for Fredericksburg and 2 1/2 minutes for College are shown in this figure. Further examples of SC vector diagrams are shown in Figure 3-1 to illustrate the fact that opposite directions of rotation of $\underset{\sim}{\Delta H}$ with storm time do occur.

In order to study the various characteristics of the SC field as manifested in the vector diagrams of $\underset{\sim}{\Delta H}$ two methods of approach were used. First, for a given latitude, the SC field was studied as a function

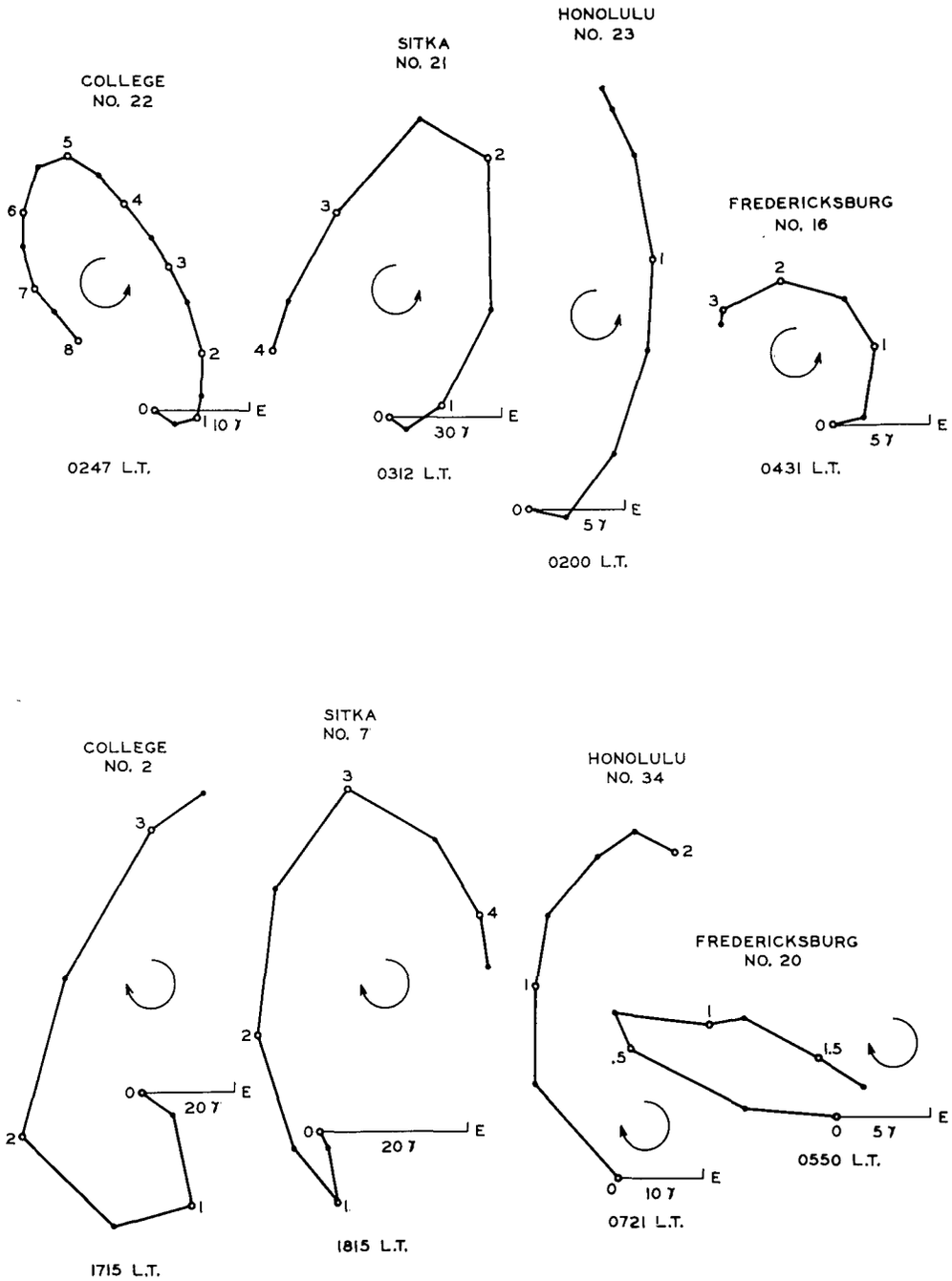

Fig. 3-1. SC vector diagrams for clockwise and counterclockwise polarization.

of longitude with respect to the sun-earth line by treating the local time of the SC's at the station as equivalent to this spatial variable. The 579 vector diagrams for the 17 stations to which this first statistical approach to the description of the SC field was applied are shown in Figures 3-2, 3-3, 3-4 and 3-5. In order to test to what extent individual SC's agree with the results derived for the SC field from the above statistical approach using many SC's at the 17 individual stations, a second analysis was carried out using 10 SC's (as listed in Table 3-2) for 18 to 30 stations. The 247 vector diagrams for this second method of study of the SC field are shown in map form in Figures 3-6 through 3-15 for each of the 10 SC's. In all of these Figures 3-2 through 3-15 the shape and orientation of the vector diagrams are accurately drawn, however, the time and magnitude scales are not all the same.

The most remarkable feature of these 826 vector diagrams is the predominance of SC's in which the locus of $\underset{\sim}{\Delta H}$ is elliptical in form rather than linear. This rotation that makes the vector diagram of elliptical shape characterizes the polarization of the SC, and in what follows this characteristic is referred to simply as the polarization of the SC. Some of the vector diagrams show an almost perfect elliptical or circular polarization while for others it is less regular but still clearly polarized either in a clockwise or counterclockwise direction. At lower latitudes there are more linear than polarized forms of vector diagrams, but even at Honolulu ($\underset{\sim}{\Phi} = 21.0°$) there are some clearly elliptically polarized SC's. This high degree of polarization of SC's emphasizes the necessity of taking the D variations into account when one attempts to describe the SC field.

The complexity and great range of variability of SC's in magnitude, rise time and shape of the vector diagram as illustrated above preclude the possibility of a simple description of the SC field or of a single explanation which can cover all the possible types of SC's. However, there are certain general features of the SC field that can be established from the study of the vector diagrams. The two most prominent features of the SC field as manifested by the vector diagrams are the type of polarization, (circular, elliptical or linear), and the direction of polarization (clockwise or counterclockwise). In order to discuss the nature of the polarization of the SC field the following nomenclature will be used to describe the shape of the SC vector diagrams. An SC will be said to be: a) linearly polarized if its vector diagram is similar to the four shown in Figure 3-2 for Honolulu around 2300 hours; b) irregularly polarized if the vector diagram shows an irregular rotation such as the two in Figure 3-3 at College around 1300 hours; c) elliptically polarized if the vector diagram is approximately elliptical, even though only part of an ellipse is traced out, such as the three in Figure 3-2 at Honolulu from 0100 to 0200 hours; d) circularly polarized if the vector diagram is clearly an ellipse or circle such as those in Figure 3-2 at College between 0800 and 0900 hours. Because of the complexity of SC's not even these four types of vector diagram classifications will suffice to unambiguously describe all SC's.

The variations with both local time and latitude of the degree of polarization of the SC field for the northern hemisphere as determined from the vector diagrams in Figures 3-2 to 3-5 are summarized below in terms of the classifications of polarization defined above.

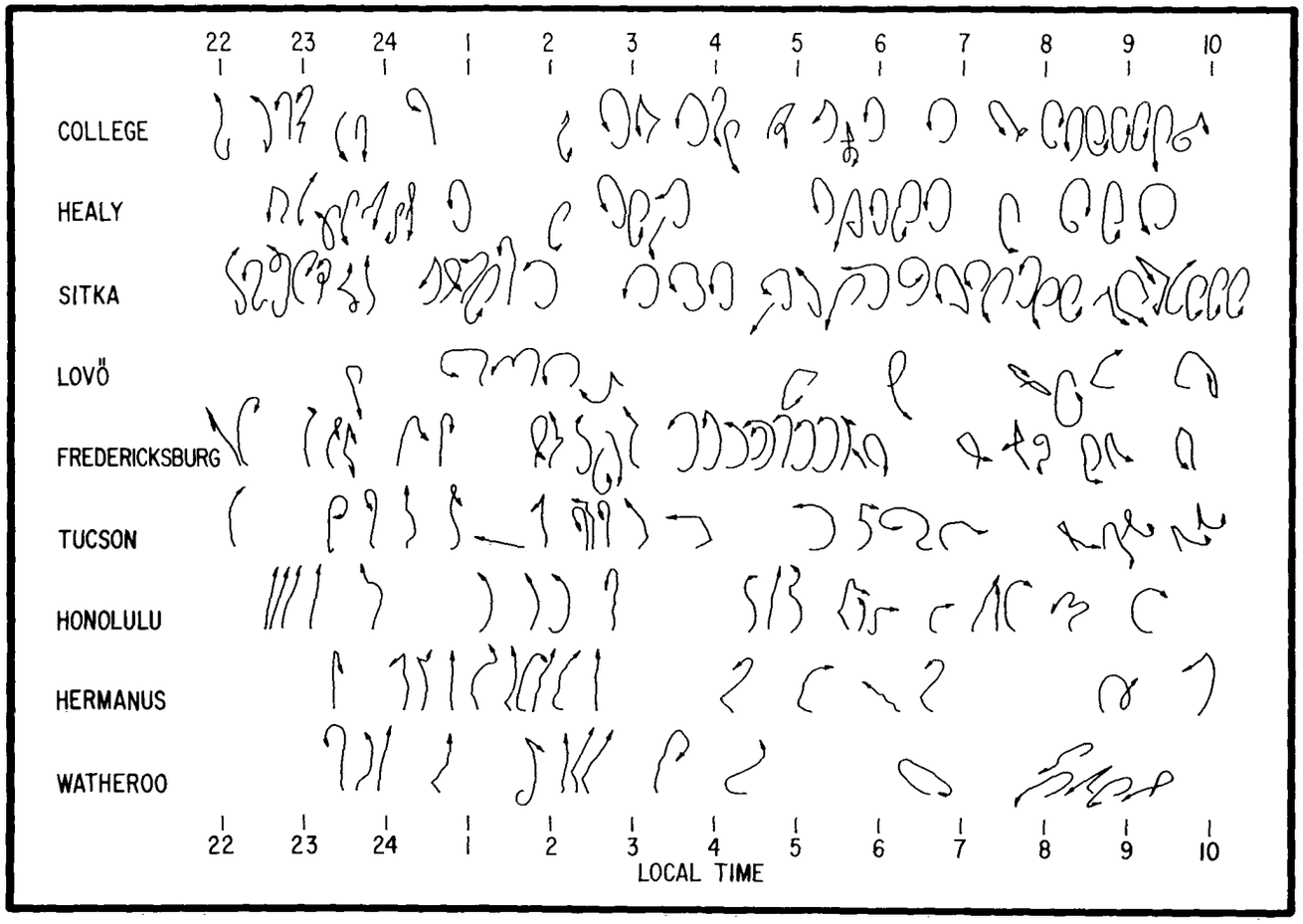

Fig. 3-2 SC vector diagrams for $\Phi < 65^{\circ}$ and L.T. 2200 to 1000 hours.

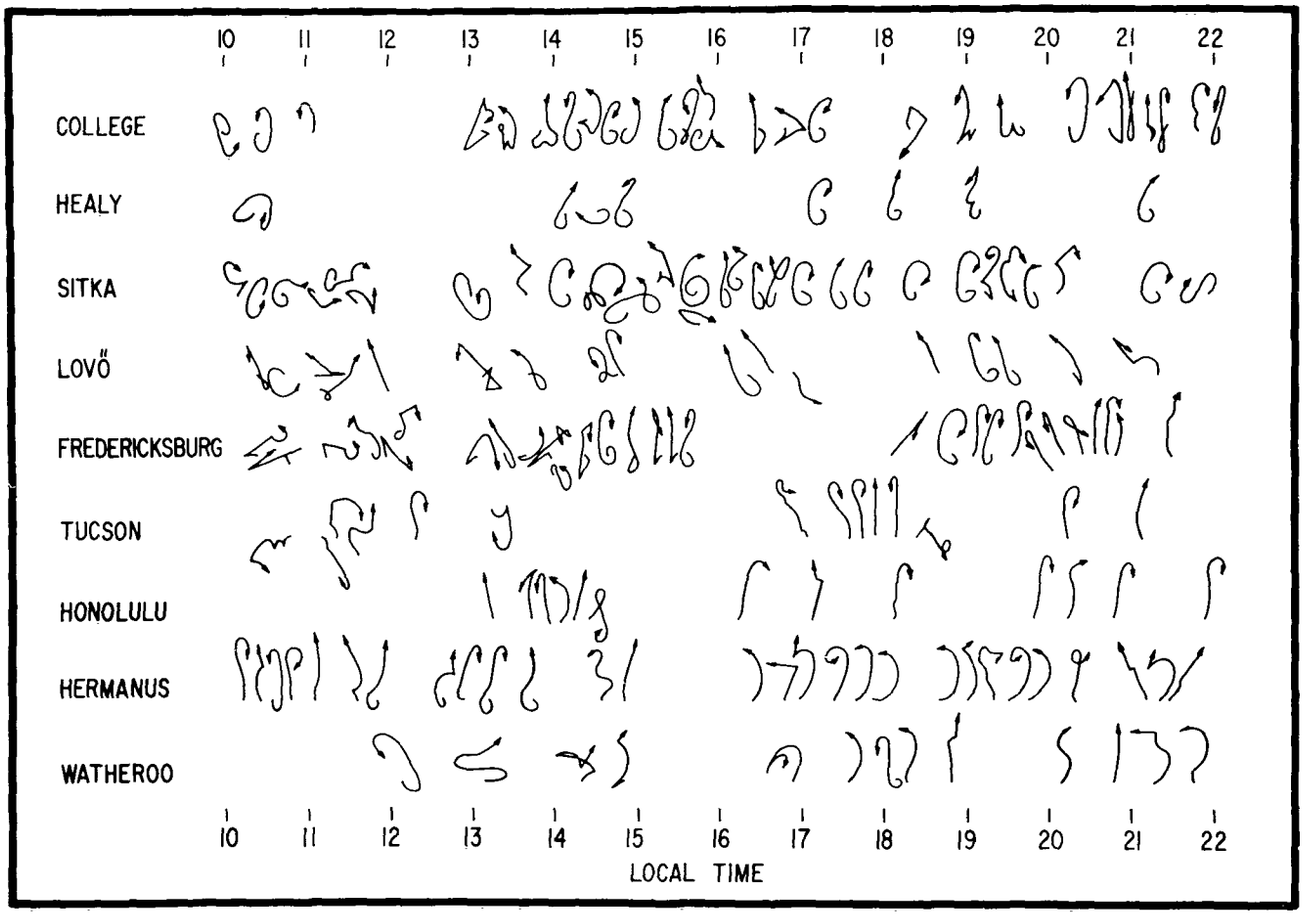

Fig. 3-3 SC vector diagrams for $\Phi < 65^{\circ}$ and L.T. 1000 to 2200 hours.

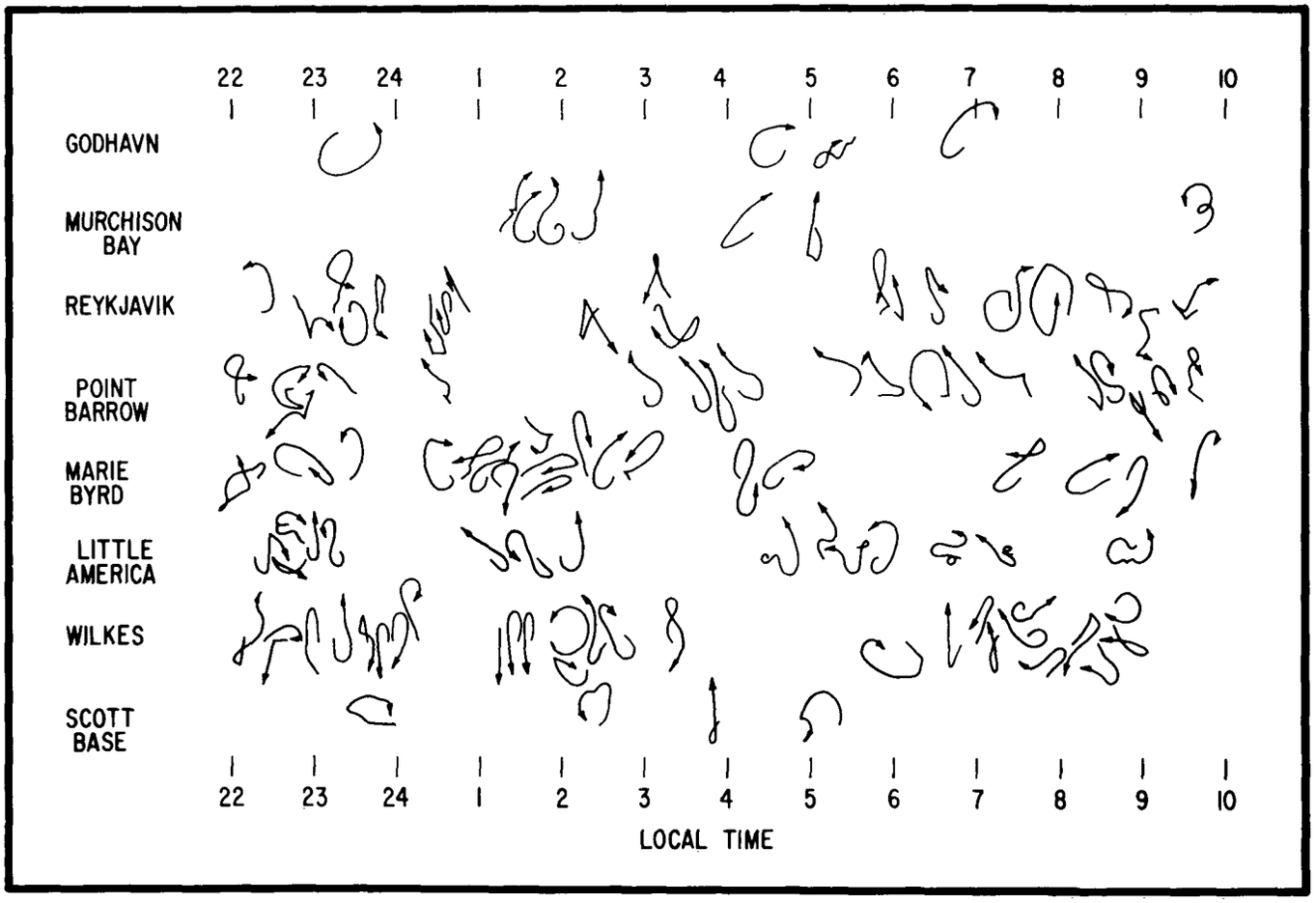

Fig. 3-4 SC vector diagrams for $\Phi > 65^{\circ}$ and L.T. 2200 to 1000 hours.

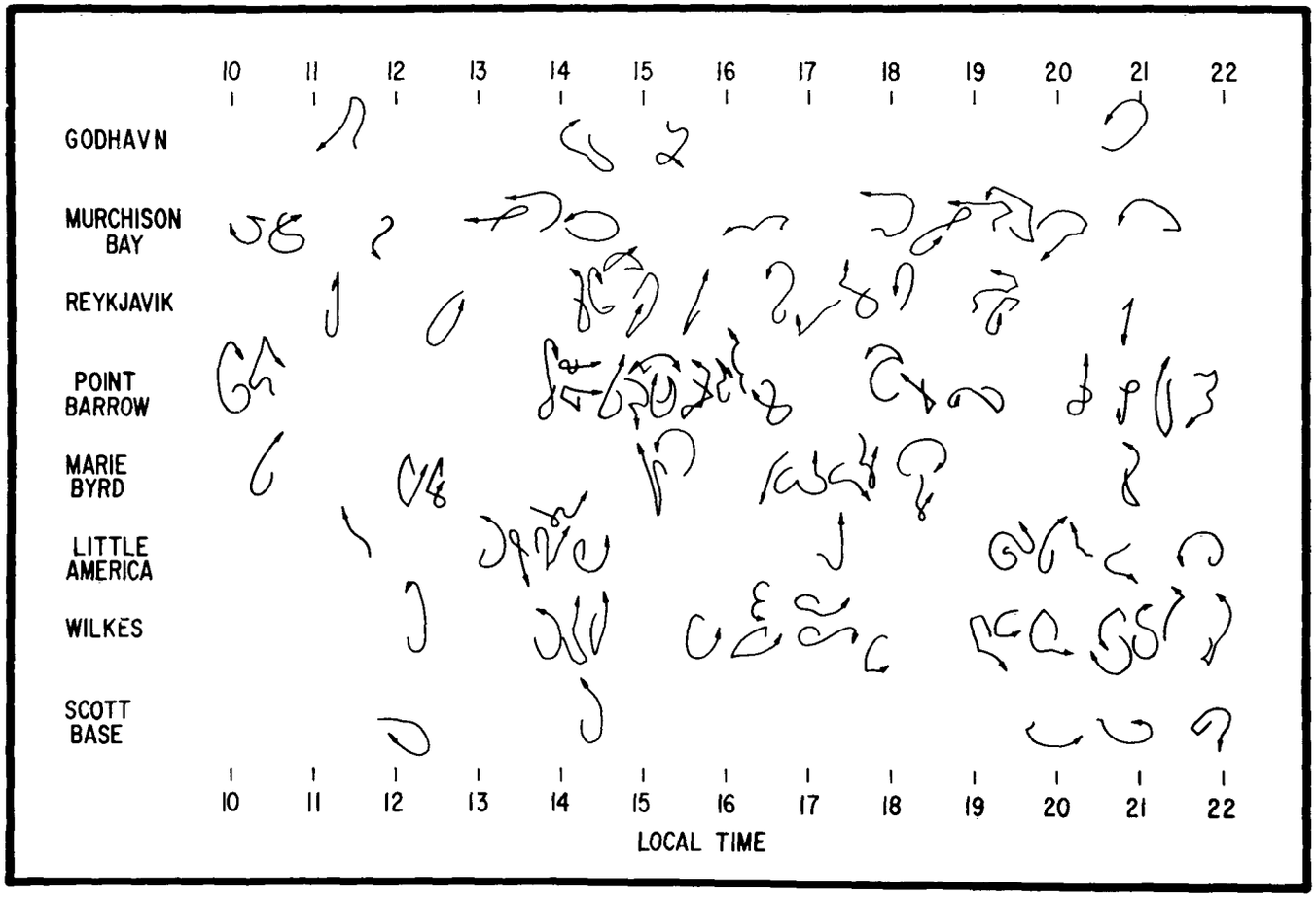

Fig. 3-5 SC vector diagrams for Φ >65° and L.T. 1000 to 2200 hours.

1) For stations with a geomagnetic latitude $\underline{\Phi} \geq 60°$ virtually all the SC's are either elliptically or circularly polarized depending on the local time. Thus, with the exception of stations very near the auroral zone such as Point Barrow and Reykjavik where the SC field is very disturbed, SC's at stations with $\underline{\Phi} \geq 60°$ are circularly polarized between 0100 and 1000 hours of local time and elliptically polarized at all other times.
2) For stations such that $60° > \underline{\Phi} \geq 45°$ SC's are circularly polarized from 0100 to 1000 hours, elliptically polarized from about 1800 to 0100 hours and irregularly polarized from 1000 to 1800 hours.
3) For low latitude stations with $45° > \underline{\Phi} \geq 0$ the polarization is either linear or irregular in the time zone 1000 to 2400 hours, and either irregular or elliptical in the time zone 2400 to 1000 hours.

There is not sufficient data for the latitudes from 45° to 70° in the southern hemisphere to determine the variation of the degree of polarization for this section. The direction of polarization for the southern hemisphere SC's at very high latitude for $\underline{\Phi} > S70°$ seems to agree in general with that in the northern hemisphere. From the data at Hermanus and Watheroo the SC polarization can be said to be elliptical or irregular from 1600 to 2200 hours and irregular or linear from 2200 to 1600 hours for $S45° > \underline{\Phi} \geq 0$. The above latitude zones of the type of polarization are only meant to be approximate.

If the SC magnetic perturbation observed at a station were due to a transverse hydromagnetic wave propagating along a field line, its polarization would be circular, whereas, if it were due to a longitudinal

hydromagnetic wave its polarization would be linear. The change in the type of polarization thus reflects the distribution over the earth of the ratio of transverse to longitudinal SC hydromagnetic waves. Transverse hydromagnetic waves predominate over the longitudinal hydromagnetic wave component of the SC field with increasing latitude until they constitute the major part of an SC above, say, 60°. At the local time zones within a few hours of 0400 and 1600 hours of local time there is a strong enhancement of the transverse hydromagnetic waves such that even at very low latitudes circularly polarized SC's appear when the SC is very large. In column 5 of Table 3-1 the percentage of elliptically polarized SC's for each of the 17 stations in Figures 3-2 to 3-5 are given. The decrease in this percentage from the pole to the equator illustrates the predominance of transverse SC hydromagnetic waves at higher latitudes. Because these figures were derived on the basis of the type of polarization being "circular", the percentages at College, Point Barrow and Reykjavik are lowered by the irregular disturbance due to their proximity to the auroral zone.

That the type of polarization becomes more circular at higher latitudes can also be seen in Figures 3-6 through 3-15 for the 10 selected SC's. The vector diagrams are drawn at the projected positions of the stations on the equatorial plane. Thus the linear forms of the vector diagram which appear in Figures 3-8 and 3-13 lie near the equator. At higher latitudes the SC's are almost all elliptically or circularly polarized. The predominance of circular polarization for the stations within the zones near 0400 and 1600 hours of local time can be seen in Figure 3-7 for the SC of 0315 U.T. October 22, 1958. Thus, in this particular SC, the transverse hydromagnetic wave component was strong as close to the equator as Apia (#31) at Φ = S16.0°

The variation of the direction of polarization of the SC vector diagrams in Figures 3-2 to 3-5 can be seen to be systematic with local time by looking, say, at Sitka. If the direction of polarization is noted for only those SC's which are elliptically or circularly polarized, then there are two local time zones of opposite polarization at Sitka; namely, counterclockwise (when the direction of rotation of $\underset{\sim}{\Delta H}$ is viewed looking downward at the center of the earth) from 2200 to 1000 hours and clockwise from 1000 to 2200 hours. This division of the direction of polarization of the vector diagrams into two local time zones of opposite polarization, as illustrated by data for many SC's from one station (Sitka), can also be seen to be the case for any particular SC at many stations; for example, refer to Figure 3-8 for the SC of 0315 U.T. October 22, 1958.

An indication of the relation between the directions of polarization of SC's that are observed in opposite hemispheres at stations with the same local time can be found in Figure 3-3. Thus the six SC's at Hermanus in the southern hemisphere from 1700 to 1900 hours are elliptically polarized in a counterclockwise direction, whereas at Sitka in the northern hemisphere there is a group of five SC's within the same period of local time for which the polarization is clearly reversed, namely clockwise. An example of SC's exhibiting the opposite direction of polarization from the northern to the southern hemisphere for a particular SC can be seen in Figure 3-13 for the SC of 1652 U.T. May 31, 1958. Thus the directions of polarizations of the SC at Honolulu (#26) in the northern and Apia (#31) is the southern hemisphere are opposite. Also the counterclockwise polarization of this SC at Hermanus (#32) in the southern hemisphere is opposite to all the others of the same local time zone because they are in the northern hemisphere.

A complete analysis of all the vector diagrams in Figures 3-2 through 3-15 has been made in order to investigate the systematic behavior of the direction of polarization of elliptically or circularly polarized SC's. From this analysis of a total of more than seven hundred vector diagrams the following two rules have been determined for the direction of polarization of elliptically polarized SC's, either clockwise or counterclockwise, when viewed downward on the earth's surface.

1) In each of the northern and southern hemispheres the direction of polarization is opposite in two quadrants separated by the meridian plane through 1000 and 2200 hours of local time.

2) In each meridian plane the direction of polarization of the magnetic vector $\underset{\sim}{\Delta H}$ is opposite in the northern and southern hemispheres.

In the northern hemisphere the direction of polarization is clockwise from 1000 to 2200 hours; this specifies the direction of polarization in the remaining three quadrants according to the rules given above.

The above two rules can be combined into one, namely, that the transverse circularly polarized component of the SC hydromagnetic perturbation is transmitted to the earth in the ordinary mode in the morning hemisphere (2200 to 1000 hours) and in the extraordinary mode in the evening hemisphere (1000 to 2200 hours). For a discussion of the direction of polarization of the O and the E wave with respect to the field line see the section on the phase of the transverse wave in chapter V.

The data from the statistical study of many SC's at a given station from which these rules were determined are presented in column 6 of Table 3-1 in the form of the percentage of the elliptically polarized SC's for a given station which obey the polarization rules. The percentages of cases

in which the elliptically polarized SC's obey the two rules ranges from 91% to 69% with a mean 84%, (excluding the high latitude stations for which $\bar{\Phi} > 65°$). The percentage of agreement with the polarization rules is independent of latitude. Even at stations for which the elliptically polarized SC's are not very frequenct, i.e. Fredericksburg, Tucson and Honolulu, the majority of the elliptically polarized SC's follow the pattern set by the rules.

In order to test to what extent individual SC's obey the polarization rules an analysis was made of ten SC's (listed in Table 3-2). The stations used are listed under Table 3-2 and the number of stations for which data were analyzed is shown in column 2. The data in Table 3-2 correspond to the analysis of the vector diagram in Figures 3-6 to 3-15. From column 3 of Table 3-2 the percentage of stations at which the SC's were elliptically polarized ranges from 95% to 69% for the 10 SC's indicating a high rate of occurrence of elliptically polarized SC's. Taking only the cases in which the SC's is observed to be elliptically polarized, the percentage of stations at which the polarization of the SC agrees with the polarization rules is listed in column 4. In general this percentage is high with a mean of 77% indicating good agreement with the polarization rules for individual SC's as well.

As will be discussed in chapter VI, there is reason to believe that the magnetic field lines through stations of latitude greater than 72° may not be interhemispherically connected because of the distortion of the earth's dipole field by the steady solar wind. This being the case, one would expect that the polarization rules for the transverse hydromagnetic wave component of SC's, (which propagates from the equatorial plane in both

directions along the dipole field line to the northern and southern hemispheres), would not be obeyed by SC's in very high latitudes. This break-down in the agreement of elliptically polarized SC's with the polarization rules is illustrated by the mean of the percentages in column 6 of Table 3-1 for stations for which $\left|\Phi\right| \geq 72°$; this mean is only 49% compared to 84% for stations for which $\left|\Phi\right| < 72°$. Because there are two possible polarizations and two local time zones the percentage agreement of about 50% indicates random polarization of SC's at very high latitudes. In column 5 of Table 3-2 the percentage of stations with latitude less than 72° for which elliptically polarized SC's obey the polarization rules is given; the average percentage for the 10 SC's is now increased by the exclusion of very high latitude stations from 77% to 84%.

The polarization rules discussed above were determined solely on the basis of SC vector diagrams of either circular or clearly elliptical polarization, however, these rules should also apply to irregular polarizations that are due to the combination of the circularly polarized transverse hydromagnetic wave and a linearly polarized longitudinal hydromagnetic wave. Thus in Figure 3-4 the vector diagrams for the 8 SC's at Byrd Station between 2430 and 0245 hours all exhibit clockwise polarization in agreement with the rules.

There are other types of vector diagrams to which the polarization rules apply. These are hook or inverted hook forms. The hook form may be interpreted as an indication of the initial arrival of a predominately longitudinal wave which is linearly polarized followed by the arrival of a transverse circularly polarized wave; whereas, the situation is in the reverse sequence for the inverted hook form. Hook forms appear at Tucson

and Honolulu in Figure 3-3 between 1700 and 2200 hours and examples of inverted hook forms can be seen in Figure 3-12 at station No.'s 11, 14, 15, 16, 17, 21, 22, and in Figure 3-13 at Station No.'s 14, 17, 19, and 22.

In order to demonstrate that the polarization rules are obeyed by those SC's that exhibit a hook or an inverted hook in their vector diagrams, the sense of rotation of the magnetic vector for the hooked portion is shown in Table 3-3. Column 4 of Table 3-3 indicates for each observatory-SC the sense of rotation, clockwise (marked C) or counterclockwise (CC), expected from the quadrant polarization rules. The sense of rotation actually observed in the hooked part of each SC is shown in column 5. Agreement between columns 4 and 5 is good; 80% of the 17 observatory-SC's listed in Table 3-3 for Honolulu, Tucson, and Fredericksburg show agreement with the polarization rules.

For the SC of July 21, 1958 at 1529 U.T. illustrated in Figure 3-12, the four stations, Lerwick (11), Lovö (14), Rude Skov (16) and Hartland (17) were all on the day side of the earth. The vector diagrams for these stations showed a loop or inverted hook form, and the polarization characteristics were in agreement with those expected from the rules.

In column 6 of Table 3-3 the form of the vector diagram in each SC is indicated; here, ℓ and h signify loop and hook forms, respectively.

Table 3-1 Percentage of SC's that are elliptically polarized, and percentage of SC's (among these elliptically polarized SC's) obeying the polarization rules

1	2	3	4	5		6	
Magnetic Observatory	Geomagnetic Latitude	R_e* in earth radii	Total number of SC's, N	Elliptically polarized SC's		SC's obeying polarization rules	
				N_e	$(N_e/N)\times 100\%$	N_e*	$(N_e^*/N)\times 100\%$
Godhavn	N 79.8°	32.0	8	7	87	3	43
Murchison Bay	N 75.25	15.5	20	15	75	7	47
Reykjavik	N 70.2	8.6	33	23	70	13	57
Pt. Barrow	N 68.6	7.5	39	27	70	21	78
College	N 64.7	5.4	55	32	58	26	81
Healy	N 63.6	5.0	31	22	71	21	96
Sitka	N 60.0	4.0	67	52	78	50	96
Lovo	N 58.2	3.6	30	14	47	12	86
Fredericksburg	N 49.6	2.4	62	23	37	21	91
Tucson	N 40.4	1.7	36	11	30	10	91
Honolulu	N 21.0	1.14	37	8	21	6	75
Hermanus	S 33.3	1.45	47	20	42	16	80
Watheroo	S 41.7	1.78	34	16	47	11	69
Byrd Station	S 70.6	9.0	31	20	65	18	90
Little America	S 74.0	13.0	27	21	78	8	37
Wilkes Station	S 77.8	22.5	47	36	77	24	66
Scott	S 79.0	27.8	9	8	89	4	50
Total			613	355		271	

*R_e is the geocentric distance of the point at which the magnetic field line (of the unperturbed dipole) through the station crosses the equatorial plane.

Table 3-2

Results of Analysis of Ten SC's

1		2	3	
Time of SC		Stations for which Data were Available	Stations at which SC was Elliptically Polarized	
U.T.	Date	Number, S	Number, S_e	$(S_e/S)x100\%$
0042	July 5, 1957	23	17	74%
0315	Oct. 22, 1958	26	23	88
0843	Sept. 3, 1958	26	18	69
0930	Sept. 16, 1958	29	24	83
1050	Jan. 25, 1958	27	22	81
1300	Sept. 4, 1957	18	16	89
1529	July 31, 1958	30	26	87
1652	May 31, 1958	22	17	77
1821	Nov. 6, 1957	22	21	95
1920	Aug. 29, 1957	24	18	75
		Total 247	Total 202	Mean 82

Table 3-2 (Con'd)

4		5		
Stations at which Elliptically Polarized SC Obeyed the Rules		Same as Columns 3 and 4, Excluding Stations with $\Phi > 72^{o}$ ($R_e > 10.5$)		
Number, S_e^*	$(S_e^*/S_e) \times 100\%$	S_e' (S_e with $\Phi < 72^{o}$)	$S_e'^*$	$(S_e'^*/S_e') \times 100\%$
12	70%	12	10	83%
19	83	18	17	95
13	72	14	11	79
23	96	18	17	95
16	73	16	11	69
13	81	11	10	91
17	56	20	15	75
14	82	13	13	100
13	62	17	11	65
17	95	13	12	92
Total 157	Mean 77	Total 152	Total 127	Mean 84

Table 3-2 (Con'd)

Stations (Geomagnetic Latitude)

A021*	1.	Thule (N 89°.0)	C147*	25.	Kakioka (N 26°.0)
A049	2.	Godhavn (N 79°.8)	C277	26.	Honolulu (N 21°.0)
A010	3.	Murchison Bay (N 75°.3)	E575	27.	Paramaribo (N 17°.0)
A103	4.	Reykjavik (N 70°.2)	E556	28.	Guam (N 3°.9)
A039	5.	Point Barrow (N 68°.6)	E606	29.	Koror (S 3°.3)
A047	6.	Tromsö (N 67°.2)	E625	30.	Hollandia (S 12°.5)
A060	7.	Kiruna (N 65°.3)	E653	31.	Apia (S 16°.0)
A092	8.	College (N 64°.7)	C957	32.	Hermanus (S 33°.3)
A102	9.	Big Delta (N 64°.4)	C925	33.	Watheroo (S 41°.7)
A107	10.	Healy (N 63°,6)	A997	34.	Byrd Station (S 70°.6)
A140	11.	Lerwick (N 62°.5)	A995	35.	Little America (S 74°.0)
A149	12.	Sitka (N 60°.0)	A979	36.	Dumont d'Urville (S 75°.5)
B038	13.	Eskdalemuir (N 58°.4)	A977	37.	Wilkes (S 77°.8)
B009	14.	Lovö (N 58°.2)	A991	38.	Scott Base (S 79°.0)
B098	15.	Valentia (N 56°.7)			
B114	16.	Rude Skov (N 55°.9)			
B119	17.	Hartland (N 54°.6)			
B132	18.	Manhay (N 52°.0)			
B136	19.	Dourbes (N 52°.0)			
B318	20.	Fredericksburg (N 49°.6)			
B321	21.	Ponta Delgada (N 45°.6)			
C098	22.	Toledo (N 43°.9)			
C236	23.	Tucson (N 40°.4)			
C034	24.	Memambetsu (N 34°.1)			

*IGY station designation

Table III-3

Analysis of SC Vector Diagrams of Looped or Hooked Form

1	2	3			4	5	6
Station	Geomagnetic latitude	Time of SC Date	U.T.	L.T.	Rotation expected from rules	Rotation in loop or hook, observed	Form of vector diagram
	21.0	Feb.11,1958	0125	1425	C	CC	ℓ
		Aug.6, 1957	0508	1808	C	C	h
		Oct.28,1958	0650	1950	C	C	h
		Jul.8, 1958	0748	2048	C	C	h
		Jul.2, 1957	0857	2157	C	C	h
		Sep.22,1957	1345	0245	CC	CC	h
Tucson	40.4	Jul.5, 1957	0042	1742	C	C	h
		Jun.7, 1958	0046	1746	C	C	h
		Sep.16,1958	0930	0230	CC	CC	h
		Dec.19,1957	0937	0237	CC	CC	h
		Aug.29,1957	1920	1220	C	C	h
Fredericks-burg	49.6	Sep.29,1957	0016	1916	C	C	h
		Jul.7, 1957	0042	1942	C	C	h
		Jan.5, 1959	0137	2037	C	C	h
		May 24,1959	0540	0040	CC	C	h
		Dec.19,1957	0937	0437	CC	CC	h
		Jan.29,1960	1937	1437	C	C	ℓ
Lerwick	62.5	Jul.31,1958	1529	1529	C	C	ℓ
Lovo	58.2	Jul.31,1958	1529	1629	C	C	ℓ
Rude Skov	55.9	Jul.31,1958	1529	1629	C	C	ℓ
Hartland	54.6	Jul.31,1958	1529	1529	C	C	ℓ

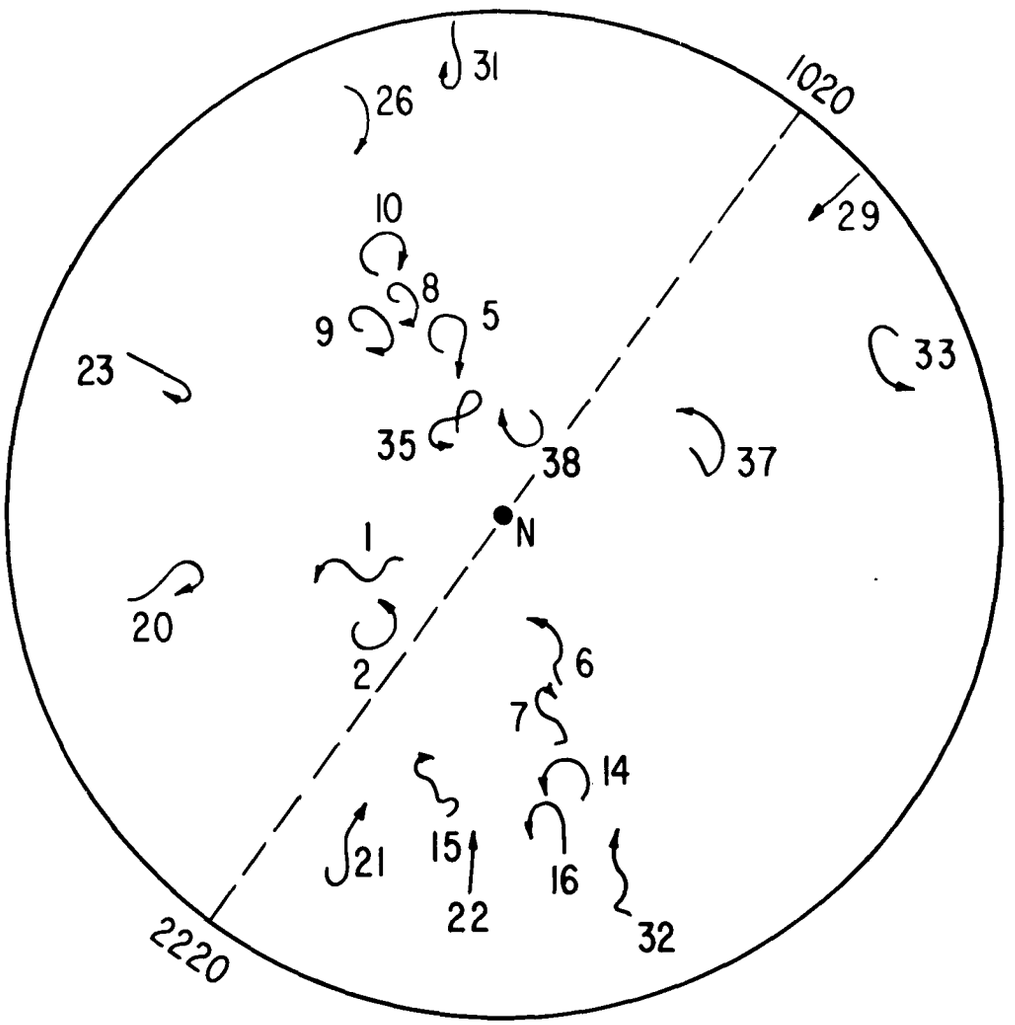

0042 U.T. JULY 5, 1957

Fig. 3-6 Equatorial plane map of vector diagrams for SC of 0042 U.T. July 5, 1957.

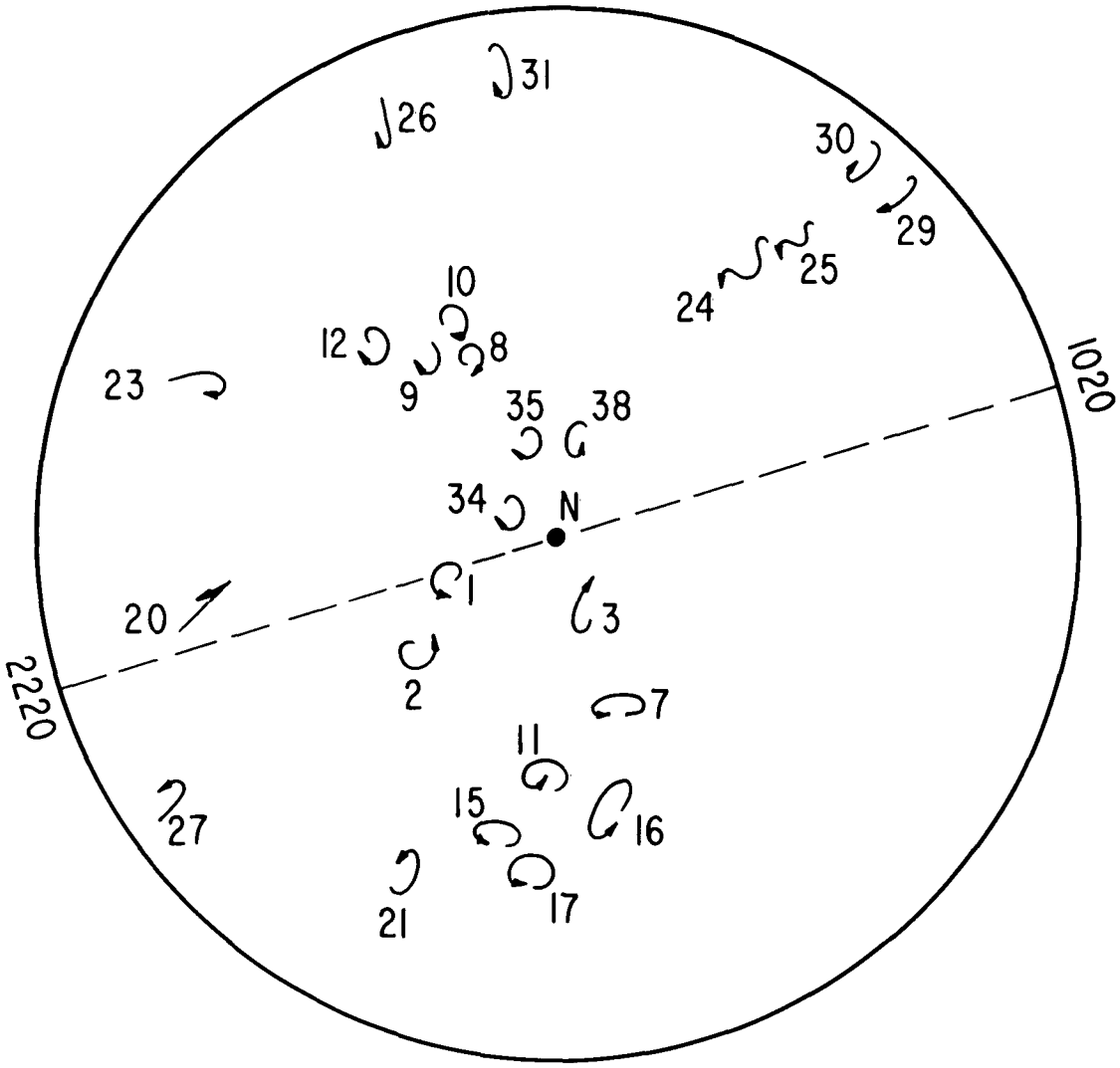

0315 U.T. OCTOBER 22, 1958

Fig. 3-7 Equatorial plane map of vector diagrams for SC of 0315 U.T. October 22, 1958.

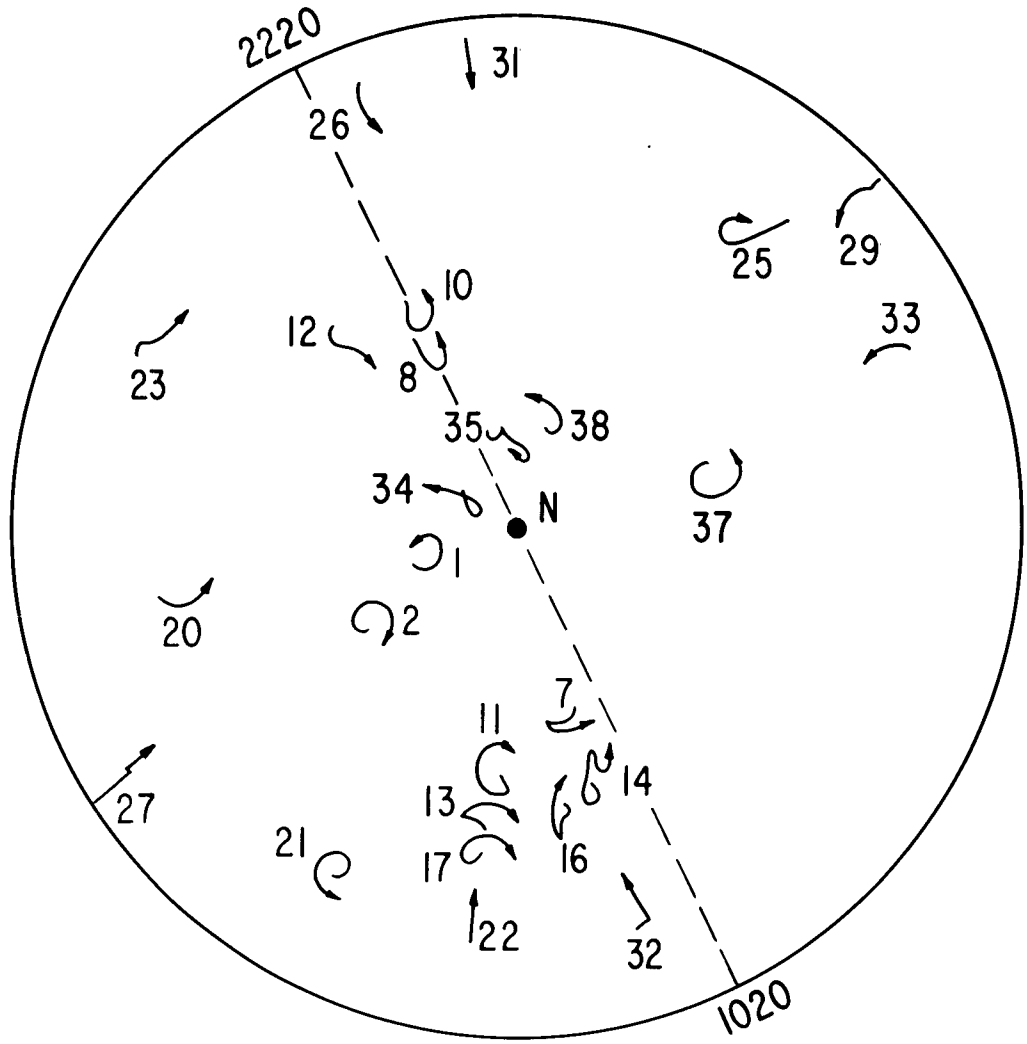

0843 U.T. SEPTEMBER 3, 1958

Fig. 3-8 Equatorial plane map of vector diagrams for SC of 0843 U.T. September 3, 1958.

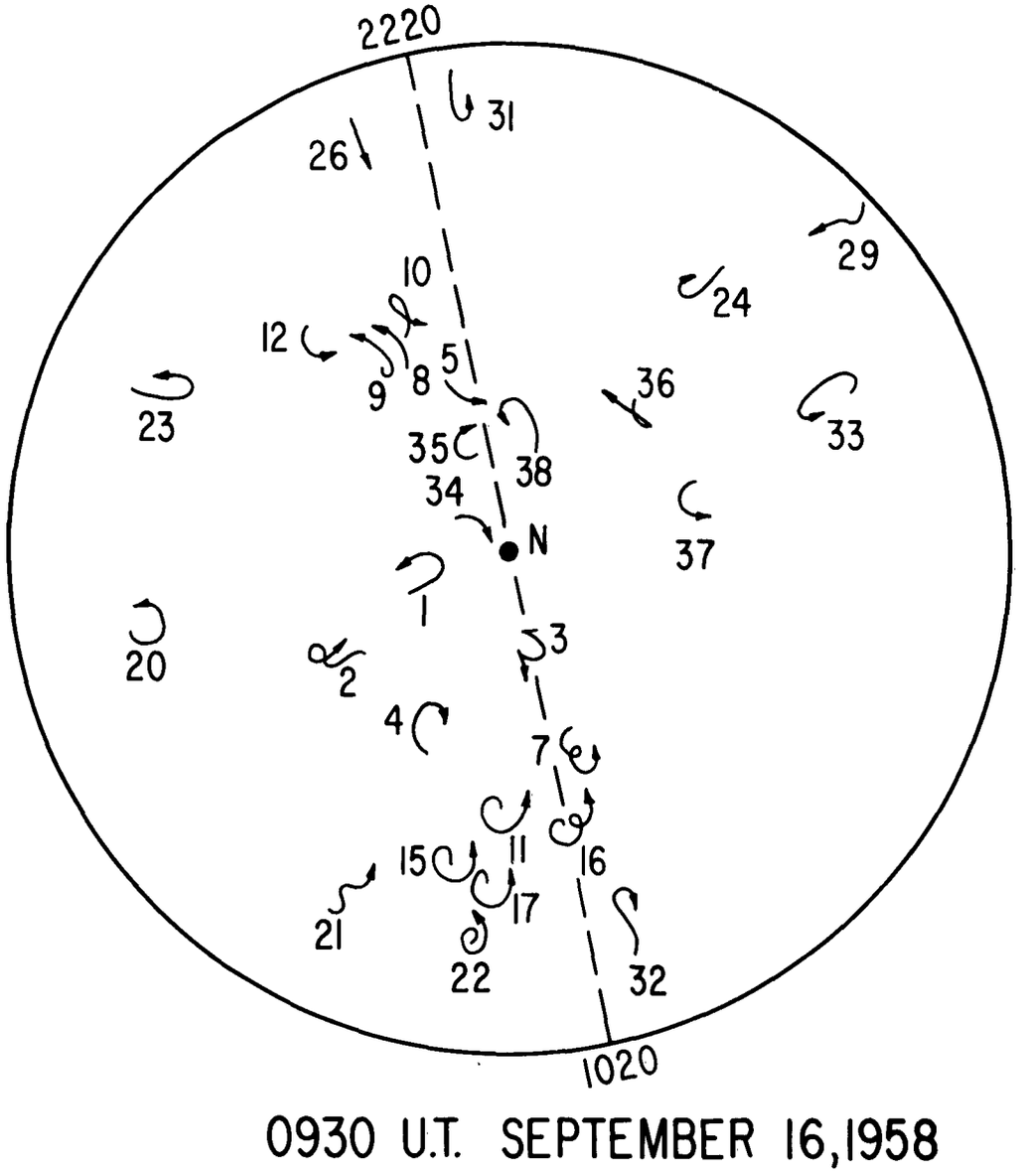

Fig. 3-9 Equatorial plane map of vector diagrams for SC of 0930 U.T. September 16, 1958.

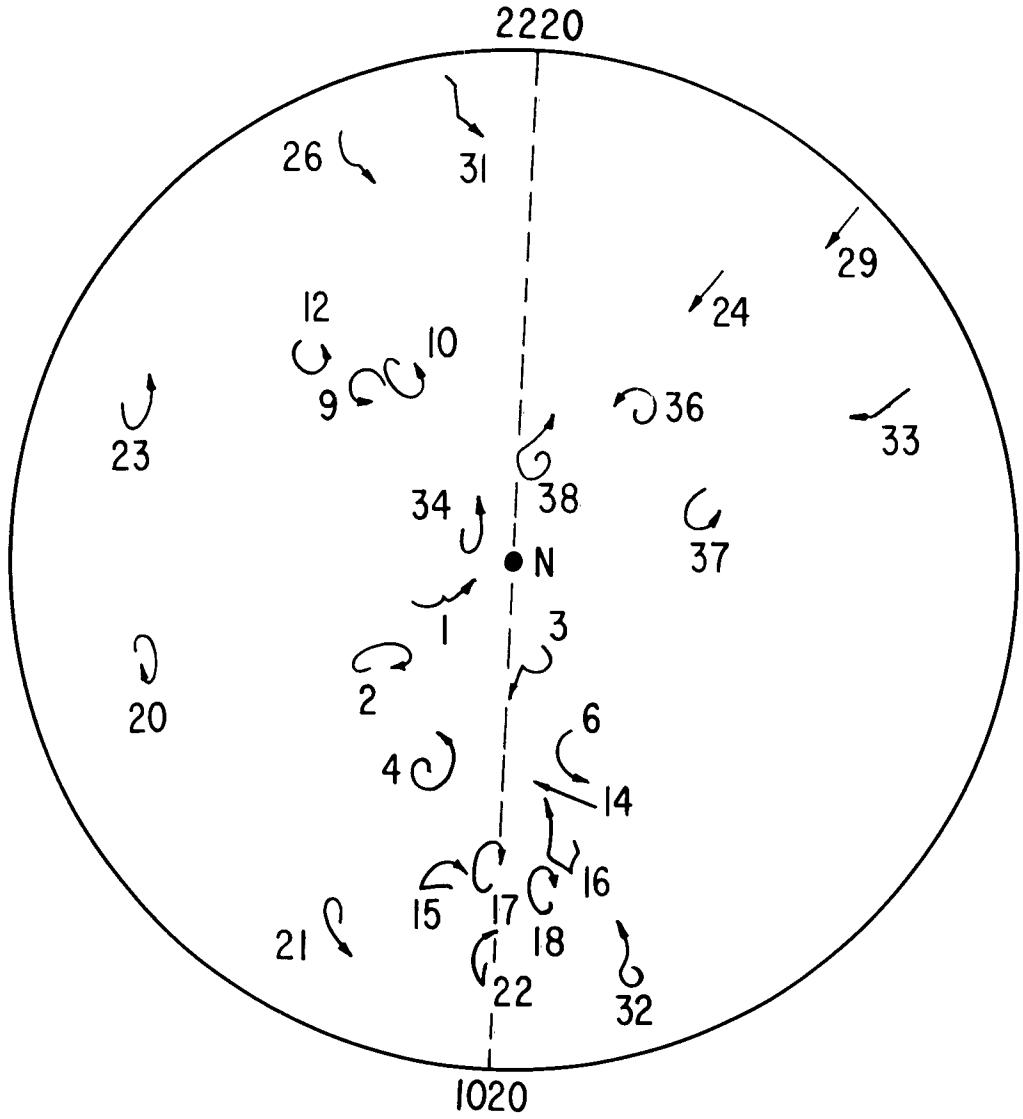

1050 U.T. JANUARY 25, 1958

Fig. 3-10 Equatorial plane map of vector diagrams for SC of 1050 U.T. January 25, 1958.

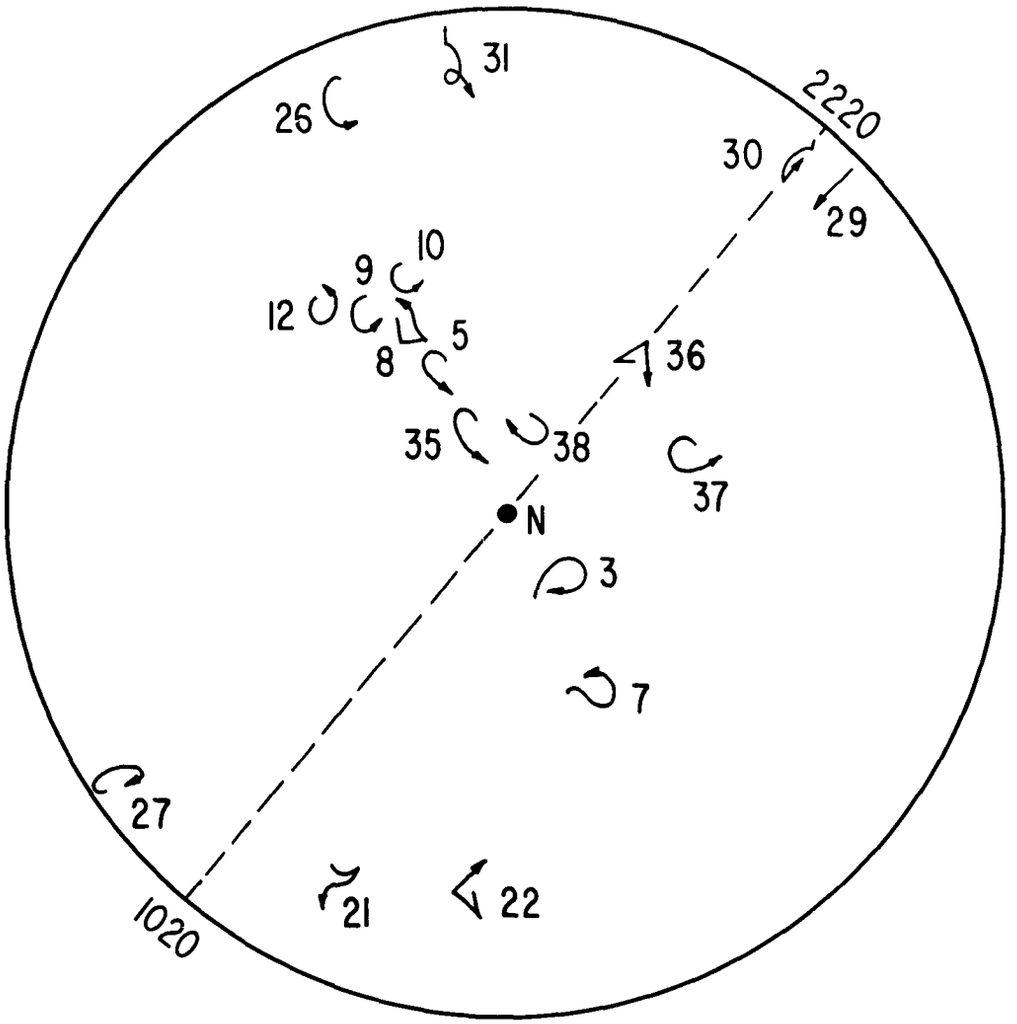

1300 U.T. SEPTEMBER 4, 1957

Fig. 3-11 Equatorial plane map of vector diagrams for SC of 1300 U.T. September 4, 1957.

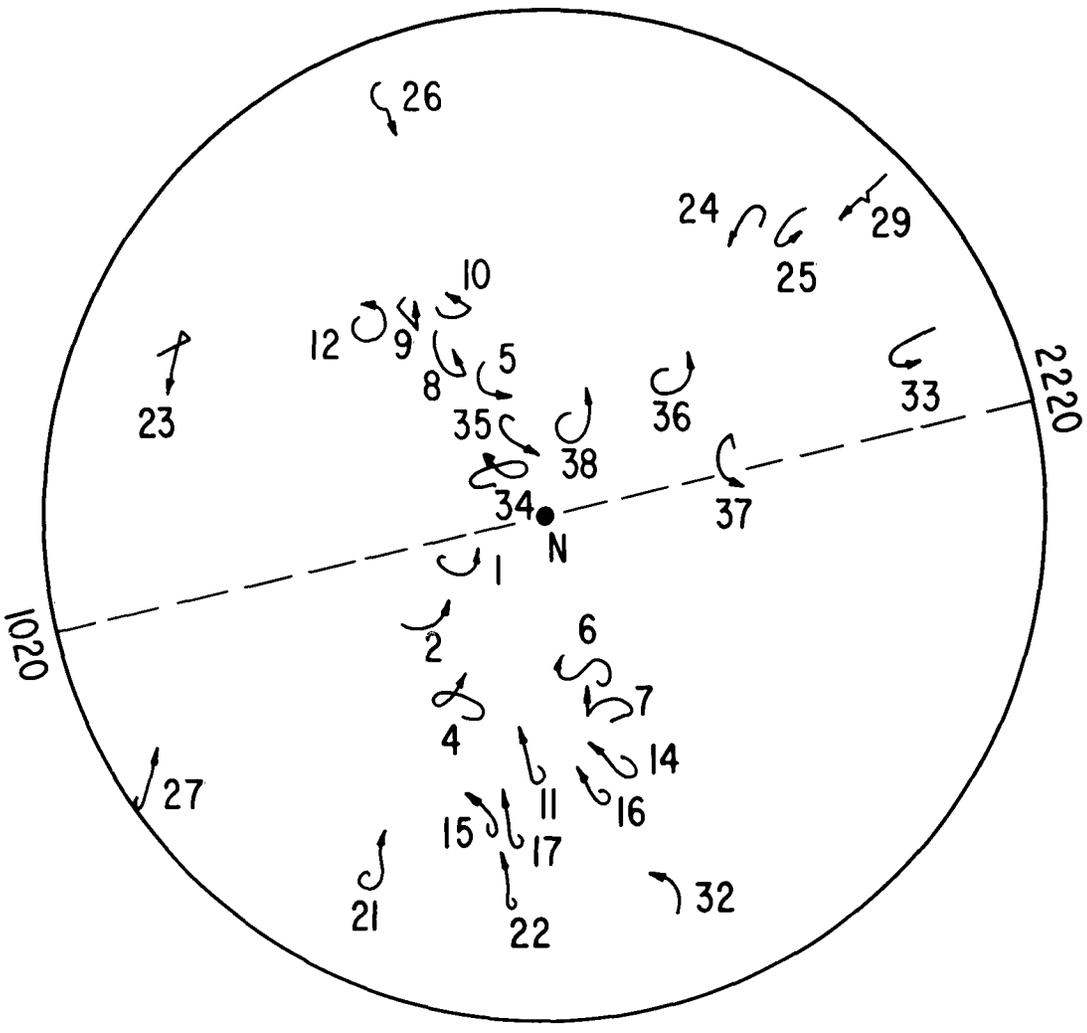

1529 U.T. JULY 31, 1958

Fig. 3-12 Equatorial plane map of vector diagrams for SC of 1529 U.T. July 31, 1958.

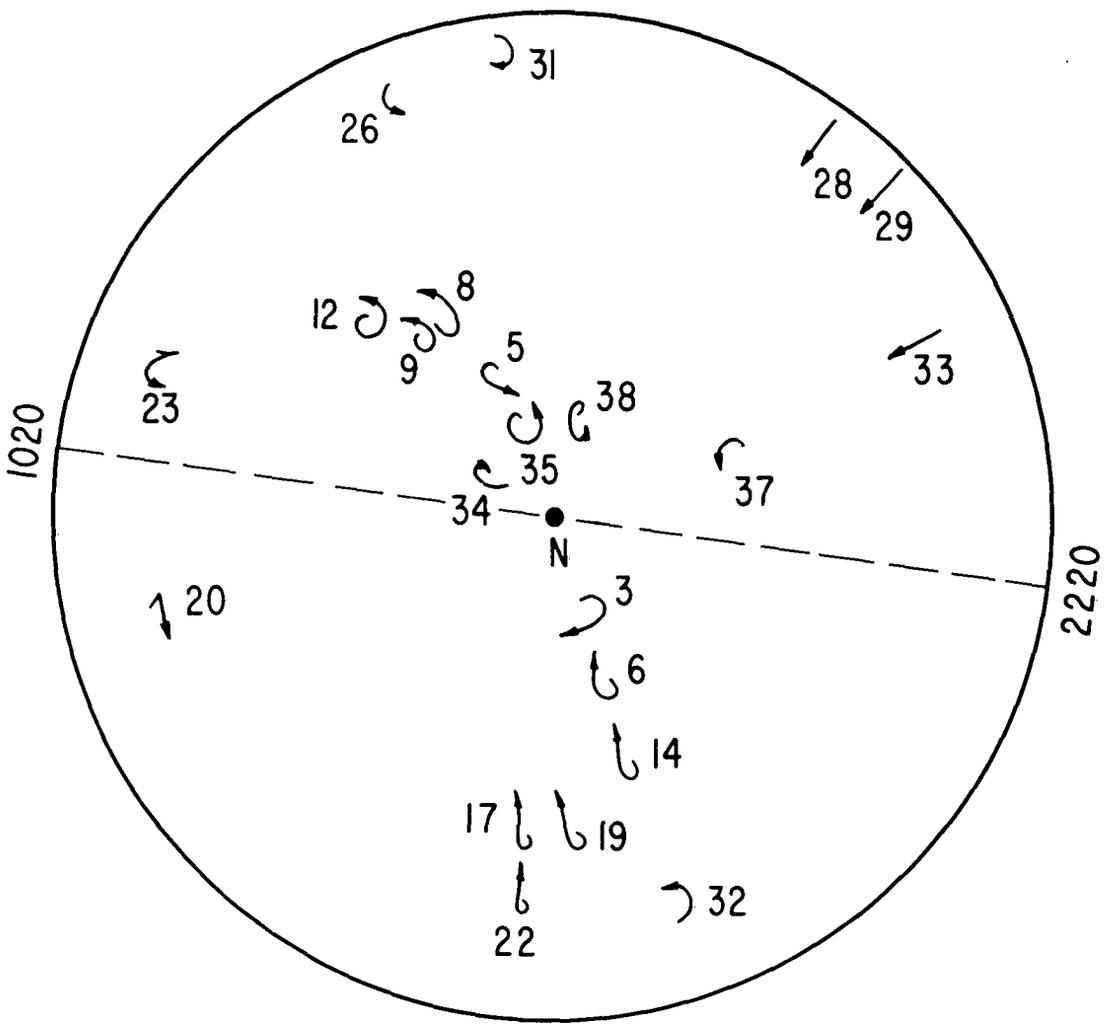

Fig. 3-13 Equatorial plane map of vector diagrams for SC of 1652 U.T. May 31, 1958.

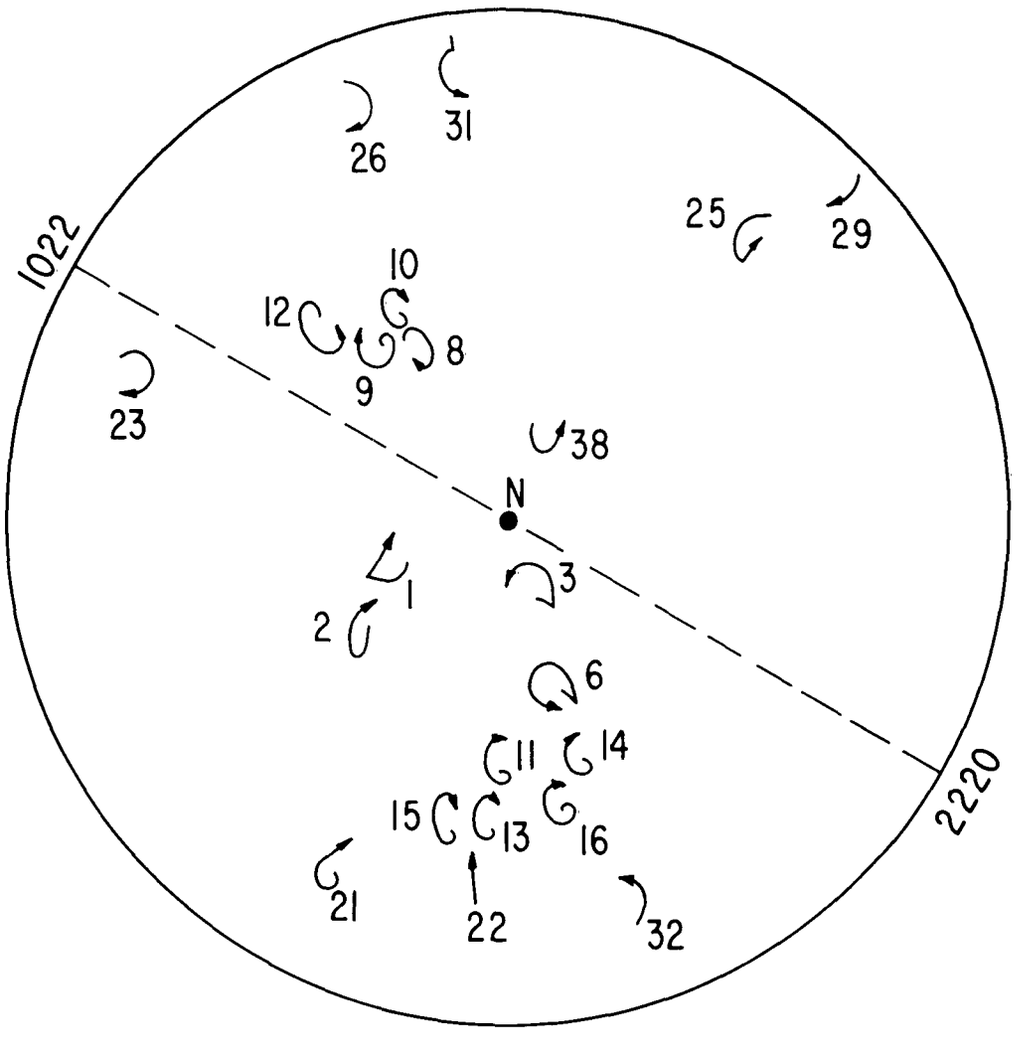

1821 U.T. NOVEMBER 6, 1957

Fig. 3-14 Equatorial plane map of vector diagrams for SC of 1821 U.T. November 6, 1957.

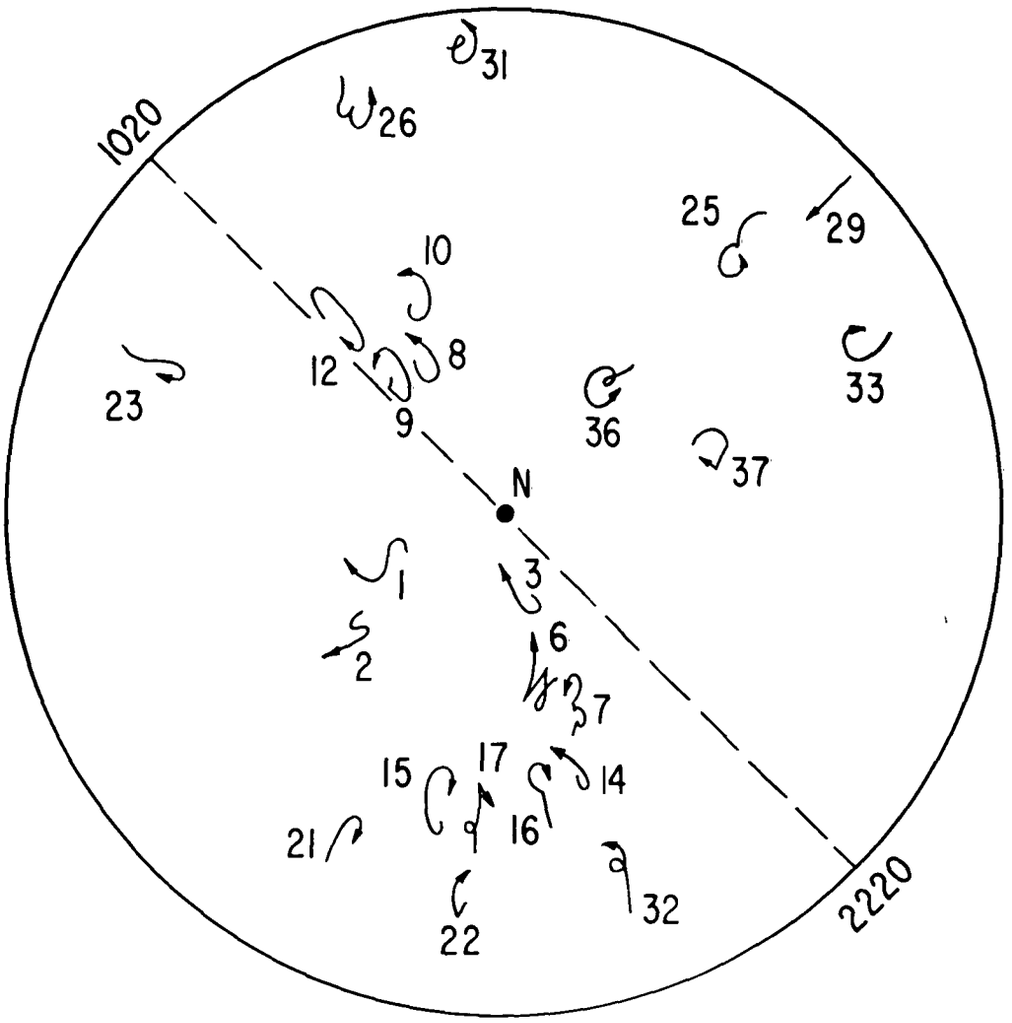

1920 U.T. AUGUST 8,1957

Fig. 3-15 Equatorial plane map of vector diagrams for SC of 1920 U.T. August 8, 1957.

CHAPTER IV

SUDDEN COMMENCEMENT OSCILLATIONS

Oscillatory disturbance of the magnetic field following SC's has been reported by many researchers. From the morphological studies it is clear that there are at least two different types of oscillations associated with SC's. First, there is a damped type rapid pulsation accompanying an SC as described by Kato and Saito (1958), Kato (1959) and Benioff (1960); the pulsations of this type have been studied extensively with induction magnetometers. The damped rapid pulsations are found to occur in the sunlit hemisphere and most frequently around 0900 hours local time with a period of 20 seconds, and a damping ratio of 0.85 as observed in Japan by Kato and Saito (1958). The second type of oscillatory disturbance of the SC field, which will be referred to as SC oscillation, has been described by Watanabe (1956), Wilson and Sugiura (1961) and Sano (1962). The main differences between SC oscillation and the damped pulsation accompanying SC's are; 1) the SC oscillation period is longer; 2) the amplitude of SC oscillation is not rapidly damped and the oscillation can thus continue for tens of cycles; 3) the local time dependence of frequency of occurrence is reversed, thus SC oscillations occur most frequently around 2200 hours local time; 4) the direction of rotation of the disturbance vector for damped typed pulsations observed by Kato and Saito (1958) depends on local time differently from that of the SC oscillation found by Wilson and Sugiura (1961) and Watanabe (1956).

Damped rapid pulsations accompanying SC's have been found at Fredericksburg from around 0800 to 1500 hours local time. The periods, the duration of the pulsation given in the number of cycles and the components

in which the pulsation occurs are given for ten SC's at Fredericksburg in Table 4-1. The pulsation always occurs in Z, in half of the cases in Z and H and only in one fifth of the cases in all three components; this fact suggests that, in general, the pulsation is not transverse to the field line (in which case it would show elliptical polarization) but is parallel to $\underset{\sim}{B}_o$ and is thus probably due to the fast or E mode. The local time of maximum occurrence of around 1200 hours for these damped pulsations lends support to the suggestion that they may be due to the fast or transverse propagation mode. Thus Piddington (1959) stated that an E wave would be generated in the noon meridian by the impact of the solar wind on the magnetosphere. Kato and Saito (1958) and Berthold (1960) suggest that hydromagnetic oscillation of the magnetosphere due to the impact of the solar wind is ultimately responsible for damped type pulsations accompanying SC's.

Table 4-1

Damped Rapid Pulsations Accompanying SC's at Fredericksburg

U.T.	L.T.	Date	Components which show oscillation	Period seconds	Duration in cycles
1348	0848	Nov. 12, 1960	Z	35	9
1452	0952	Oct. 24, 1960	Z,H	48	6
1525	1025	Dec. 23, 1959	Z	54	4
1529	1029	July 31, 1958	Z	40	4
1702	1202	July 14, 1960	Z,H,D	52	8
1804	1304	Dec. 7, 1960	Z,H	50	4
1859	1359	Jan. 13, 1960	Z,H	54	6
1909	1409	Nov. 30, 1960	Z	52	4
2000	1500	Apr. 27, 1960	Z,H,D	47	9
2020	1520	May 4, 1959	Z	60	4

Because of the disturbed nature of the SC field at high latitudes damped type SC pulsations, if they occur, are obscured by the more violent fluctuations. In the analysis of the SC's presented here many SC oscillations were found at Sitka, and most of the Point Barrow and College SC's were accompanied by strong and frequently persistent oscillation. Typical examples of SC oscillations are shown in Figure 4-1 for College, Sitka and Fredericksburg. The numbers by the station name refer to the SC number for the IGY SC's as listed in Table A-2 in the Appendix. In general the percentage of SC's which are accompanied by SC oscillations decreases rapidly with latitude south of the auroral zone. Because of the disturbed nature of the field north of this zone, it is difficult to tell whether SC oscillation persists for $\overline{\Phi} > 70°$. A review of the records at Wilkes (at $\overline{\Phi} = 77.8°$) and Little America (at $\overline{\Phi} = 74.0°$) indicates that both the percentage of SC's that have SC oscillations and the occurrence of clear sinusoidal wave forms for SC oscillations decrease at these very high latitudes. In Table 4-2 the decrease in the percentage at lower latitudes of SC's which exhibit oscillation is given for Point Barrow, College, Sitka, Fredericksburg and Honolulu. At College 80% of the SC's are followed by strong oscillations, therefore, this station was chosen for a detailed analysis of the SC oscillations.

Table 4-2

Percentage of Occurrence of SC Oscillations

Station	Number of SC	Number of SC's with Oscillation	Percentage of SC's with Oscillation
Point Barrow	23	19	83%
College	56	45	80%
Sitka	67	43	64%
Fredericksburg	58	28	47%
Honolulu	34	4	11%

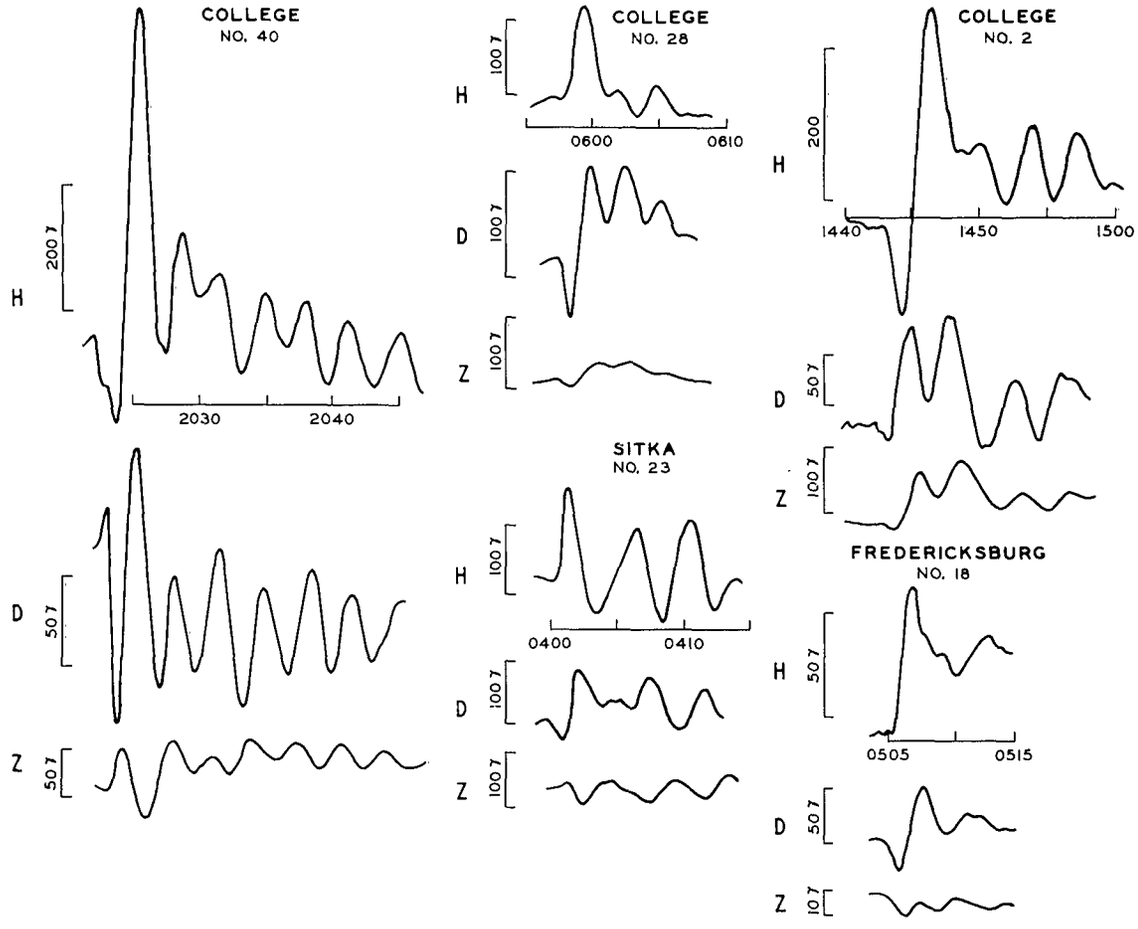

Fig. 4-1. SC oscillations at College, Sitka and Fredericksburg in H, D and Z.

Out of the 45 SC's which exhibited oscillation at College, the rapid-run magnetograms of only 29 were suitable for studying the oscillation characteristics in detail. One of the most striking features of SC oscillations at College is the smooth sinusoidal wave form that appears in all three components as is illustrated in Figures 4-1, 4-7, 4-9 and 4-10. This general characteristic of oscillation occurring in all three components in such a manner that there is a constant phase difference between the various components was found to be true for 95% of the cases at College. Thus the vector diagrams of SC oscillations are almost always open elliptical forms as can be seen in Figure 4-2 for College and Sitka. In this figure, for SC number 23 at Sitka, two vector diagrams are given; 23A is for the first 9 minutes of the SC and 23B is for the 9 minutes beginning 30 minutes after the start of the SC. These two vector diagrams were presented to show how the clear elliptical form for SC oscillations often persists for many tens of minutes without appreciable damping.

Although the position for the maximum frequency of occurrence of SC oscillations is in the auroral zone, the greater the amplitude of the SC oscillation the larger the area in which the oscillations are observed. For large oscillations the wave form is similar at stations close to each other as can be seen in Figure 4-3 for the same SC oscillation as observed at College, Big Delta and Healy, which are all within 130 km of each other. The amplitude varies to some extent but the wave form and period are nearly the same at all these stations.

There are not sufficient data with only 29 SC oscillations at College to reliably determine the dependence of the frequency of occurrence on local time. However, there is an indication of a greater tendency for SC oscillations to occur in two groups around 0800 and 2200 hours. Sugiura (1961) found a diurnal variation in the frequency of occurrence, averaged over the

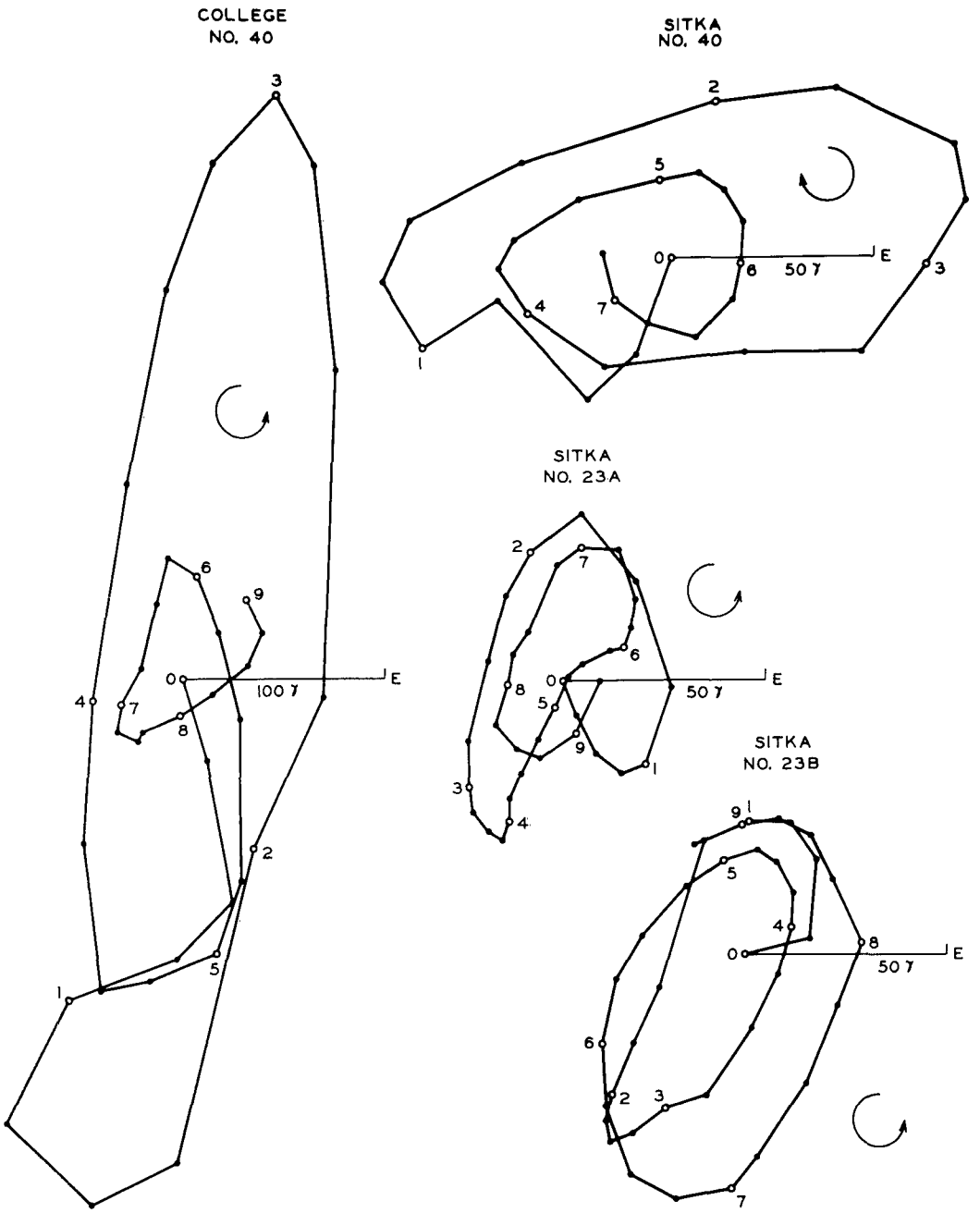

Fig. 4-2. Vector diagrams for SC oscillations at College and Sitka.

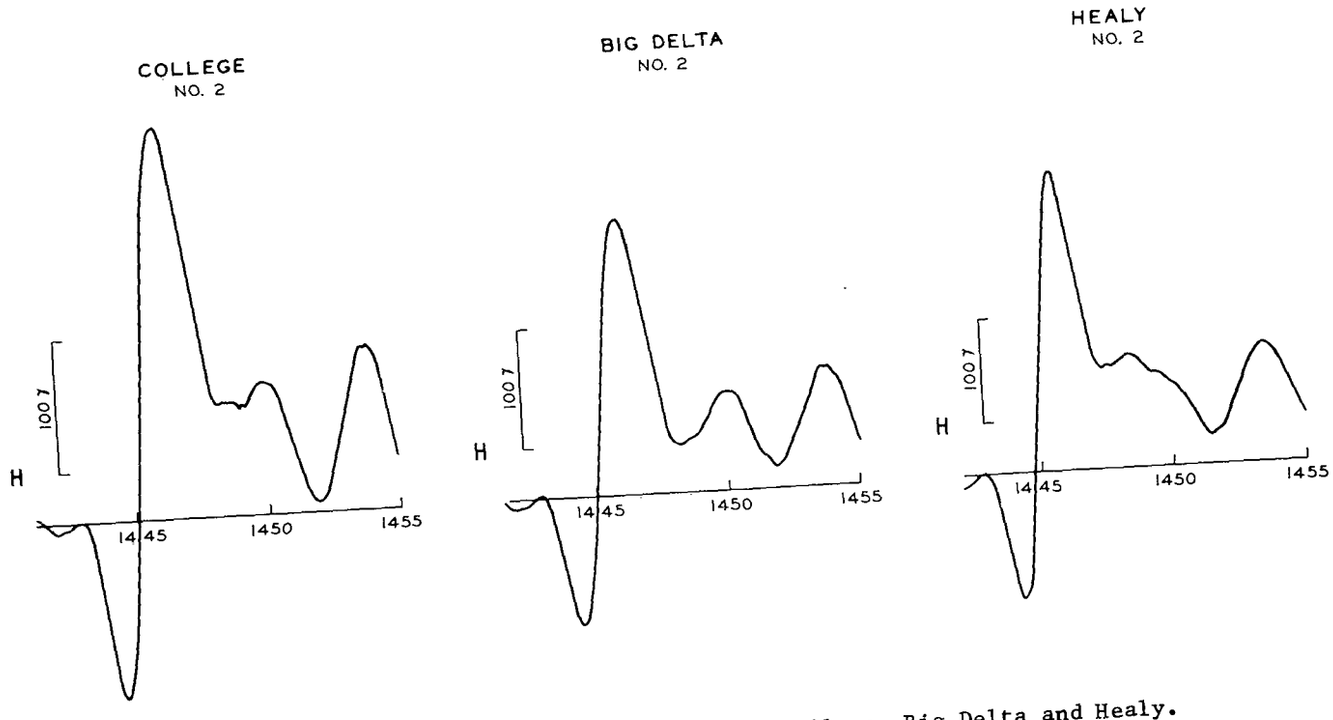

Fig. 4-3. H component of SC oscillation at College, Big Delta and Healy.

year, for giant pulsations of 4 to 8 minute periods at College, such that there were also two groups centered around 0900 and 1800 hours respectively. This tendency of SC oscillations and giant pulsations to show similar local time of occurrence relationships suggests an association between the two phenomena. This was verified when it was found that 21 of the 29 SC oscillations at College occurred during periods of giant pulsation activity. Thus if the field exhibited large amplitude pulsation activity prior to an SC then the SC would always be oscillatory. Only a few SC oscillations have been found without previous oscillational disturbance of the field. This association of SC oscillation with giant pulsations prior to the SC can be seen in Figures 4-4 and 4-5. In both the SC's of 1327 L.T. May 11, 1959 and 0828 L.T. April 9, 1959 at College, shown in Figure 4-4 for the H component, the field prior to the SC can be seen to be highly oscillatory. Frequency spectrum analyses were made of the oscillations around the epoch marked OSC in Figure 4-4, just prior to the SC in each case to determine the relationship of the periods to the SC period. For the May 11 SC, the two periods were found to be both 190 seconds and for the April 9 SC they were both 340 seconds. Although the fundamental periods of the OSC and the SC oscillations were identical for these SC's, the harmonic structures were found to differ in both cases. Vector diagrams were constructed for the OSC as well as for the SC to compare the polarizations. For the very smooth sinusoidal OSC and SC of April 9 shown in Figure 4-4, the two vector diagrams were almost identical in shape and both exhibited counterclockwise polarization in agreement with the SC polarization rules. In the case of the more highly disturbed field of the May 11 SC in Figure 4-4, the vector diagrams were not similar. The SC polarization was clockwise, in agreement with the polarization rules, but the OSC polarization was counterclockwise.

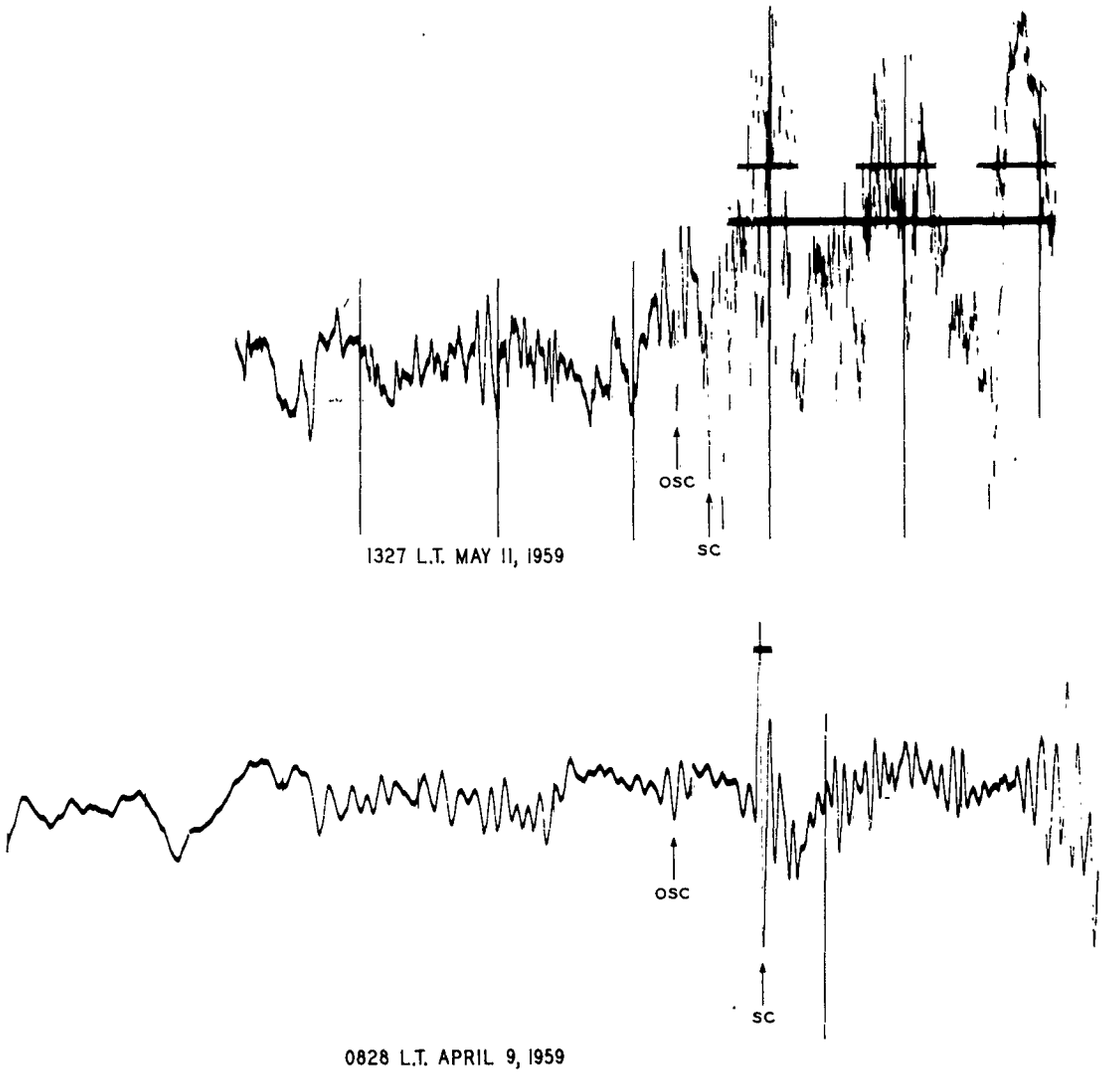

Fig. 4-4. Oscillation in H component prior to SC's at College.

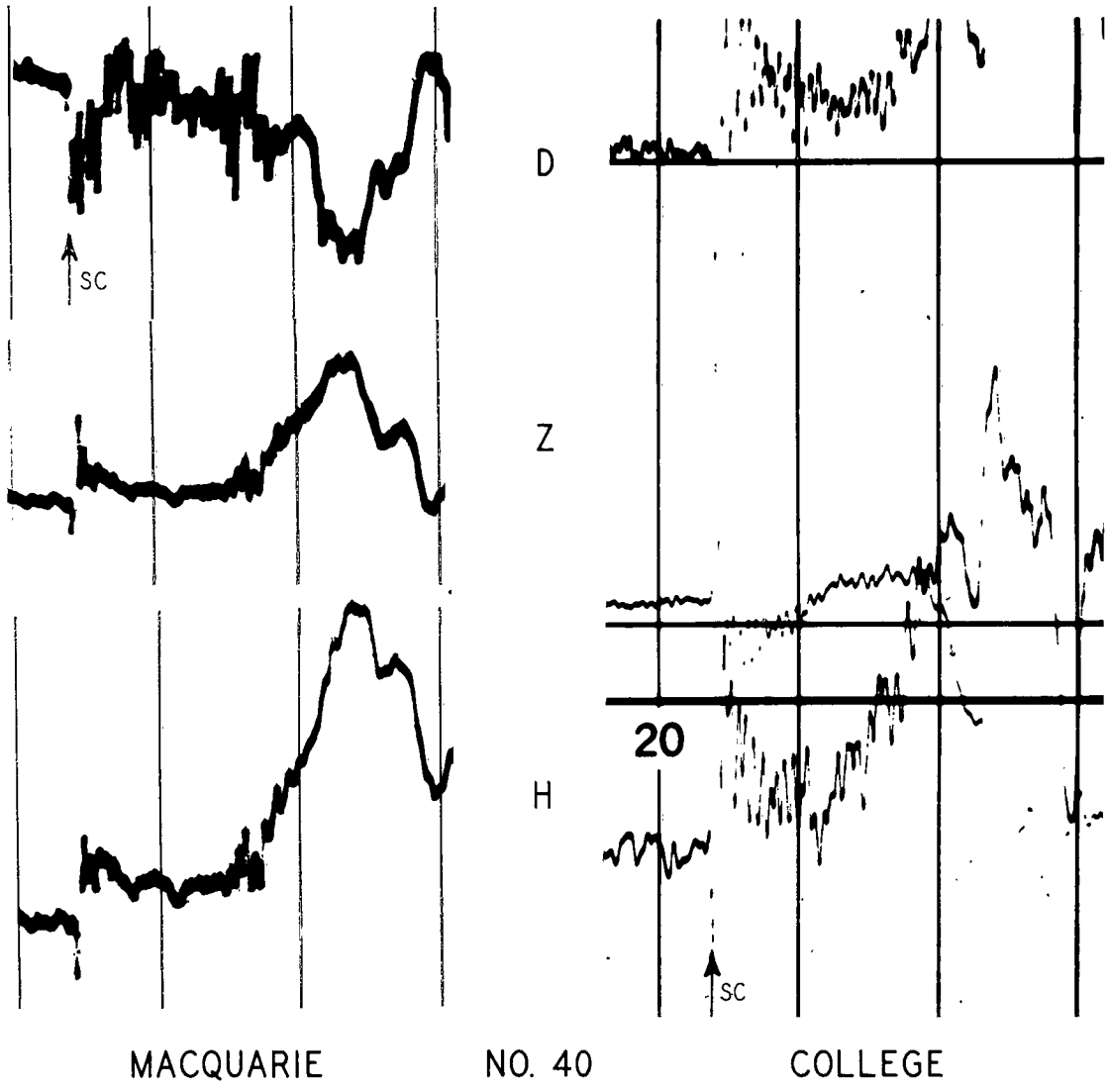

Fig. 4-5. Simultaneous SC oscillation at conjugate stations.

Watanabe (1956) has reported that SC oscillations occur on a world-wide scale. This has been found to be the case for the SC of 0622 U.T. August 17, 1958. In Figure 4-5 normal run magnetograms of this particularly fine example of a SC oscillation are shown for College and Macquarie Island. These two stations are approximately at conjugate points. The condition of the field prior to the SC can again be seen to be oscillatory in Figure 4-5. In five other SC's for which records were available at both College and Macquarie Island, SC oscillations were found to be remarkably similar in these conjugate areas.

The characteristics of the 29 SC oscillations studied for College are given in Table 4-3. The period of the SC oscillation given in column 4 in seconds was determined by a spectrum analysis of the wave form. The number of cycles for which the SC oscillation could be identified is given in column 5. The amplitude in column 6 was measured in gamma from the first positive maxima in H to the following minima in H. In order to compare the amplitude of the oscillation at College to the size of the longitudinal component of the SC, the size of the SC in H at Honolulu is given in gammas in column 7. The polarization of the SC oscillation is given in column 8 where CC is counterclockwise, C is clockwise and IR is irregular. The direction of the first extremum in H, (+ for maximum and - for minimum), and the rise time in seconds to this first extremum are given in columns 10 and 9, respectively. In the last column of Table 4-3, the phase of the oscillation in Z with respect to that in H is indicated.

No systematic relationships were found between local time and any of the following: period, duration, amplitude, rise time and phase of Z with respect to H. The direction of polarization does in general follow the local time rules. The following relationships were found between the local

Table 4-3
College SC Oscillation Data

U.T.	Date	L.T.	Period H sec	Number Cycles Duration	Amplitude H	Amplitude Honolulu H	Polarization Direction	Rise Time in H to Max Sec.	Direction H Extremum	Phase Z with Respect to H
1212	Mar 14'58	0212	370	3	418	26	CC	78	+	in
1300	Sept 4'57	0300	420	15	129	23	CC	185	+	out
1348	Nov 12'60	0348	270	4	51(D)	31	CC	290	-	in
1557	Aug 3'57	0557	172	3	124	23	CC	120	+	out
1628	Apr 6'60	0628	178	5	292	17	CC	120	+	in
1637	Jul 21'58	0637	260	15	241	25	CC	54	+	in
1652	May 31'58	0652	220	3	473	18	CC	115	+	in
1702	Jul 14'60	0702	172	4	215	15	CC	78	+	out
1821	Nov 6'57	0821	260	3	258	36	C	54	-	in
1828	Apr 9'59	0828	340	6	388	20	CC	108	+	out
1859	Jan 13'60	0859	148	17	252	24	CC	30	+	in
1909	Nov 30'60	0909	75	5	60	-	CC	24	+	out
1920	Aug 29'57	0920	110	10	194	6	CC	60	+	in
2027	Feb 17'61	1027	200	5	238	21	CC	60	-	out
2108	Sep 30'61	1108	55	9	374	-	C	24	+	out

Table 4-3 (Con'd)

U.T.	Date	L.T.	Period H sec	Number Cycles Duration	Amplitude H	Amplitude Honolulu H	Polarization Direction	Rise Time in H to Max Sec.	Direction H Extremum	Phase Z with Respect to H
2312	Apr 2'60	1312	220	10	262	26	C	24	-	out
2327	May 11'59	1327	190	7	391	24	C	54	-	out
0016	Sept 29'57	1416	320	2	177	17	C	84	-	out
0042	Jul 5'57	1442	240	4	425	33	C	84	-	out
0046	Feb 22'59	1446	220	3	41	21	CC	66	-	-
0622	Aug 17'58	2022	190	12	522	53	CC	96	-	out
0659	Dec 5'59	2059	350	1	218	22	CC	138	-	out
0718	Jan 10'60	2118	220	2	262	42	CC	108	-	in
0748	Jul 8'58	2148	215	5	561	105	C	72	+	out
0755	Feb 11'59	2155	260	5	177	10	IR	120	-	out
0803	Jul 15'59	2203	220	7	347	58	C	78	+	out
0843	Mar 26'59	2243	540	2	136	24	CC	90	+	out
0930	Sep 16'58	2330	500	2	258	28	CC	240	-	in
0937	Dec 19'57	2337	750	2	173	23	IR	138	+	-

time or direction of polarization and the direction of the first extremum in H: 1) For the group of SC oscillations occurring around 0900 ranging from 0212 to 1446 hours, the direction of the first extremum in H for counterclockwise polarization was positive in 11 out of 14 cases and for clockwise polarization it was negative in 5 out of 6 cases. 2) For the group of SC oscillations occurring around 2200 hours ranging from 2022 to 2337 hours, the situation is reversed, i.e. for CC polarization the first extremum in H is -, and for C polarization it is +).

Watanabe (1956) found that at Onagawa in Japan, the phase relationship between Z and H was constant in that when H was north (+), Z was down (+) and that at stations at other latitudes the effect was reversed. Onagawa station is on the ocean so the Z effect may be due to induction in the ocean. From column 11 of Table 4-3 it can be seen that there is no such consistent behavior between Z and H for SC oscillations at College. Thus for counterclockwise SC oscillations there were 8 cases in which H was north and Z was up, and 6 cases in which Z was down when H was north; while for clockwise SC oscillations, in 5 cases H was north and Z was up, and only in one case Z was down when H was north.

If it is assumed that the SC oscillations are due to waves in which the perturbation is transverse to the propagation direction vector, then from the phase relation between the Z and H components of the waves the plane that contains the propagation vector as well as the azimuthal direction of the incoming wave can be inferred. In Figure 4-6 the relationship between the H and Z perturbations ΔH and ΔZ, is shown for the vertical plane containing the propagation vector and for the horizontal plane. From this figure it can be seen that the azimuthal direction of the incoming wave will

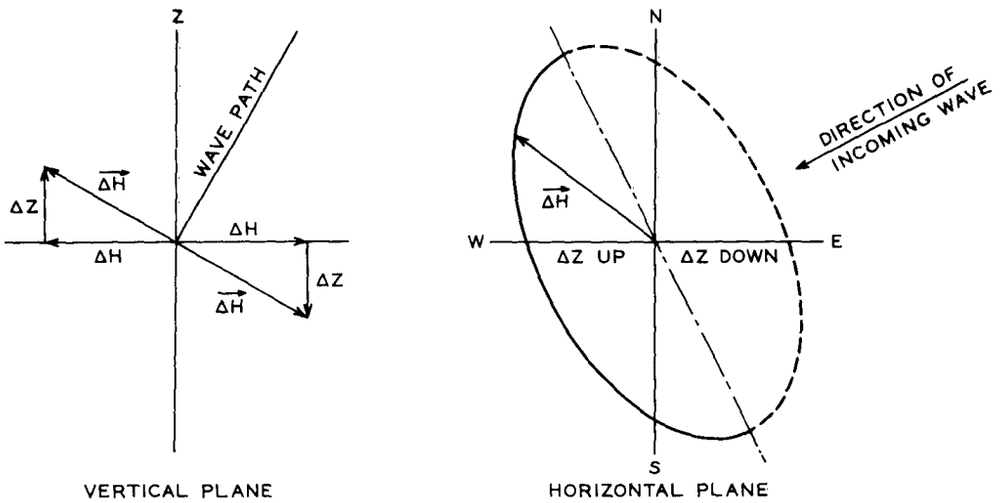

Fig. 4-6. Relation between components of a circularly polarized wave.

be given by the azimuth of the normal to the dot-dash line in the figure that separates the half of the ellipse over which ΔZ is up from that half over which ΔZ is down. In the above discussion it is assumed that there is very little ground reflection as has been found by Dawson and Sugiura (1963) for pearl-type micropulsations; if the ground reflection were complete, ΔZ would be zero.

An analysis of this sort to determine the direction of the incoming SC oscillation wave for the SC of 0622 U.T. August 17, 1958 has been made using data from six stations. At college ΔZ was plotted for this SC oscillation as a function of the azimuth of the total horizontal disturbance vector. The two azimuths at which ΔZ changed from up to down were 180° apart and remained constant for the five cycles of the wave that were plotted. From similar plots at five other stations, the azimuth of the direction of the incoming wave was found to be about 30° west of the sun-earth line. The data are presented in Table 4-4 below.

Table 4-4

Azimuth of Incoming Wave of SC Oscillation 0622 U.T. August 17, 1958
with Respect to Sun-Earth Line
(Azimuth measured westward from the sun-earth line)

Station	L.T.	Azimuth
Little America	1822	50°
College	2022	5°
Big Delta	2022	17°
Sitka	2122	40°
Tucson	2322	30°
Fredericksburg	0122	55°
		average = 33°

The fact that the direction of the incoming wave of this SC oscillation is from the 1000 hour local time meridian, which is thought to be the direction of the incoming solar plasma, is highly significant.

Frequency spectrum analyses for SC oscillations at College and Sitka were made in order to determine whether or not these oscillations have harmonic structure as would be implied if this origin were due to a resonance mechanism in the magnetosphere as was first suggested by Dungy (1954). The details of the frequency spectrum analysis are covered in the Appendix in section II. In Table 4-5 the results of the spectrum analysis are presented for 29 SC oscillations at College and 16 simultaneous SC oscillations at Sitka. The periods for the various harmonics of each SC oscillation listed in Table 4-5 are given in seconds with the relative power per cycle per second for each harmonic component listed under each period in arbitrary units. Examples of the frequency spectra themselves are shown in Figures 4-7 through 4-11. The rapid-run magnetograms of the SC oscillations are reproduced in these figures to show the nature of the oscillations. The analysis of the data in Table 4-5 reveals the following results:

1) The SC oscillations at College and Sitka all show harmonic structure and all have fairly sharp spectra as may be seen in Figures 4-7 through 4-11.

2) Almost 90% of the energy is concentrated in the fundamental period.

3) There are only a few main frequencies (and their harmonics); and their occurrences do not seem to show any systematic relationship to local time. The four sequences of harmonic periods are listed below in Table 4-6 in seconds.

Table 4-5

Frequency Analysis of SC Oscillations at College and Sitka
(period in seconds and relative power per cycle per second)

U.T.	Date	College				Sitka			
0016	Sep. 29'57	320	140	70					
		2.75	0.50	0.40					
0042	Jul. 5'57	240	430	120	50				
		2.1	1.95	0.25	0.25				
0046	Feb. 22'59	220	65	35		220	35		
		2.6	0.20	0.12		1.56	0.15		
0622	Aug. 17'58	190	60			230	540	90	45
		3.0	0.35			2.15	0.9	0.25	0.20
0659	Dec. 5'59	350	110						
		-	0.4						
0718	Jan. 10'60	220	70						
		1.3	0.50						
0748	Jul. 8'58	215	60			340	180	90	
		2.5	0.25			1.8	1.3	0.20	
0755	Feb. 11'59	260	100	55		440	170	75	
		2.0	0.25	0.25		2.05	0.50	0.15	
0803	Jul. 15'59	220	140	70	35	110	320	35	
		0.65	0.40	0.10	0.08	0.36	0.24	0.10	
0843	Mar. 26'59	540	140	70		490	220	140	88
		2.7	0.4	0.15		3.1	0.55	0.3	0.25
0930	Sep. 16'58	500	140						
		-	0.4						
0937	Dec. 19'57	750	350	70					
		2.1	1.05	0.02					
1212	Mar. 14'58	370	220	88		350	220	60	
		0.85	0.15	0.12		0.8	0.75	0.15	
1300	Sep. 4'57	420	220			240	550	45	
		2.1	1.0			2.4	0.25	0.25	
1348	Nov. 12'60	270	90	45		260	90		
		3.5	0.40	0.25		1.7	0.20		
1557	Aug. 3'57	172	44			160	70	35	
		2.95	0.40			1.35	0.38	0.05	
1628	Apr. 6'60	178	56	30		178	55		
		3.05	0.35	0.25		0.75	0.25		

Table 4-5 (Con't)

U.T.	Date	College				Sitka			
1637	Jul. 21'58	260	100	45					
		2.10	0.40	0.25					
1652	May 31'58	220							
		0.75							
1702	Jul. 14'60	172	70	40					
		2.35	0.70	0.40					
1821	Nov. 6'57	260	90	45		150	350		
		3.5	0.8	0.3		2.3	0.45		
1828	Apr. 9'59	340	90			340	140	70	35
		3.5	0.40			3.5	1.05	0.45	0.20
1859	Jan. 13'60	148	640	35					
		3.0	1.25	0.3					
2027	Feb. 17'61	200	110	55	350				
		1.2	0.70	0.25	3.5				
1909	Nov. 30'60	75	110						
		2.1	3.1						
1920	Aug. 29'57	210	350	110	35	220	350	110	37
		0.70	0.65	0.25	0.15	1.4	0.70	0.30	0.15
2108	Sep. 30'61	55	110						
		1.4	2.1						
2312	Apr. 2'60	220	350	70	35	290	90		
		2.25	2.50	0.20	0.24	2.4	0.30		
2327	May 11'59	190	45			170	45		
		2.8	0.35			2.7	0.37		

Table 4-6

Harmonic Sequences of Periods in Seconds for SC Oscillations at College

A	B	C	D
? - 340	1 - 140	1 - 270	1 - 180
1 - 220	2 - 70	3 - 90	3 - 60
2 - 110	4 - 35	6 - 45	6 - 30
4 - 55			

An example of a type C harmonic sequence can be seen in Figure 4-7 for the SC oscillation at College of 1821 U.T. November 6, 1957. The relative power on an arbitrary scale is plotted against period in seconds on a logarithmic scale.

4) The spectra of any particular SC oscillation may begin with any of the periods listed in harmonic sequences A of Table 4-6; however, in the other three sequences the longest period, i.e. 140, 270 or 180, of the particular sequence always occurs as the fundamental period. In sequence A the 220 second period occurs most often as the fundamental; the 340 second period occurs as the fundamental the next most often and the 110 second period occurs the least often as the fundamental. In Figure 4-8 the spectra for three SC oscillations at College are shown together with the oscillations themselves to illustrate how in sequence A, for example, either 340 seconds, 220 seconds or 110 seconds can be the "fundamental" period excited in any particular SC. Thus in the SC of 2027 U.T. February 17, 1961, the period with the most power is 340 seconds and the 220 second harmonic component shows as a bump on the 340 second peak, while the 110 second and 55 second harmonic components are discrete maxima. In the SC of 0046 U.T. February 22, 1959, the "fundamental" period is 220 seconds, whereas 110 seconds is the "fundamental" period for the SC of 2108 U.T. September 30, 1961 at College.

5) In any particular SC oscillation the harmonic components in sequences A and B occur mixed together and so do those in C and D mix together in any one SC oscillation; mixing between A, B and C, D occurs infrequently.

6) The two pairs of spectral sequences A, B and C, D do not always

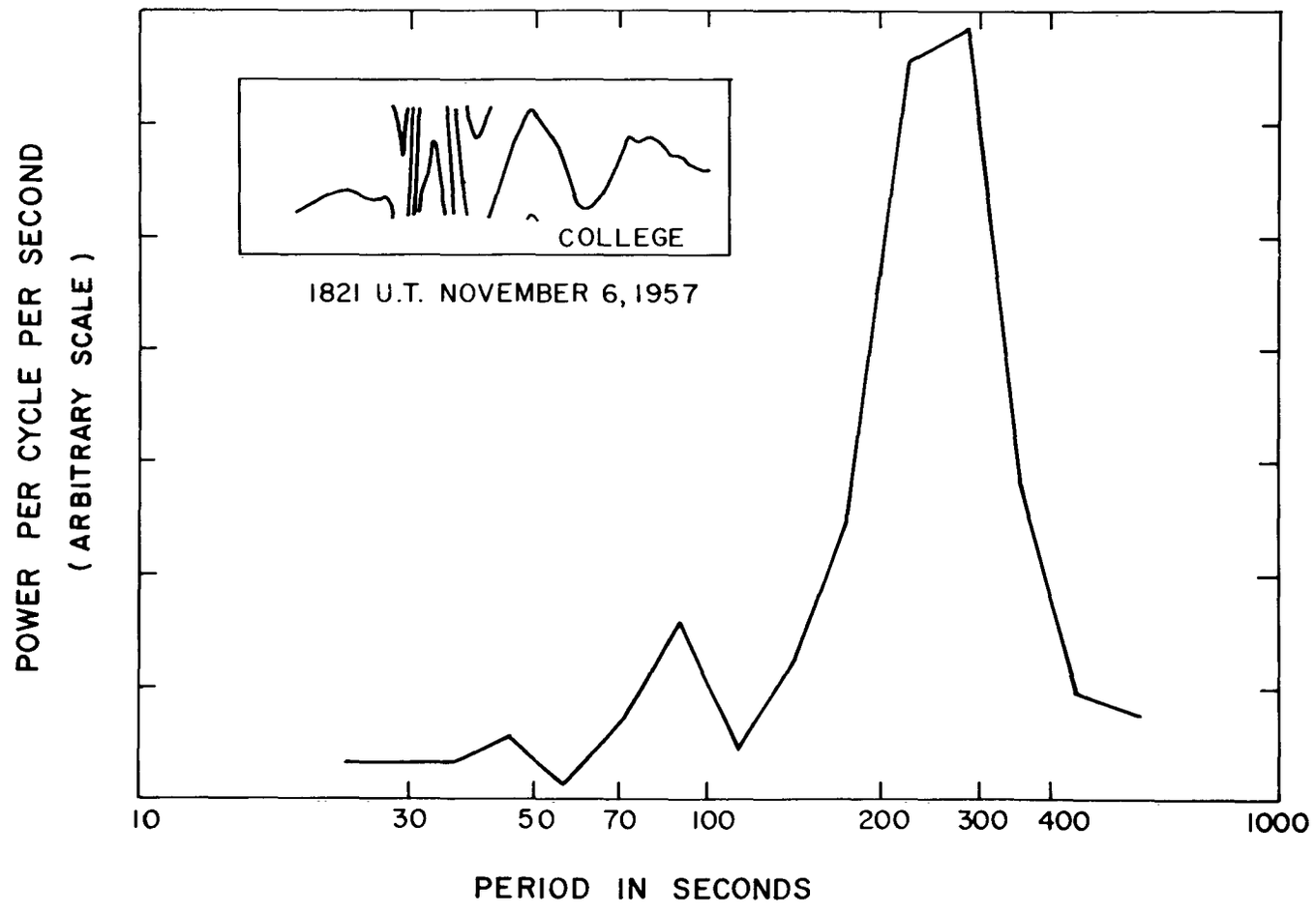

Fig. 4-7 Power spectrum SC oscillation 1821 U.T. November 6, 1957 at College.

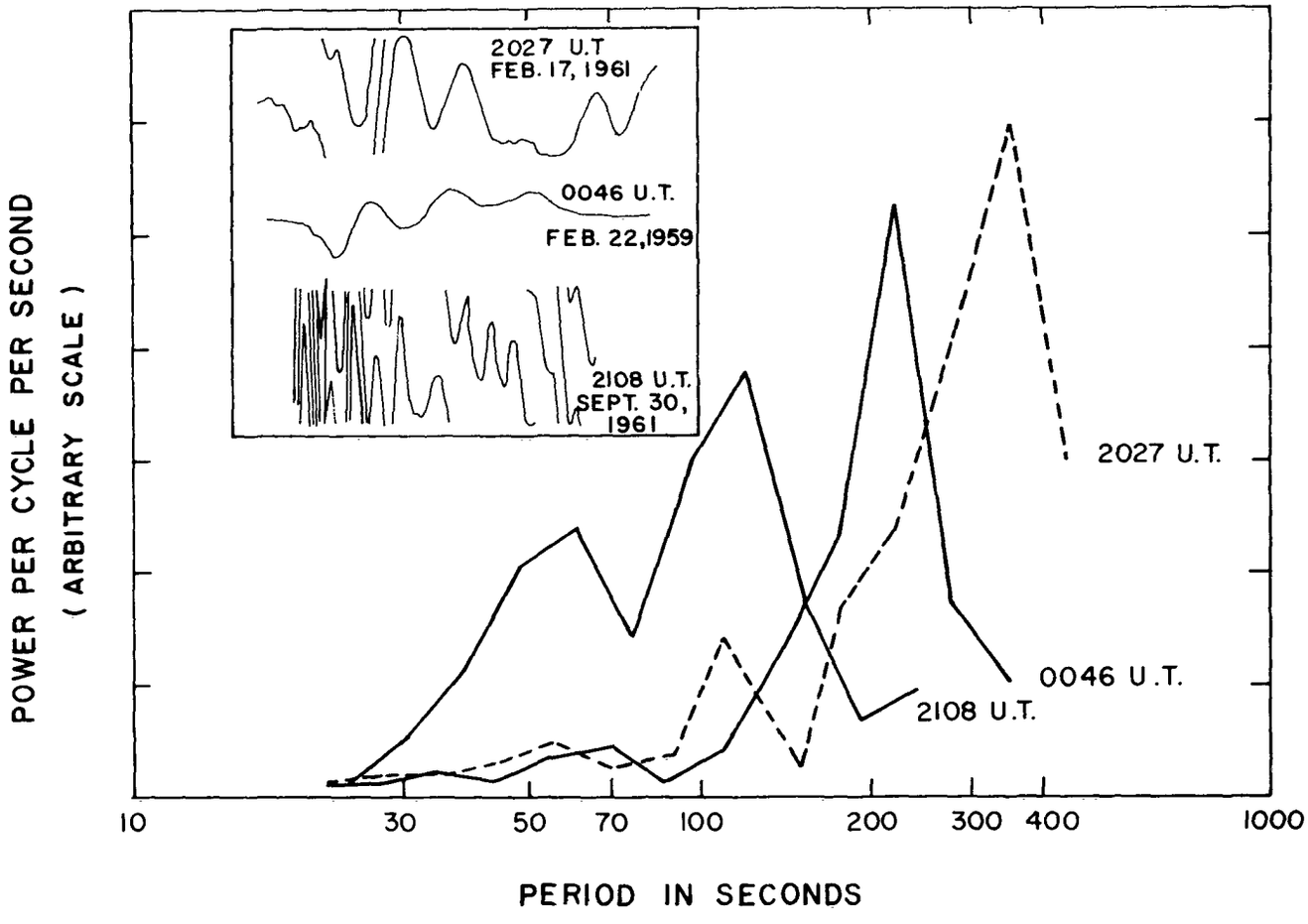

Fig. 4-8 Power spectra SC oscillations of 2027 U.T. Feb. 17, 1961, 0046 U.T. Feb. 22, 1959, 2108 U.T. Sept. 30, 1961.

occur within any definite local time range; however, the C, D sequences seem to occur slightly more frequently around 0300 to 0800 hours local time.

7) There does not seem to be any definite relation between the "fundamental" period (or the type of harmonic sequence) and direction of polarization of the SC oscillation.

As was shown in Table 4-1 the frequency of occurrence of SC oscillation decreases rapidly south of the auroral zone. The same can be said of the amplitude of the SC oscillation as can be seen in Figures 4-9, 4-10 and 4-11. In these figures the harmonic spectra as well as the oscillations for the same SC at both College and Sitka are shown for comparison at the two stations. In all three SC oscillations, the amplitude at College is much greater than the corresponding amplitude at Sitka.

Out of the 16 examples for which simultaneous SC oscillation spectra were made at both College and Sitka, 8 exhibited close agreement of the "fundamental" periods at both stations and 8 did not. There were many SC oscillations for which the fundamental period as well as the harmonic structure of the oscillations agreed for both stations as is illustrated in Figures 4-9 and 4-10. Agreement or disagreement between College and Sitka in the "fundamental" periods and harmonic sequences for simultaneous SC oscillations depends upon the agreement or disagreement of the polarization of the SC oscillation at the two stations. Thus for the 8 SC oscillations for which there was agreement between the spectra at College and Sitka, the polarization for the SC oscillation was the same at the two stations, and for the 8 cases in which there was not agreement the polarizations in 7 out of 8 of these cases were different at the two stations. This state of affairs follows logically, for if the polarizations are not the same for the

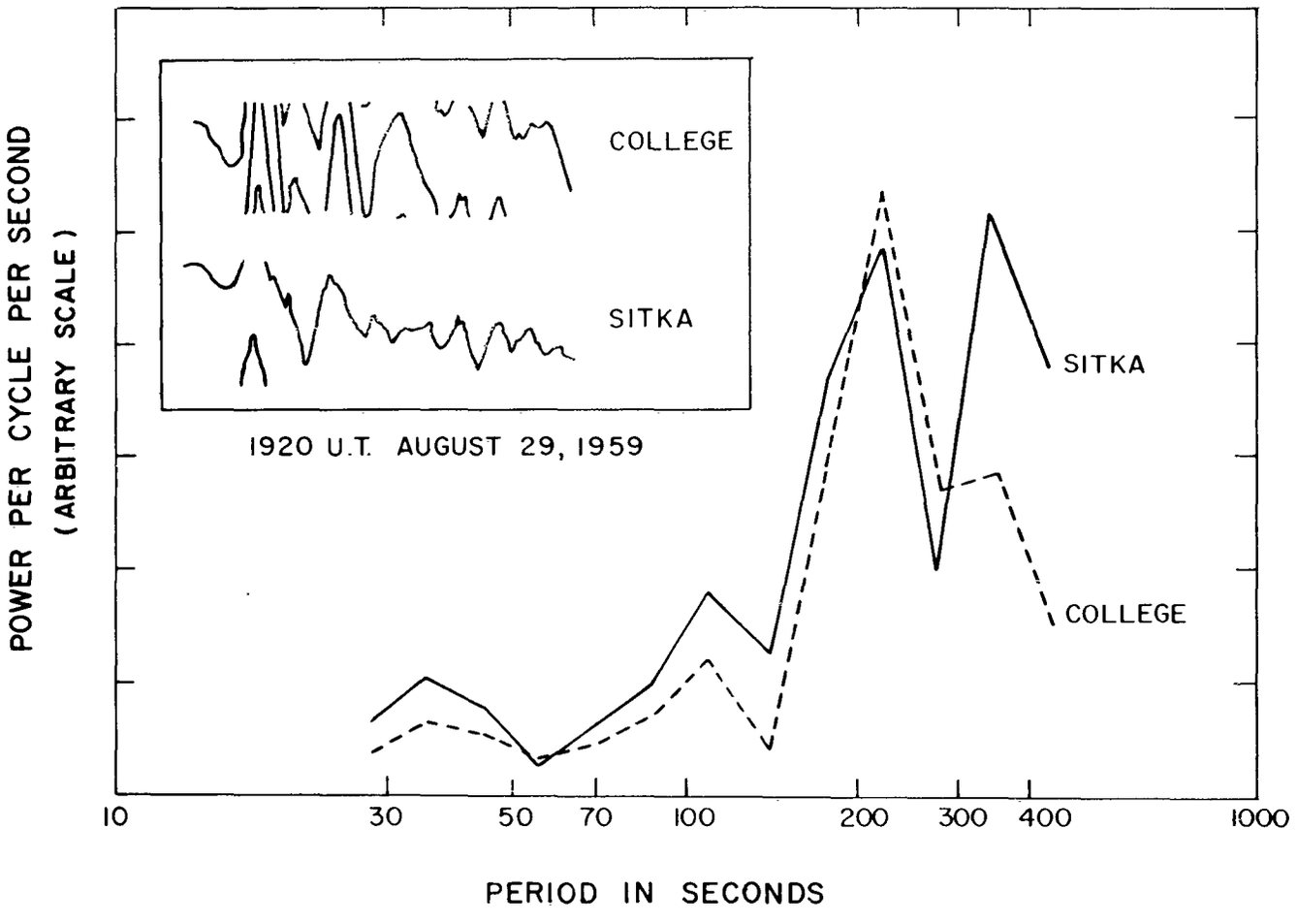

Fig. 4-9 Power spectra SC oscillations of 1920 U.T. Aug. 29, 1959 at College and Sitka.

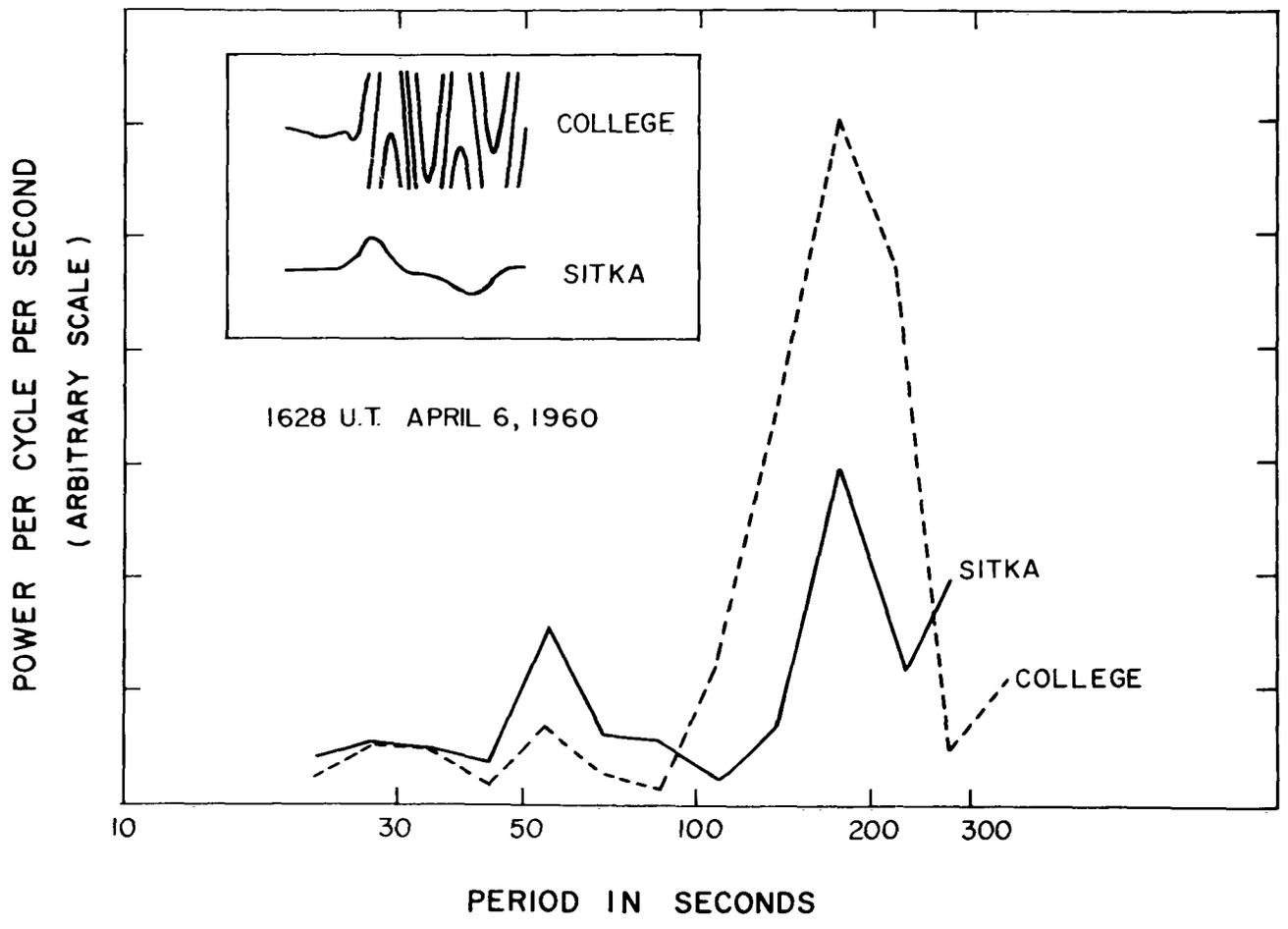

Fig. 4-10 Power spectra SC oscillation of 1628 U.T. April 6, 1960 at College and Sitka.

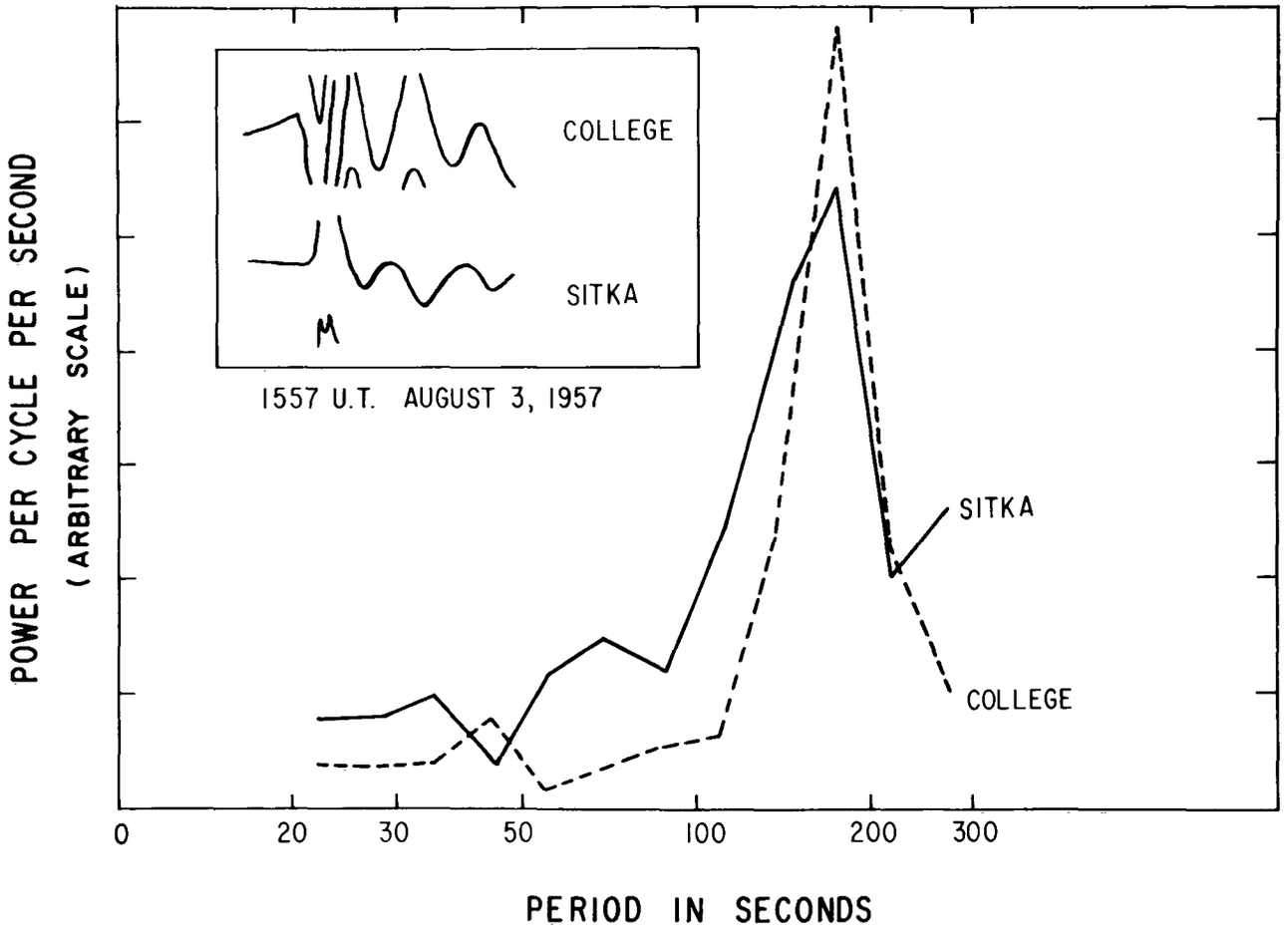

Fig. 4-11 Power spectra of SC oscillation of 1557 U.T. August 3, 1957 at College and Sitka.

SC oscillation at the two stations then the two oscillations would not be due to the same wave and thus would not be expected to exhibit similar frequency spectra.

The results of the spectral analysis of the SC oscillation of 0622 U.T. August 17, 1958 at 8 different stations are shown in Table 4-7. For stations south of the auroral zone there is a tendency for the SC oscillation to show the same period independent of latitude if the direction of polarization is the same. Thus at College $\overline{\Phi} = 64.7^{\circ}$ and at Fredericksburg $\overline{\Phi} = 49.6^{\circ}$ for which the SC oscillation exhibits the same counterclockwise

Table 4-7

Frequency Analysis of SC Oscillation 0622 U.T. August 17, 1958

Station	Component	Period in seconds Relative power per cycle per second				L.T.	Polarization
Point Barrow	H	540 4.0	180 0.80	90 0.25		2022	IR
College	H	188 1.35				2022	CC
	D	200 3.0	60 0.35				
	Z	195 2.5	60 0.30				
Sitka	H	230 2.2	540 0.8	90 0.24	45 0.20	2122	C
Fredericksburg	D	198 1.3	60 0.17	45 0.17		0122	CC
Tucson	D	190 2.1	45 0.25			2322	C
Lovo	Z	185 1.25	108 2.0	300 0.6	30 0.3	0722	-
Reykjavik	Z	340 2.1	140 1.0	90 0.56	45 0.25	0522	-
Byrd	D	550 3.0	340 2.3	70 0.38		2222	CC

polarization, the fundamental period is the same at about 200 seconds. At Sitka where the polarization of this SC oscillation is clockwise, the period is 230 seconds. At the very high latitude stations of Byrd and Point Barrow, the SC spectra have a longer fundamental period of about 550 seconds.

Thus it appears that if the direction of polarization of SC oscillations is the same at two stations then in spite of the fact that they may be widely separated in latitude and local time (as in the case of College and Fredericksburg above) then the period of the SC oscillation can be the same.

In order to relate the observed SC oscillation periods to the resonance excitation of a field line in the magnetosphere, a calculation was carried out as follows. The method for the calculation of the fundamental period of the SC oscillation is the same as that used by Dungey (1955) and Obayashi (1958) for giant pulsations. It is assumed that the distortion of the field line propagates as an Alfvén wave to the earth and is reflected back up along the field line to the opposite hemisphere from whence it is again reflected to produce an oscillation. The length of the field line is assumed to represent one half the fundamental wavelength. This is consistent with the fact that the field line is tied to the earth at each end (nodes) and that the maximum perturbation occurs at the equatorial plane (antinode).

The fundamental period for the oscillation of a field line in the Alfvén is given by four times the integral of ds/v taken from the equatorial plane to the earth or from $\pi/2$ to θ_o, the co-latitude of the station through which the field line passes. The velocity is given by the Alfvén velocity $B_o/\sqrt{4\pi\rho}$ where B_o is the field in gauss and ρ is the

positive ion density in gm/cm^3. The field is taken to be that of an earth centered dipole given by:

$$B_o = \frac{a}{R_e^3} \frac{\sqrt{1+3\cos^2\theta}}{\sin^6\theta} \qquad 4\text{-}1$$

where a is the dipole moment of the earth given by $a = 8.1 \times 10^{25}$ gauss-cm^3; R_e is the geocentric distance to the point where the field line crosses the equatorial plane; and θ is the polar angle from the dipole axis to the point in question on the field line. The line element along the field line is given by:

$$ds = R_e \sin\theta \sqrt{1+3\cos^2\theta}\ d\theta \qquad 4\text{-}2$$

The positive ion density ρ in the expression for the Alfvén velocity was determined from the gyrofrequency model given by Smith (1961) for the magnetosphere from an analysis of nose whistler data. The average value of the proton mass density in gm/cm^3 is thus:

$$\rho = 1.2 \times 10^{-2} \frac{B_o e m_i}{2\pi C m_e} \qquad 4\text{-}3$$

where $e = 1.60 \times 10^{-20}$ e.m.u.; $m_i = 1.67 \times 10^{-24}$ gm; $m_e = 9.1 \times 10^{-28}$ gm; $c = 3 \times 10^{10}$ cm/sec and B_o is given by equation 4-1. Combining equations 4-1, 4-2 and 4-3 with the Alfvén velocity expression in the time integral, the period of the fundamental field line oscillation in seconds is given by:

$$T = 37.28 \times 10^{-23} (R_e)^{5/2} \int_{\pi/2}^{\theta_o} \sin^4\theta\ (1+3\cos^2\theta)^{\frac{1}{4}}\, d\theta \qquad 4\text{-}4$$

The above integral was evaluated by numerical integration and the values of R_e in cm were taken from Chapman and Sugiura (1956).

The period in seconds for the SC oscillation fundamental mode is plotted in Figure 4-12 as a function of geomagnetic latitude. There is a seasonal variation in the ion density in the magnetosphere, Smith (1961), such that the ion density is greater in December than in June by a factor of two. This produces a seasonal variation in the calculated period as is shown in Figure 4-12 by vertical lines at every 5° of Φ.

The results of the above calculation agree with those of MacDonald (1961) for his vorticity mode for the high density model of the magnetosphere in which, for $\Phi = 60°$, MacDonald finds a period for the fundamental mode, $n = 1$, of 74.4 seconds whereas the present calculation gives 78 seconds.

Data for the period of the fundamental mode of SC oscillations at College ($\Phi = 64.7°$), Point Barrow ($\Phi = 68.6°$) and Byrd ($\Phi = 70.6°$) are plotted in Figure 4-12 for comparison of the observations with the calculations of T from the above model.

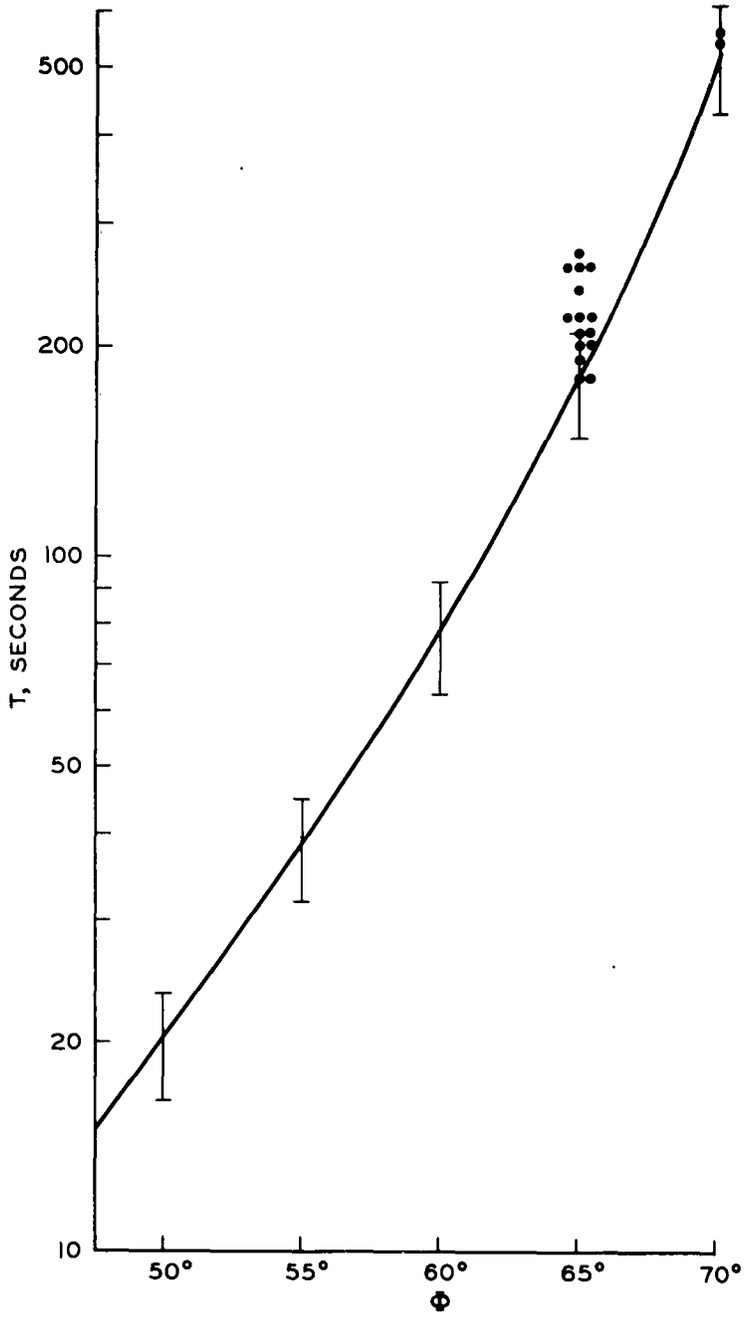

Fig. 4-12. Fundamental resonance period T as a function of geomagnetic latitude Φ.

CHAPTER V

Sudden Commencement Vector Diagrams

It is not certain whether the SC hydromagnetic perturbation propagates through the magnetosphere in a single coupled mode or in separate transverse and longitudinal modes. However, the magnetic perturbation of an SC observed at a station may be described as the sum of transverse and longitudinal components. In the following discussion the transverse component will be understood to mean the circularly polarized perturbation that is perpendicular to the magnetic field line; whereas the longitudinal component will refer to the perturbation parallel to the field line.

The projection on to the earth's surface of the longitudinal component of the SC perturbation can be represented by a time dependent vector $\underset{\sim}{\Delta H}_L$ that is always parallel to the local magnetic meridian. The projection of the transverse component on the earth's surface is similarly described by a vector $\underset{\sim}{\Delta H}_T$ whose amplitude and direction both depend on time. Thus the magnitude and direction of the total horizontal disturbance vector $\underset{\sim}{\Delta H}$, (where $\underset{\sim}{\Delta H} = \underset{\sim}{\Delta H}_T + \underset{\sim}{\Delta H}_L$) will depend on time in a complicated way. $\underset{\sim}{\Delta H}$ will be a function of the amplitude, period and initial phase of $\underset{\sim}{\Delta H}_T$ and $\underset{\sim}{\Delta H}_L$.

If the vector $\underset{\sim}{\Delta H}$ is resolved into its geomagnetic north and east components, $\Delta X'$ and $\Delta Y'$ respectively, then the shape of the vector diagram can be represented by the following functions:

$$\Delta X' = g(t) + h(t) \sin (\pm \omega t + \psi_o) \qquad 5\text{-}1$$

$$\Delta Y' = h(t) \cos (\pm \omega t + \psi_o) \qquad 5\text{-}2$$

where $g(t)$ and $h(t)$ give the amplitudes of the longitudinal and transverse components respectively, ω is the angular frequency of the circularly

polarized wave, and ψ_o is its initial phase. Positive ω or negative corresponds to counterclockwise or clockwise polarization respectively. In an attempt to understand the complexities of the vector diagrams shown in Figures 3-2 to 3-5, three different models for g(t) and h(t) have been chosen in order to construct the vector diagrams shown in Figures 5-1, 5-2 and 5-3.

In the first model, called model I in Figure 5-1, the amplitudes of both components were assumed to increase from zero linearly with time, with the same rise time, to a maximum A for the longitudinal component and to a maximum B for the transverse component. The period of the circularly polarized component was taken to be equal to the rise time of the amplitudes for this first model. To show the effect of the change in magnitude of longitudinal component on vector diagrams three different ratios of the maximum amplitudes of the two components were chosen. In Figure 5-1, for four different directions of the initial phase of the transverse component (i.e. E, N, W, S) three sets of vector diagrams are given for B = A, 2B = A and B = 2A. To the left of each diagram the projection of the vector diagram on the X' axis is given as a function of time to show how H would vary for an SC having a perturbation that would produce the vector diagram as shown.

To show the effect of a fast rise time in the transverse component h(t) was taken in model II to reach its constant maximum value of B in one quarter of the rise time of g(t). In both models II and III g(t) was taken to be given by $\frac{B}{2}\ (1 + \sin \frac{2\pi t}{T})$ where the argument goes from $-\pi/2$ to $\pi/2$ and T is the period of rotation of the transverse component. In Figure 5-2 the vector diagrams for model II in which the final amplitudes of the longitudinal and transverse components are the same are shown for four different initial phases of $\Delta \underset{\sim}{H}_T$.

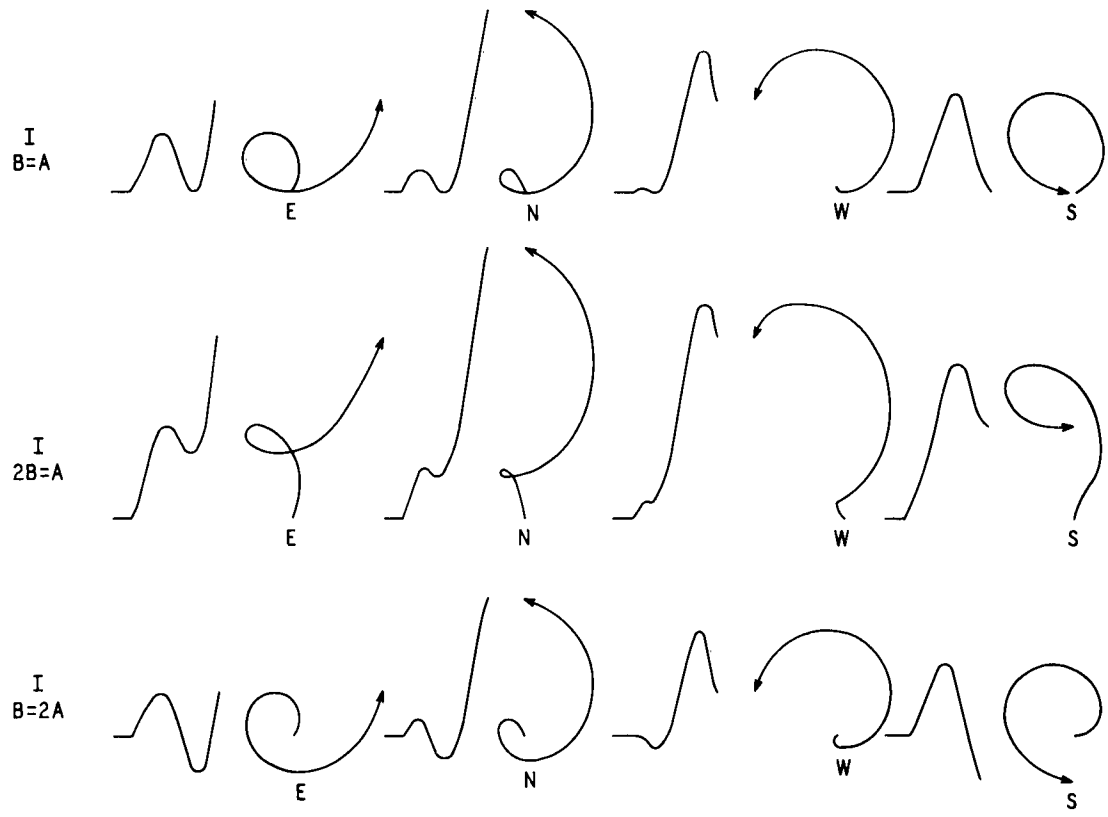

Fig. 5-1. Model I synthesized SC vector diagrams; counterclockwise.

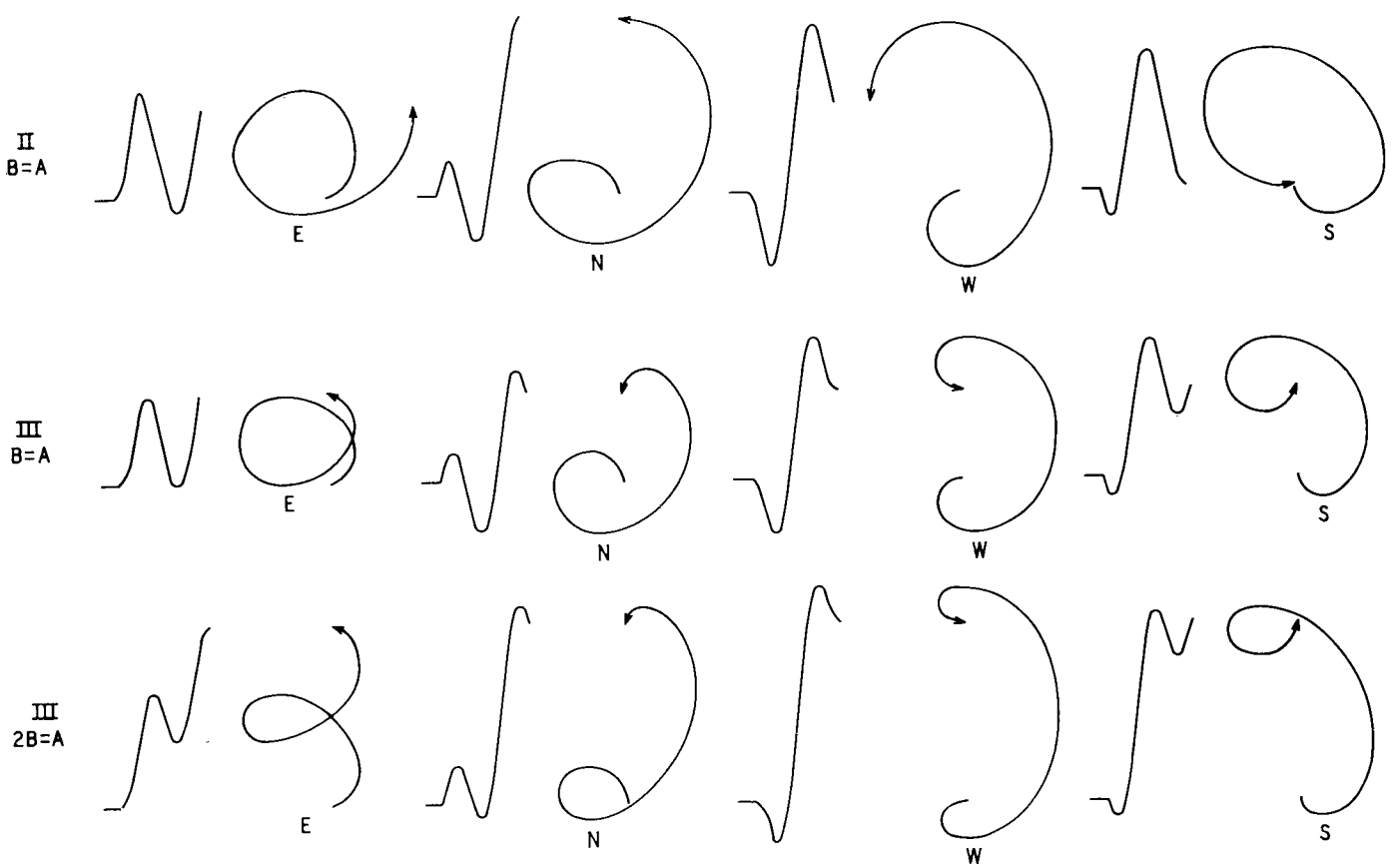

Fig. 5-2. Model II and III synthesized SC vector diagrams; counterclockwise.

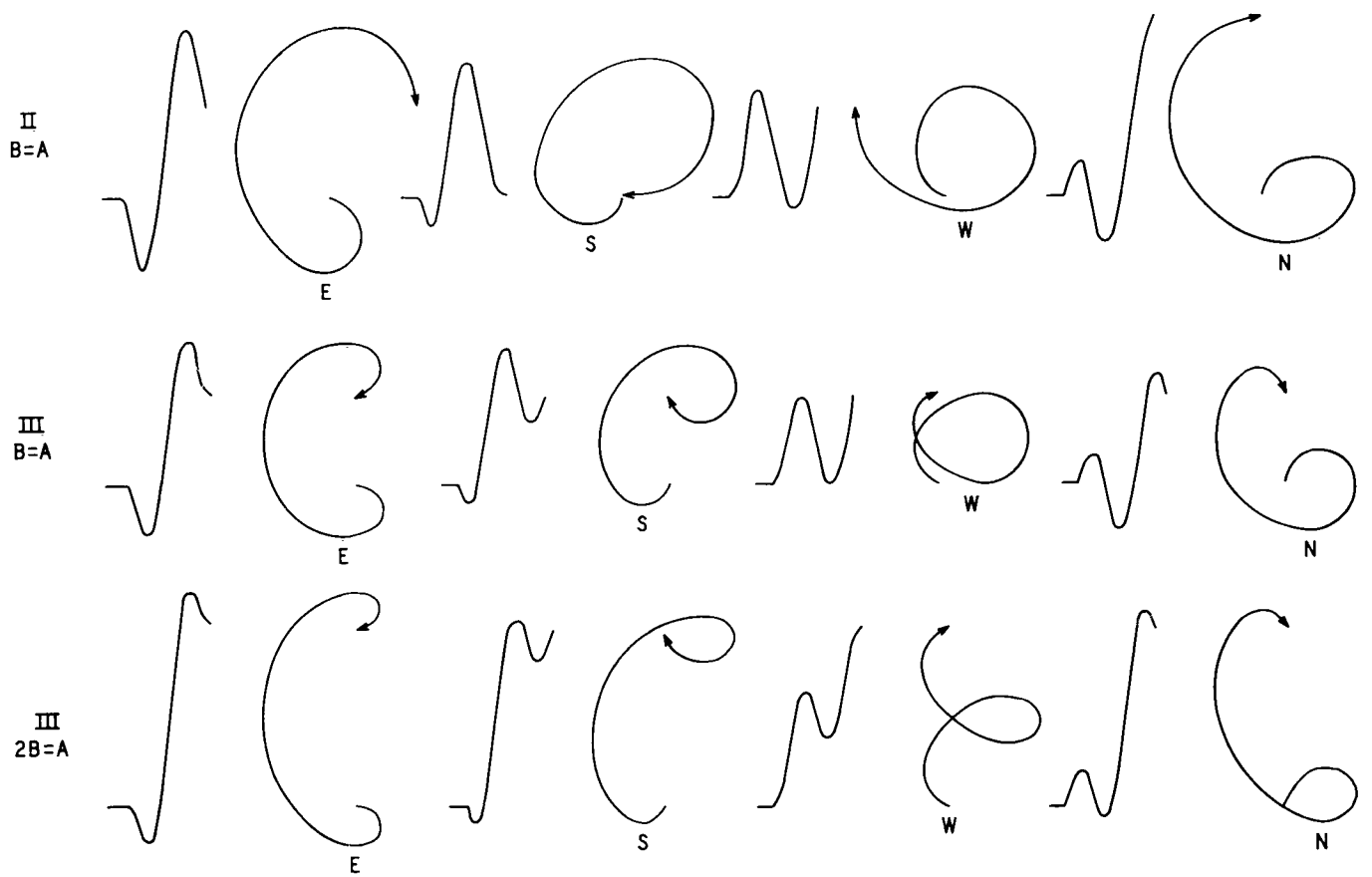

Fig. 5-3. Model II and III synthesized SC vector diagrams; clockwise.

In model III vector diagrams were constructed for the case in which $h(t)$ is given by $h(t) = B \sin \frac{\pi t}{T}$, where the argument goes from 0 to π. Thus in this third model the transverse component reaches its maximum value of B when the longitudinal component is only half its maximum value and the transverse component will have decayed to zero when the longitudinal component is a maximum. In Figure 5-2 vector diagrams for the third model are given for $B = A$ and $2B = A$ for four initial phase values of the circularly polarized component.

The synthesized vector diagrams in Figures 5-1 and 5-2 are for a counterclockwise rotation of the circularly polarized transverse component of the SC perturbation. The corresponding vector diagrams for models II and III are given in Figure 5-3 for the case of clockwise polarization. When the initial phase of ΔH_T is north or south the pairs of vector diagrams for clockwise or counterclockwise polarization are reflections of each other about the X' axis. However, the vector diagrams for clockwise polarization for east and west initial phases are reflections about the X' axis of the counterclockwise vector diagrams for west and east respectively as can be seen by a comparison of Figures 5-2 and 5-3.

From the 24 diagrams in Figures 5-1, 5-2 and 5-3, it can be seen that the resultant shape of the vector diagram depends much less on the function $h(t)$ assumed for the variation of the amplitude of the transverse component than it does on the initial phase of this component and on the ratio, B/A, of the maximum amplitudes of the two components. The variations in shape of the vector diagrams of the SC's shown in Figures 3-2 to 3-15 can be explained for a given latitude in terms of the change in the initial phase of the transverse wave as a function of local time, and for a given local time in terms of the change in the ratio of the amplitudes of the

longitudinal and transverse waves as a function of latitude. These features are discussed in the end of this chapter in more detail.

In order to show the correspondence between the synthesized vector diagrams and the observed ones, 18 vector diagrams are presented in Figure 5-4 and 5-5. The approximate correspondence between the shape of the SC vector diagrams in Figures 5-4 and 5-5 and the synthesized vector diagrams in Figures 5-1, 5-2 and 5-3 is given in Table 5-1. Although the correspondence between the forms is not exact, the general agreement in the shape of the pairs of vector diagrams is further evidence that the SC field can be described in terms of the resultant of a circularly polarized transverse wave and a longitudinal wave.

Because of the great changes which take place in the shape of the vector diagram with changes in the initial phase of the circularly polarized component for even the simple model of the synthesis of the vector diagram that was given above, it is important to try and see how the initial phase will vary over the earth for the model that was proposed. This can be done for the 0 wave to give a pattern of the initial phase vector for the morning hemisphere (2200 to 1000 hours) that agrees with the observed initial phase of SC's at College, Sitka and Fredericksburg for SC's which are clearly circularly polarized.

The initial phase for the E wave over the evening hemisphere (1000 to 2200 hours) is more difficult to describe. In the case of the 0 wave the energy is propagated along the field line and thus the 0 wave is circularly polarized along its entire path from the equatorial plane to the earth's surface. According to Piddington (1955) the E wave propagates not only along the field line but in all directions from the source. The polarization of the E wave varies from being plane to circular in a manner that depends

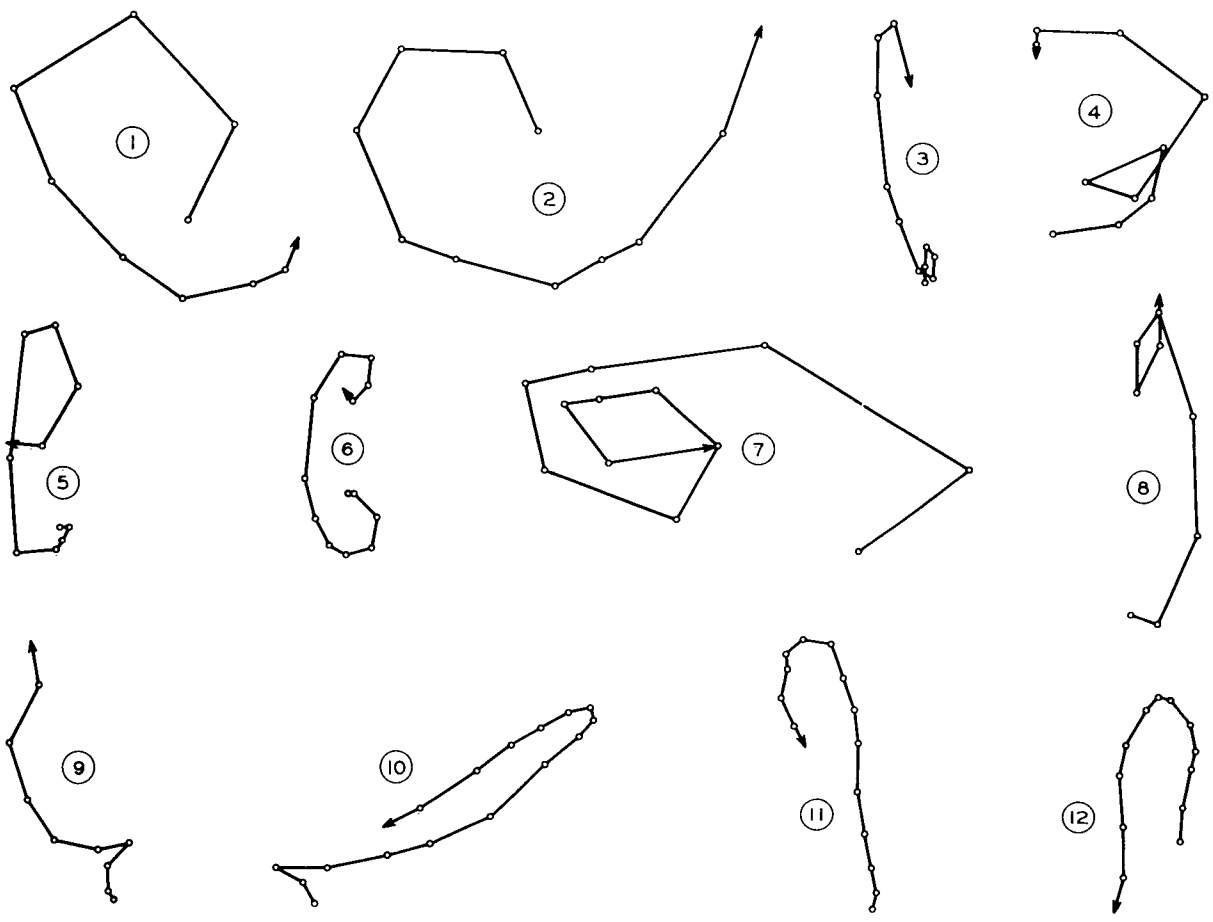

Fig. 5-4. SC vector diagrams; numbers refer to Table 5-1.

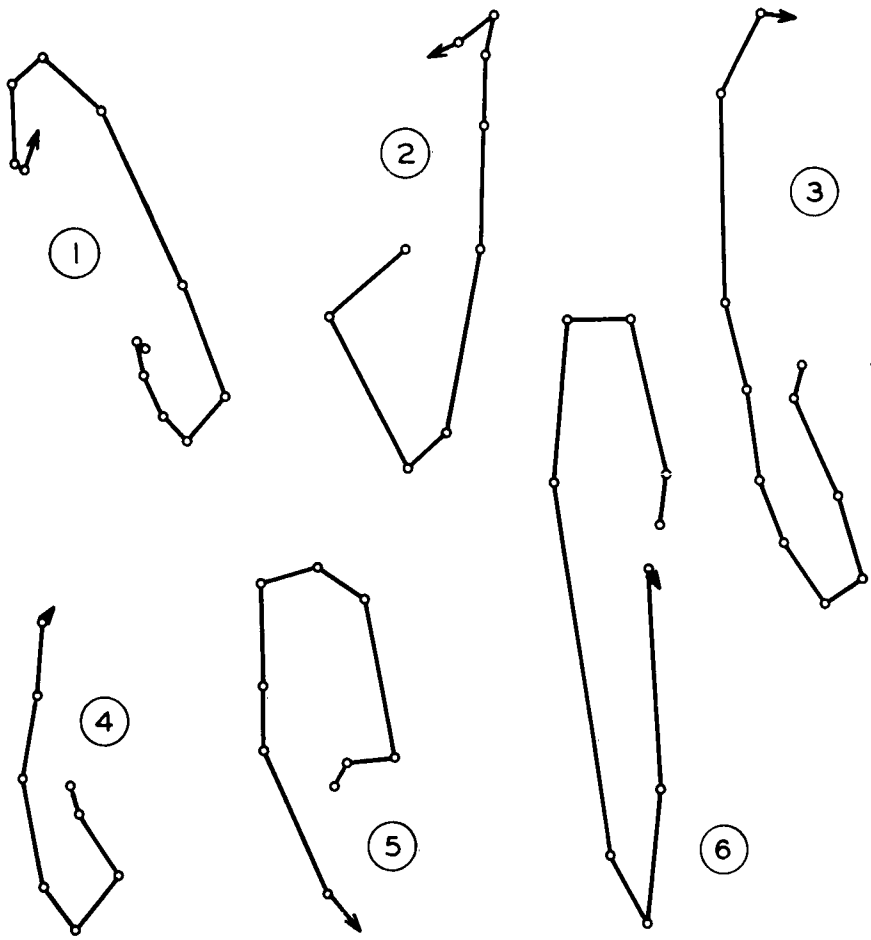

Fig. 5-5. SC vector diagrams; number refer to Table 5-1.

Table 5-1

Correspondence Between the SC Vector Diagrams in Figures 5-4 and 5-5 and the Synthesized Vector Diagrams in Figures 5-1, 5-2 and 5-3

No.	L.T.	Date	Station	Corresponding Synthesized Vector Diagram
			Figure 5-4	
1	0802	July 14, '60	Sitka	5-2, II, B = A, E
2	0950	Jan. 25, '58	Reykjavik	5-1, I, B = 2A, E
3	1439	June 29, '60	Fredericksburg	5-3, III, 2B = A, N
4	0943	Sept. 3, '58	Murchison Bay	5-2, III, 2B = A, E
5	1903	Aug. 16, '59	Sitka	5-3, III, 2B = A, E
6	1715	Oct. 22, '58	Healy	5-3, III, 2B = A, E
7	0315	Oct. 22, '58	Eskdalemuir	5-2, III, B = A, S
8	2248	July 8, '58	Sitka	5-2, III, 2B = A, S
9	1545	June 27, '60	Point Barrow	5-1, I, 2B = A, N (reflected)
10	0250	Jan. 25, '58	Byrd	5-1, I, 2B = A, W
11	0135	Apr. 23, '59	Sitka	5-1, I, 2B = A, S
12	2243	Sept. 3, '58	College	5-1, I, 2B = A, S
			Figure 5-5	
1	1027	Feb. 17, '61	College	5-2, III, 2B = A, W
2	1448	June 25, '57	College	5-2, III, B = A, W
3	1947	July 14, '60	Sitka	5-3, III, 2B = A, S
4	1730	Sept. 4, '60	Sitka	5-3, III, 2B = A, S
5	0928	June 14, '58	Sitka	5-2, II, B = A, N
6	0909	Nov. 30, '60	College	5-2, II, B = A, N

on the frequency of the wave as the angle between the propagation vector and the magnetic field changes from 90° to 0. The E wave disturbance changes its degree of polarization as it propagates directly in from the distorted field across the magnetic field line to the earth's surface. This produces a complicated change in the phase of the perturbation at the earth that makes the problem of the initial phase of the circularly polarized component of the E wave in the evening hemisphere difficult to solve even for our simple model.

The pattern of the initial phase of the 0 wave can be described in terms of the variation over the earth of the angle ψ, measured east of north, between the perturbation vector $\underset{\sim}{b}'$ and the north direction.* The distortion of the line of force for the frozen-in field by the pressure of the enhanced solar wind is shown schematically in Figure 5-6 for the field line in the 0800 hour meridian. The vectors $\underset{\sim}{B}_o$, $\underset{\sim}{b}$, and $\underset{\sim}{B}$ represent the undisturbed field, the perturbation causing the distortion of the line, and the distorted field line respectively. It is assumed that $\underset{\sim}{b}$ is initially directed toward the solar wind and thereafter rotates in a clockwise direction as seen along the direction opposite to $\underset{\sim}{B}_o$. However, the subsequent rotation of $\underset{\sim}{b}$ does not concern us here because it is the initial phase or direction of $\underset{\sim}{b}$ that we are concerned with.

To describe the propagation of $\underset{\sim}{b}$ along the field line to the earth an orthogonal right-handed XYZ coordinate system is chosen such that Z is in the direction of $\underset{\sim}{B}_o$ (and is thus always parallel to the field line) and Y is normal to the meridian plane of the undisturbed dipole field line. In Figure 5-7 the initial perturbation vector $\underset{\sim}{b}$ is shown in the equatorial

---

*The angle ψ here is not to be mistaken as the declination of the geomagnetic meridian used in equations 3-1 and 3-2 in Chapter III.

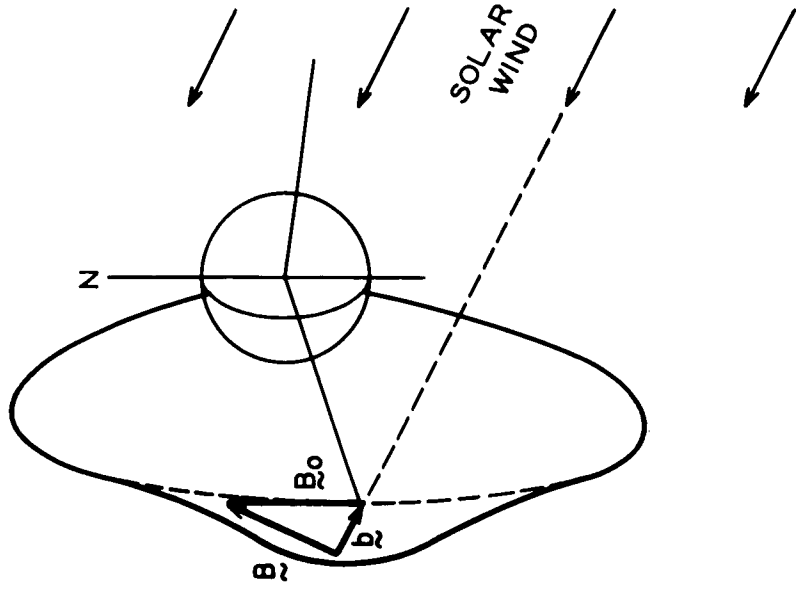

Fig. 5-6. Distortion of an earth field line by the solar wind.

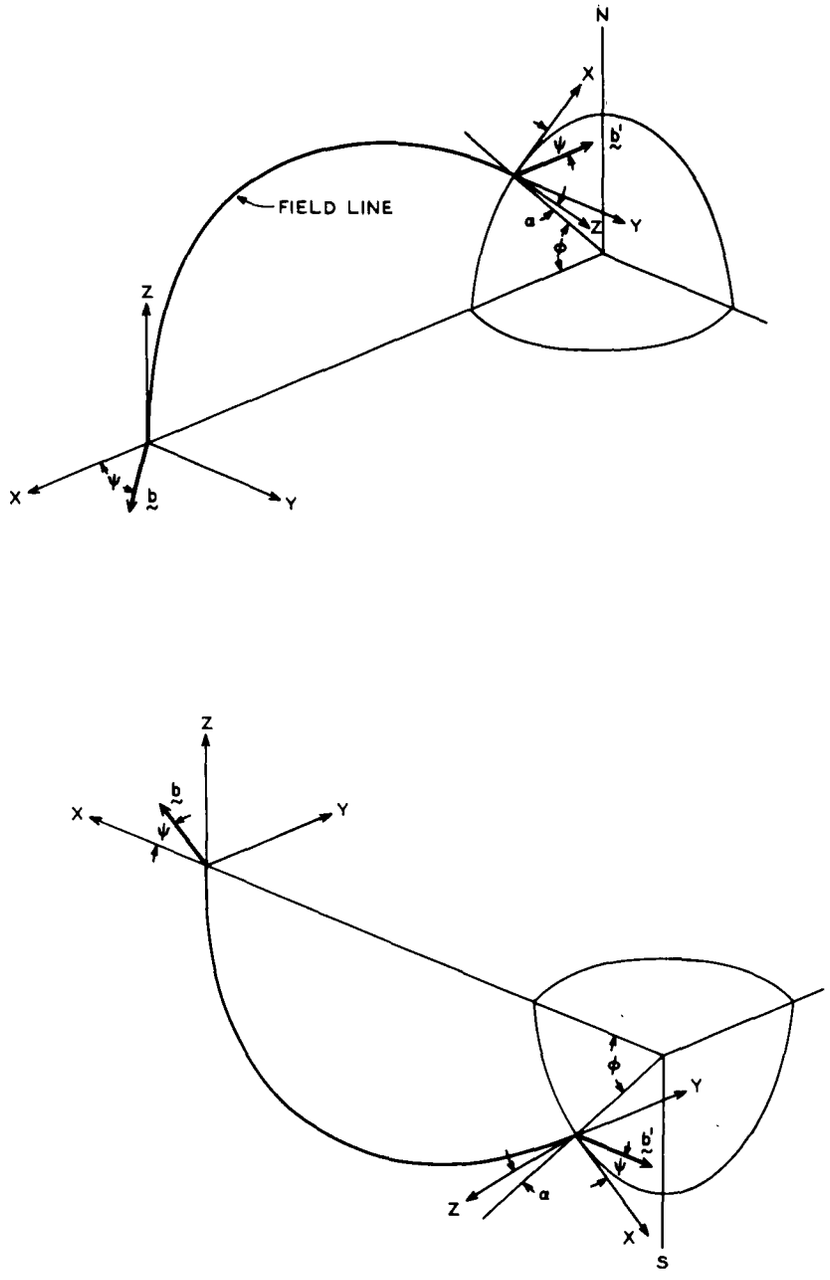

Fig. 5-7. Propagation of perturbation $\underset{\sim}{b}$ to northern and southern hemispheres.

plane where it makes an angle ψ with the X axis and lies in the XY plane. The angle ψ gives the direction of the solar wind with respect to the plane of the field line.

The distortion of the field line produces a pair of O waves which propagate in opposite directions from the equatorial plane along the field line to the northern and southern hemispheres. The propagation of the initial phase of these two oppositely directed O waves is shown in Figure 5-7 to the northern and southern hemispheres respectively. The orientation of the initial perturbation vector $\underset{\sim}{b}'$ at the earth as the result of the propagation along the field line of $\underset{\sim}{b}$ from the equatorial plane can be found as follows.

Consider a monochromatic elliptically polarized plane wave of angular frequency ω propagating in the Z direction. This wave can be represented by two plane polarized waves in the X and Y planes as follows:

$$\underset{\sim}{b} = \underset{\sim}{b}_x + \underset{\sim}{b}_y \qquad 5\text{-}3$$

$$\underset{\sim}{b}_x = \text{Real} \left\{ \underset{\sim}{b}_{xo} e^{i(\omega t - kz)} \right\} \qquad 5\text{-}4$$

$$\underset{\sim}{b}_y = \text{Real} \left\{ \underset{\sim}{b}_{yo} e^{i(\omega t - kz)} \right\} \qquad 5\text{-}5$$

Because the propagation vector $\underset{\sim}{k}$ is along the direction of the magnetic field in the case of the O wave the polarization constant R from equation 2-13 becomes $R = b_{yo}/b_{xo} = i$ and thus equations 5-4 and 5-5 become:

$$b_x = b_{xo} \cos(\omega t - kz) \qquad 5\text{-}6$$

$$b_y = -b_{xo} \sin(\omega t - kz) \qquad 5\text{-}7$$

These equations show that the O wave is circularly polarized and that, for a given Z, the sense of rotation of the perturbation vector $\underset{\sim}{b}$ is counter-clockwise when viewed along the direction of the field.

If the XYZ coordinate system in Figure 5-7 moves along the field line with the phase velocity of the wave, then the vector $\underset{\sim}{b}$ in this moving coordinate system has constant phase, $(\omega t - kz)$, and thus b_x and b_y, the components of $\underset{\sim}{b}$, do not change. Thus the orientation of $\underset{\sim}{b}$ does not change, for a constant phase as it propagates from the equatorial plane to the earth's surface. If we choose this constant phase as the initial phase of the perturbation vector $\underset{\sim}{b}$ when the solar wind first distorts the field line at the equatorial plane, then we see from the above considerations that the initial phase of the circularly polarized O wave propagates to the earth without any rotation in the XYZ field line coordinate system. However, because the field line orientation itself changes along the line, the initial phase of $\underset{\sim}{b}$ changes to the orientation shown by $\underset{\sim}{b}'$ in Figure 5-7. From the rotation of the XYZ coordinate system the pattern of $\underset{\sim}{b}'$ as a function of local time can be found if it is assumed that the initial perturbations produced by the solar wind on each field line are all parallel and are directed toward the solar wind. Thus the initial phase of the circularly polarized O wave component of sudden commencements is represented in Figure 5-8 by $\underset{\sim}{b}'$ over the morning hemisphere for a given latitude. Because the field line is not radial, but makes an angle α with the radial direction, the XY plane is not horizontal. The projection of $\underset{\sim}{b}'$ from the XY plane on to the horizontal plane changes the angle ψ to ψ' such that $\tan \psi' = \tan \psi \sec \alpha$. However, this effect is small for high latitudes and its neglect is consistent with the other approximations of the model.

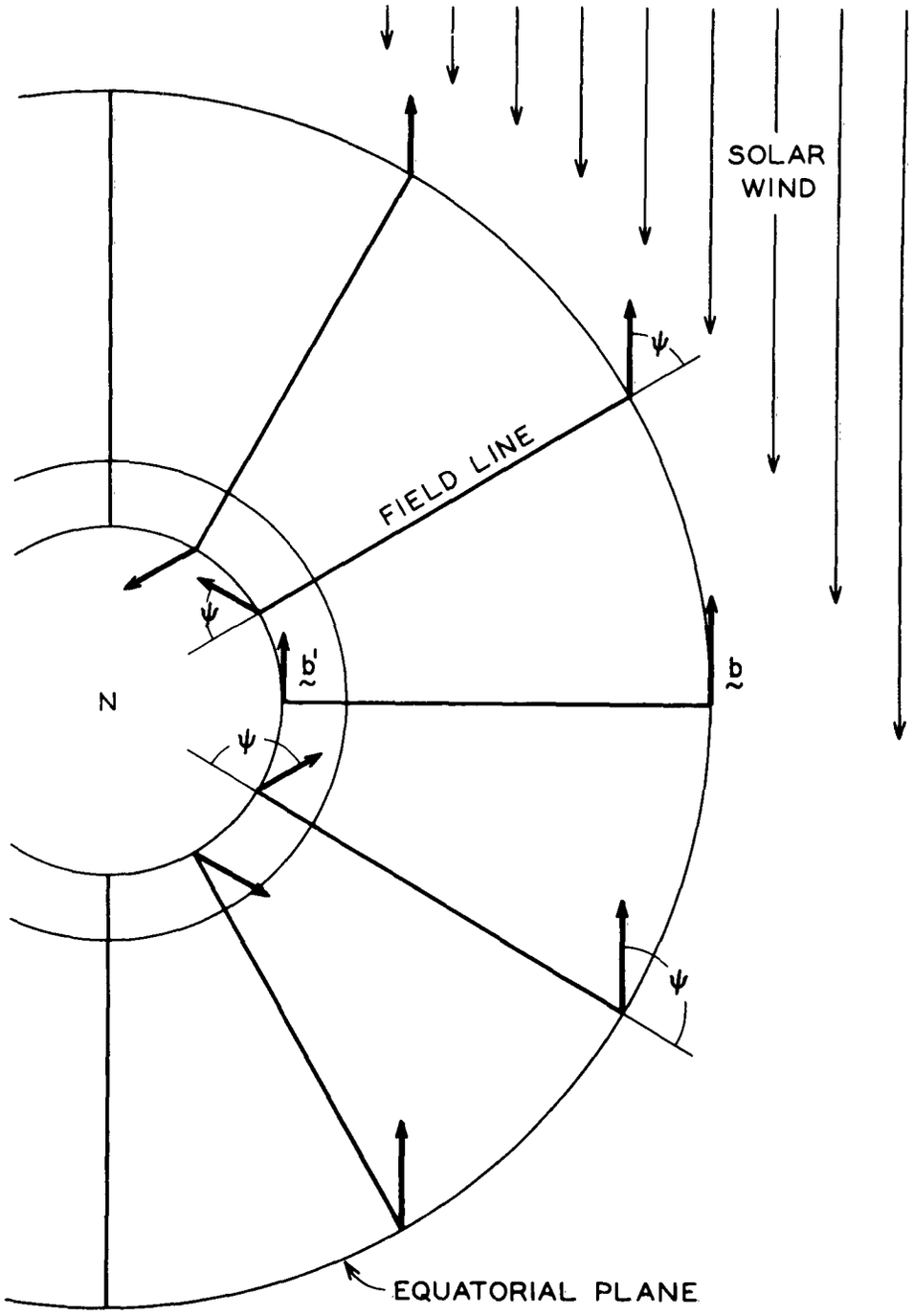

Fig. 5-8. Initial phase of polarized component $\underset{\sim}{b}'$ over northern hemisphere.

The orientation of $\underset{\sim}{b}'$ in the southern hemisphere relative to that of $\underset{\sim}{b}'$ in the northern hemisphere can be found by a reflection of $\underset{\sim}{b}'$ about the Y axis in the XY plane as can be seen from Figure 5-7.

Although the field lines are not twisted in the meridian plane through 1000 and 2200 hours, a continuation of the pattern of $\underset{\sim}{b}'$ to this plane shows that as the local time increases from 2200 to 1000 hours the initial phase of the polarized component of the sudden commencement rotates from south to east to north in the northern hemisphere and from north to east to south in the southern hemisphere. This effect can be seen for the 0 wave in Figure 5-9 in which the angle ψ measured east of north for the phase of the horizontal perturbation vector $\underset{\sim}{\Delta H}$ at 30 seconds after the beginning of the SC is plotted as a function of local time of the SC for College, Sitka and Fredericksburg.

The above discussion has referred specifically to the phase of $\underset{\sim}{b}'$, the circularly polarized transverse wave. The initial phase given in Figure 5-9 is the initial phase of $\underset{\sim}{\Delta H}$ (measured 30 seconds after the beginning of the SC) on the SC vector diagrams themselves. Because of the effect of the longitudinal component the phase of $\underset{\sim}{\Delta H}$ will differ from that of $\underset{\sim}{b}'$ (called $\underset{\sim}{\Delta H}_T$ in the discussion of the synthesis of the vector diagrams). In order to see how much the two phases differ the phase of $\underset{\sim}{\Delta H}$ at a time of 1/6 the period after the beginning was measured for the synthesized vector diagrams in Figures 5-1, and 5-3. The true "initial" phase, of course, can not be measured because at $t = 0$ the amplitude of $\underset{\sim}{\Delta H}$ is zero. The results are presented in Table 5-2. The first column gives the phase $\psi_o(\underset{\sim}{b}')$ of the circularly polarized component at $t = 0$; the second column gives the phase $\psi(\underset{\sim}{b}')$ of this component at 1/6 period

Table 5-2

Phase of $\underset{\sim}{\Delta H}$ and $\underset{\sim}{b}'$ at 1/6 Period of Rotation of Polarized Component

Counterclockwise Polarization

Model I

$\psi_o(\underset{\sim}{b}')$	$\psi(\underset{\sim}{b}')$	B=A $\psi(\underset{\sim}{\Delta H})$	2B=A $\psi(\underset{\sim}{\Delta H})$	B=2A $\psi(\underset{\sim}{\Delta H})$
E	30°	15°	12°	21°
N	300	330	345	326
W	210	300	335	250
S	120	60	24	90

Model II

E	30°	30°	
N	300	307	
W	210	220	
S	120	117	

Model III

E	30°	30°	23°
N	300	304	313
W	210	215	220
S	120	112	115

Clockwise Polarization

Model I

$\psi_o(\underset{\sim}{b}')$	$\psi(\underset{\sim}{b}')$	B=A $\psi(\underset{\sim}{\Delta H})$	2B=A $\psi(\underset{\sim}{\Delta H})$	B=2A $\psi(\underset{\sim}{\Delta H})$
E	150°	60°	25°	110°
S	240	300	346	270
W	330	345	348	339
N	60	30	15	34

Model II

E	150°	140°
S	240	243
W	330	330
N	60	53

Model III

E	150°	145°	140°
S	240	248	245
W	330	330	337
N	60	56	47

(after 60° of rotation); the columns labeled ψ ($\underset{\sim}{\Delta H}$) give the phase of the total horizontal disturbance vector $\underset{\sim}{\Delta H}$ at 1/6 period for the various models and values of B/A as shown. The correspondence between $\psi(\underset{\sim}{b}')$ and ψ ($\underset{\sim}{\Delta H}$) is poor for model I and good for B = A for both models II and III for which the synthesized vector diagrams are more nearly elliptical. Figure 5-9 was prepared by using vector diagrams which satisfied the following conditions: a) they were clearly elliptical; b) they did not have a very large longitudinal component.

When the phase of $\underset{\sim}{\Delta H}$ at 30 seconds was plotted in Figure 5-9 for all the available SC's that obey the above criterion, the points were found to be scattered about a line which is shown as a dashed line in Figure 5-9. The slope of this line is -180°/12 hours and the line intercepts the ψ axis between 180° and 200°. Thus the phase of the O wave component of polarized SC's obeys the pattern given in Figure 5-8 for the morning hemisphere of local time from 2200 to 1000 hours.

As was previously mentioned the phase of the E wave over the evening hemisphere from 1000 to 2200 hours is much more difficult to describe because the propagation may not only be along the field line. However, we put forward a hypothesis that the pattern of $\underset{\sim}{b}'$ for the E wave can be approximated by the mirror image across the 1000 to 2200 hour meridian plane of the pattern given in Figure 5-8 for the morning hemisphere. One would then expect that for a southern hemisphere station the phase ψ of $\underset{\sim}{\Delta H}$ should rotate from south at 1000 hours local time to west at 1600 hours to north at 2200 hours. The data for all the clearly circularly polarized SC's at Wilkes station are plotted in Figure 5-9; the clustering of the data points about the dashed line supports the above hypothesis.

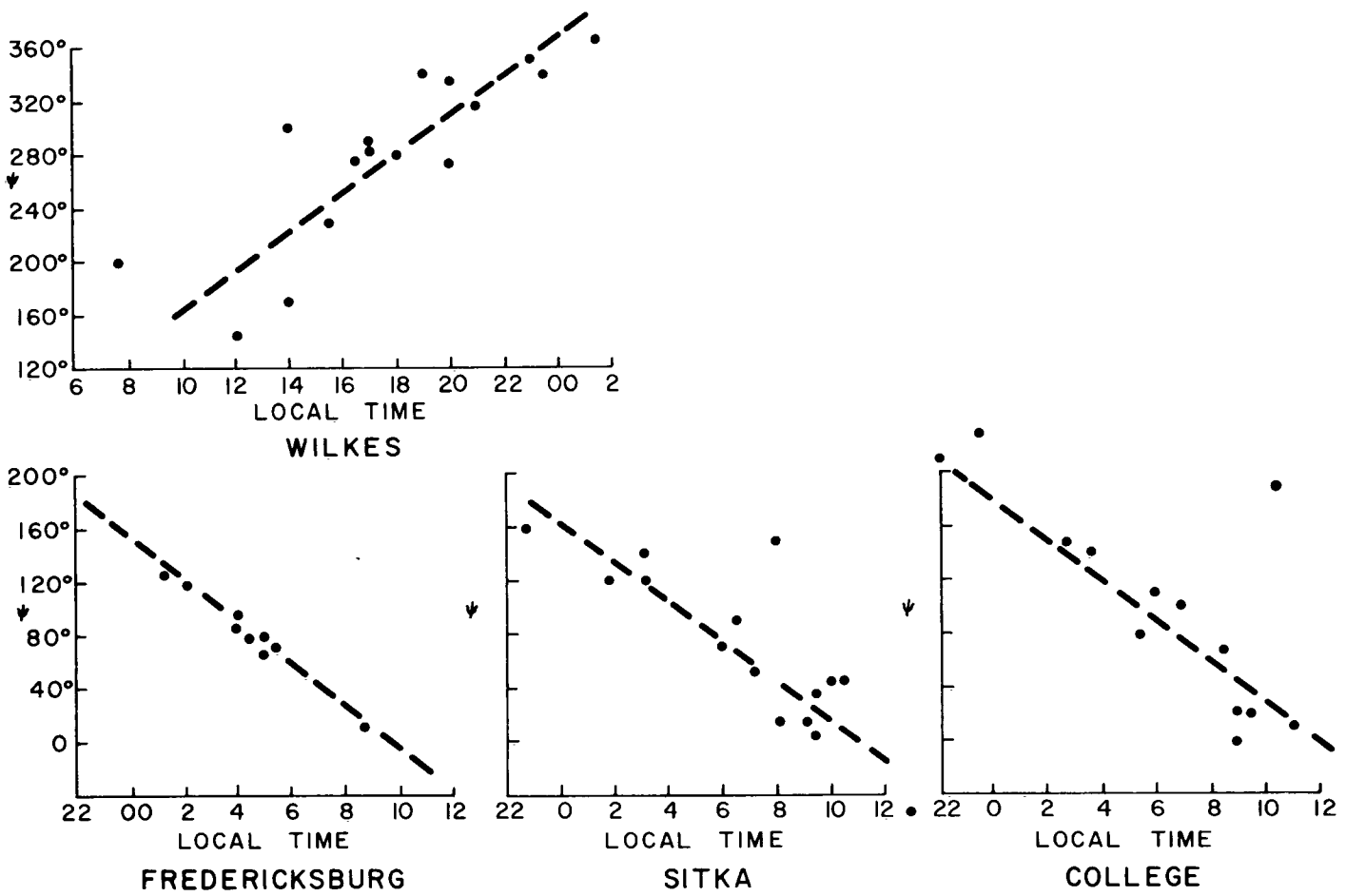

Fig. 5-9 Phase of $\underset{\sim}{\Delta H}$ at 30 sec. after SC as a function of local time at Fredericksburg, Sitka, College and Wilkes.

Because there are no data available for magnetically conjugate observatories, it is difficult to illustrate the mirror image effect with respect to the Y axis or east-west direction for the phase of the 0 wave. However, because of the great wavelength of the sudden commencement hydromagnetic wave and the consequent "leaking" of the 0 wave of one field line to adjacent field lines, stations which are not too far from being conjugate can be used to study conjugate effects of sudden commencement hydromagnetic waves. In Figure 5-10 the vector diagrams for elliptically polarized SC's are plotted for three SC's for pairs of stations in the northern and southern hemispheres.

The two vector diagrams of the SC of 0315 U.T. October 22, 1958 at Byrd and Godhavn show how, (for SC's in which there is very little longitudinal components), the variations in the two hemispheres are mirror images with respect to the east-west line. In the SC's of 1828 U.T. June 14, 1958 and1652 U.T. May 31, 1958 the pairs of vector diagrams for College and Byrd show an approximate mirror image relationship.

If there is no longitudinal component then, as suggested above, the vector diagrams of SC's in the northern and southern hemispheres will be mirror images of each other across the Y axis or east-west direction. If there is a substantial longitudinal component then the conjugate relationship of the vector diagrams of the total horizontal disturbance vector $\underset{\sim}{\Delta H}$ and not just of the circularly polarized component $\underset{\sim}{b}'$ must be considered. The initial phase of $\underset{\sim}{b}'$, the circularly polarized component, can always be found by reflection with respect to the Y axis from the northern to the southern hemisphere. Consider, for example, the conjugate relationship for an SC that has a vector diagram like that in Figure 5-2 for model III,

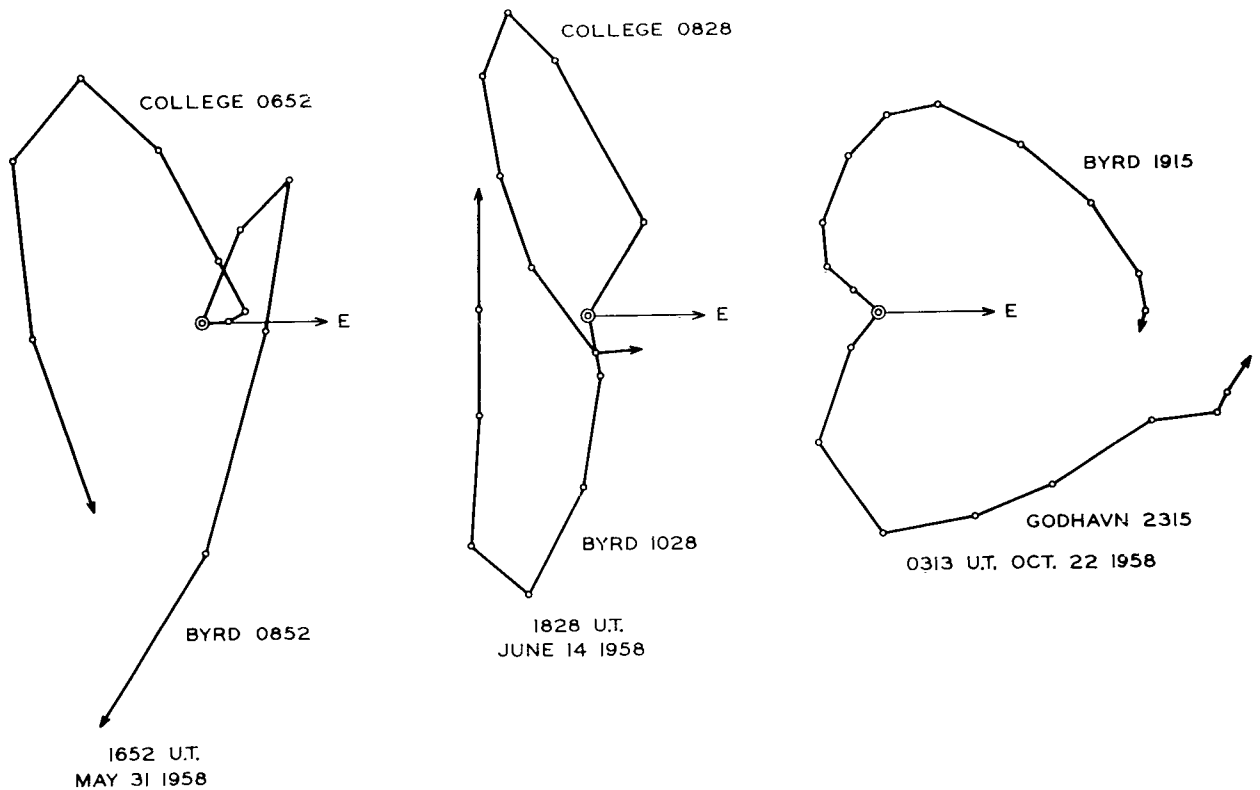

Fig. 5-10. Simultaneous vector diagrams for stations in conjugate areas.

B = A in which the initial phase of $\underset{\sim}{b}'$ is N (north). Reflection of this initial phase about the Y axis gives the initial phase of S (south) for the conjugate point in the southern hemisphere. The polarization in the southern hemisphere will be opposite to that of the vector diagram for the northern hemisphere, and thus will be clockwise. Hence, the conjugate vector diagram is found in Figure 5-3, model III, B = A with the initial phase given by S. The two vector diagrams are not at all similar. In the north the variation in H would classify the SC as an SC (+-) whereas in the southern hemisphere the conjugate vector diagram produces a shape in H to classify the SC as an SC(-+).

That the conjugate vector diagrams are not simply mirror images when the longitudinal component is taken into account can be seen more clearly by the following example. Consider the vector diagram in Figure 5-2 for model III, 2B = A, with an initial phase of west or W. Reflection about the Y axis still gives W for the initial phase in the southern hemisphere. The conjugate vector diagram is thus found in Figure 5-3, model III, 2B = A, W. In this example there is a dramatic difference in the shape of the two conjugate vector diagrams of $\Delta\underset{\sim}{H}$.

From the above considerations it would be expected that in Figure 5-10 the Byrd-Godhavn pair of vector diagrams at very high latitude stations, where there is very little longitudinal component, come the closest to being mirror images of each other.

In Figure 5-11 the phase is plotted as function of local time for the total horizontal disturbance vector $\Delta\underset{\sim}{H}$ at 1/2 the rise time for approximately elliptically polarized vector diagrams at College, Sitka, Fredericksburg, and Honolulu. For the counterclockwise polarization (2200

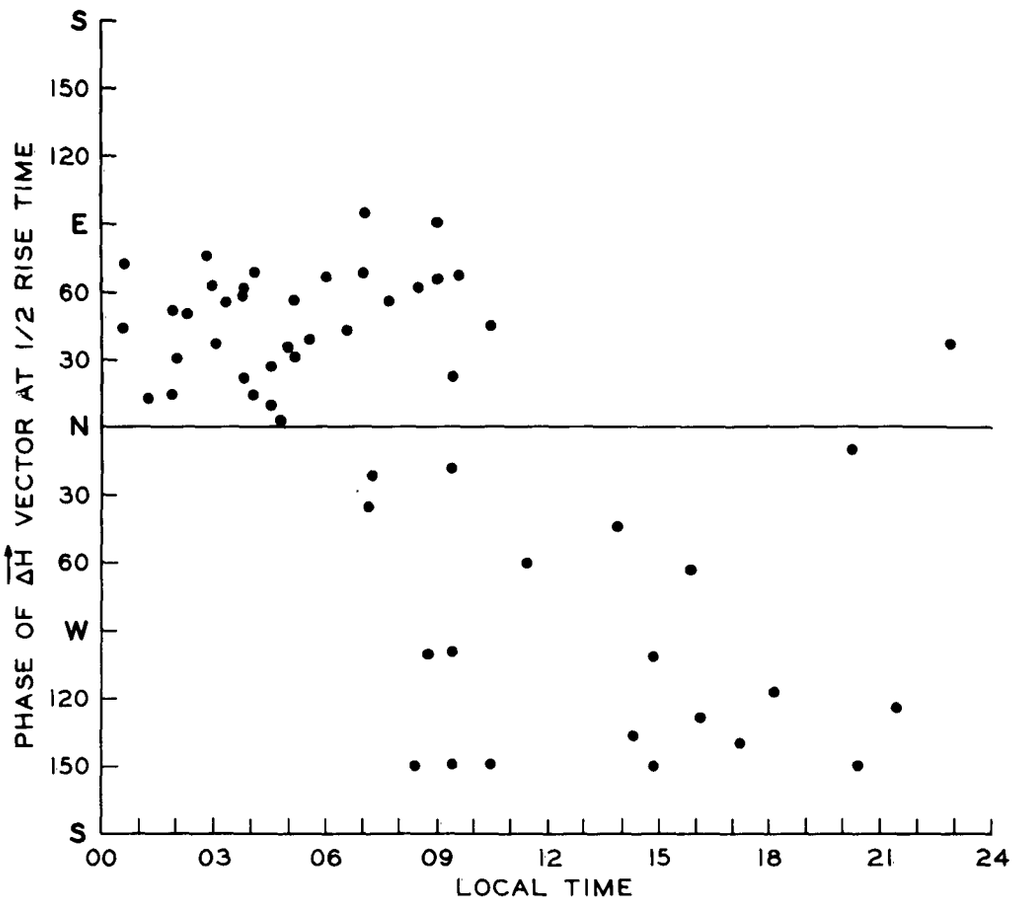

Fig. 5-11. Phase of polarized component at 1/2 rise time as a function of local time.

to 1000 hours) the points lie to the east of north whereas for the clockwise period the phase points lie to the west of north. These data lend further support to the initial phase diagram shown in Figure 5-8 for the 0 wave and to the hypothesis that the initial phase of the E wave could be considered approximately as being given by the mirror image of Figure 5-8 across the 1000-2200 hour meridian.

There is a geometrical factor to be considered. For given amplitudes of the transverse and longitudinal components, the projections of the amplitudes on to the horizontal plane at the surface of the earth varies with latitude Φ. Thus if B' is the maximum component of the transverse perturbation in the plane of the dipole field line and A' is the maximum longitudinal component of the perturbation parallel to the field line then their projections will be given by:

$$\Delta H_T = B' \cos \alpha = \frac{B' \, 2 \sin \Phi}{\sqrt{1 + 3 \sin^2 \Phi}} \qquad 5\text{-}8$$

$$\Delta H_L = A' \sin \alpha = \frac{A' \cos \Phi}{\sqrt{1 + 3 \sin^2 \Phi}} \qquad 5\text{-}9$$

where Φ is the geomagnetic latitude and α is the angle between the field line and the radial direction. Any intrinsic variation in the transverse and longitudinal perturbations will be superimposed on that given by the equations above. In any case from equations 5-8 and 5-9 it can be seen that the transverse component will vanish at the equator and the longitudinal component will vanish at the pole. In Figure 5-12, ΔH_T and ΔH_L computed by equations 5-8 and 5-9 are plotted for A' = B' = 1, that is, for

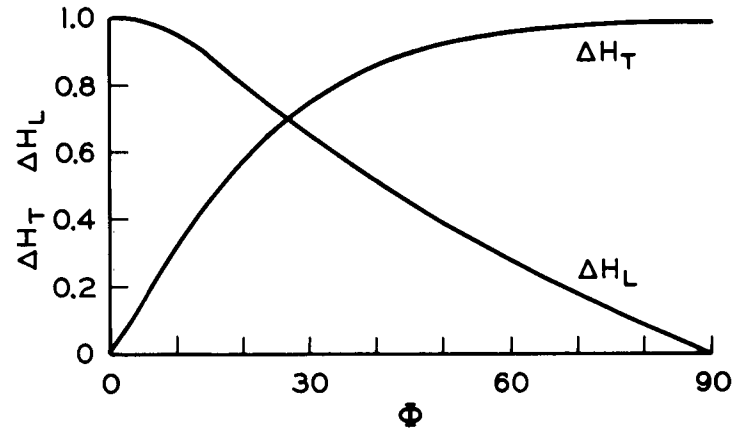

Fig. 5-12. Variations of longitudinal (ΔH_L) and transverse (ΔH_T) components as a function of geomagnetic latitude Φ.

equal transverse and longitudinal amplitudes that are the same at all latitudes. If it is assumed that the transverse SC hydromagnetic wave is the result of the twisting of the field lines due to an enhanced solar wind and that this perturbation is transmitted to the earth as an 0 wave guided along the field line over the morning hemisphere then, since the largest distortion of the field line takes place around 8 earth radii, the intrinsic variation in the transverse component would be a maximum at about $\Phi = 69°$ and diminishes towards lower latitudes. On the other hand, the transverse component may be assumed to be produced by coupling of the longitudinal hydromagnetic shock wave with the transverse waves due to the curvature of the field lines. If this coupling is most effective at about 5.5 earth radii then, in this case, the maximum amplitude of the transverse component may be expected to be at the auroral zone and the amplitude will diminish above and below auroral latitudes.

In either case there will be a strong maximum in the transverse wave amplitude at around 60° to 70° in geomagnetic latitude; also there will be a maximum in the amplitude of the transverse wave in the meridian plane at right angles to the direction of the solar wind around 0400 and 1600 hours.

Because of the dimensions of the surface of the magnetosphere, where the longitudinal component is generated, relative to the size of the earth we can assume that the longitudinal perturbation on the field lines is approximately uniform over the earth. Thus from the above considerations we would expect that ΔH_T should dominate over ΔH_L at high latitudes (60° to 70°) at all local times and also at medium latitudes (30° to 60°) around the morning and evening hours; however, ΔH_L should dominate over ΔH_T for all local times for lower latitudes.

Because the vector diagrams depend so strongly on the initial phase of the transverse component, it is very difficult to establish an unambiguous criterion for determining the relative size of the transverse and longitudinal components. Even if we choose vector diagrams around 0400 to 0600 hours when we can be fairly certain that the initial phase is east, then because of the variation of shape in the vector diagram due to the many possible different function g(t) and h(t) for the change of the amplitudes of the two components it is still very difficult to measure the ratio of B and A. Although it is virtually impossible to take meaningful quantitative measurements of B/A an examination of the vector diagrams in Figures 3-2 to 3-5 does qualitatively verify the variations of B/A with Φ and local time as discussed above.

If the rise time of a sudden commencement is defined as the time it takes the total horizontal disturbance vector $\Delta\underset{\sim}{H}$ to reach its first maximum value then this time will, in general, depend on the rise time of the transverse component amplitude, h(t), and that of the longitudinal component amplitude, g(t), (here assumed equal), and it will also differ from the rise time in H because of the dependence of the vector diagram on the initial phase of the transverse component. For example, in Figure 5-1 for B = A in model I the rise times of g(t) and h(t) were taken as both equal to the period of rotation of the transverse component. For this case when the initial phase of the transverse component is north, the rise time as determined by H would be 1/6 the rise time of g(t), h(t) and $\Delta\underset{\sim}{H}$, all of which are equal to the period of rotation for this particular choice of initial phase. If the initial phase is taken to be south, S in the diagram, then the rise time in $\Delta\underset{\sim}{H}$ would be about equal to the rise time of H but these would only be 1/2 of the actual rise time of the two components g(t) and h(t).

The physically significant quantity is the rise time in g(t) or h(t) which would, of course, be equal if the perturbation is a coupled wave. Again the complexity of the vector diagram makes it difficult to determine the actual rise time of the SC field for high latitude stations.

Any attempt to determine the period of rotation of the circularly polarized transverse component from the rotation of $\underset{\sim}{\Delta H}$ as measured on the vector diagrams will produce ambiguous results as can be seen from the following examples. In Figure 5-2, model III for B = A in one period during which the transverse component rotates through 360° the rotation of $\underset{\sim}{\Delta H}$ as measured on the vector diagrams is: 450°, 360°, 270° and 180° for the initial phases of E, N, W and S respectively. If the SC diagram contains very little longitudinal component then one would expect that the azimuth of $\underset{\sim}{\Delta H}$ would vary linearly with time and that it would sweep out 360° in one period.

Changes in the azimuth of $\underset{\sim}{\Delta H}$ are shown in several examples in Figure 5-13 for College, Sitka, Fredericksburg and in Figure 5-14 for Honolulu. The azimuth is plotted against time; the time axis is taken from left to right, and plots are made at 30 second intervals. In Figure 5-13 the three traces on the left for the three stations are for counterclockwise rotation of $\underset{\sim}{\Delta H}$; in the three examples in the middle, for College and Sitka, $\underset{\sim}{\Delta H}$ rotates clockwise. All these examples represent elliptically polarized SC's. The three examples to the extreme right for the three stations show irregular polarization. The remarkably regular rate of change in azimuth for the elliptically polarized SC's indicates the predominance of the transverse component. The linear nature of the SC vector diagrams for Honolulu on the left in Figure 5-14 indicates the predominance of the longitudinal component for this low latitude station. The constant azimuth for SC's at

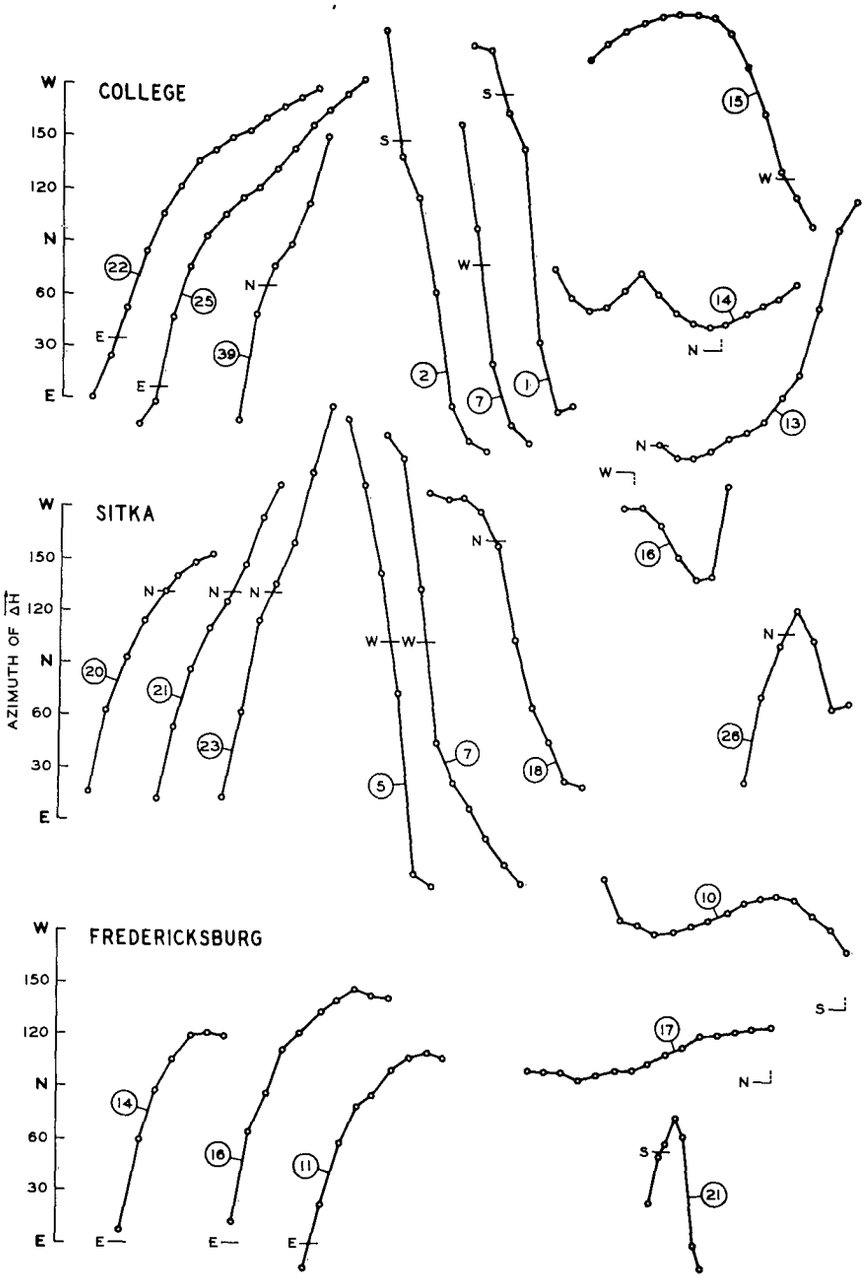

Fig. 5-13. Variations in azimuth of $\underset{\sim}{\Delta H}$ with time.

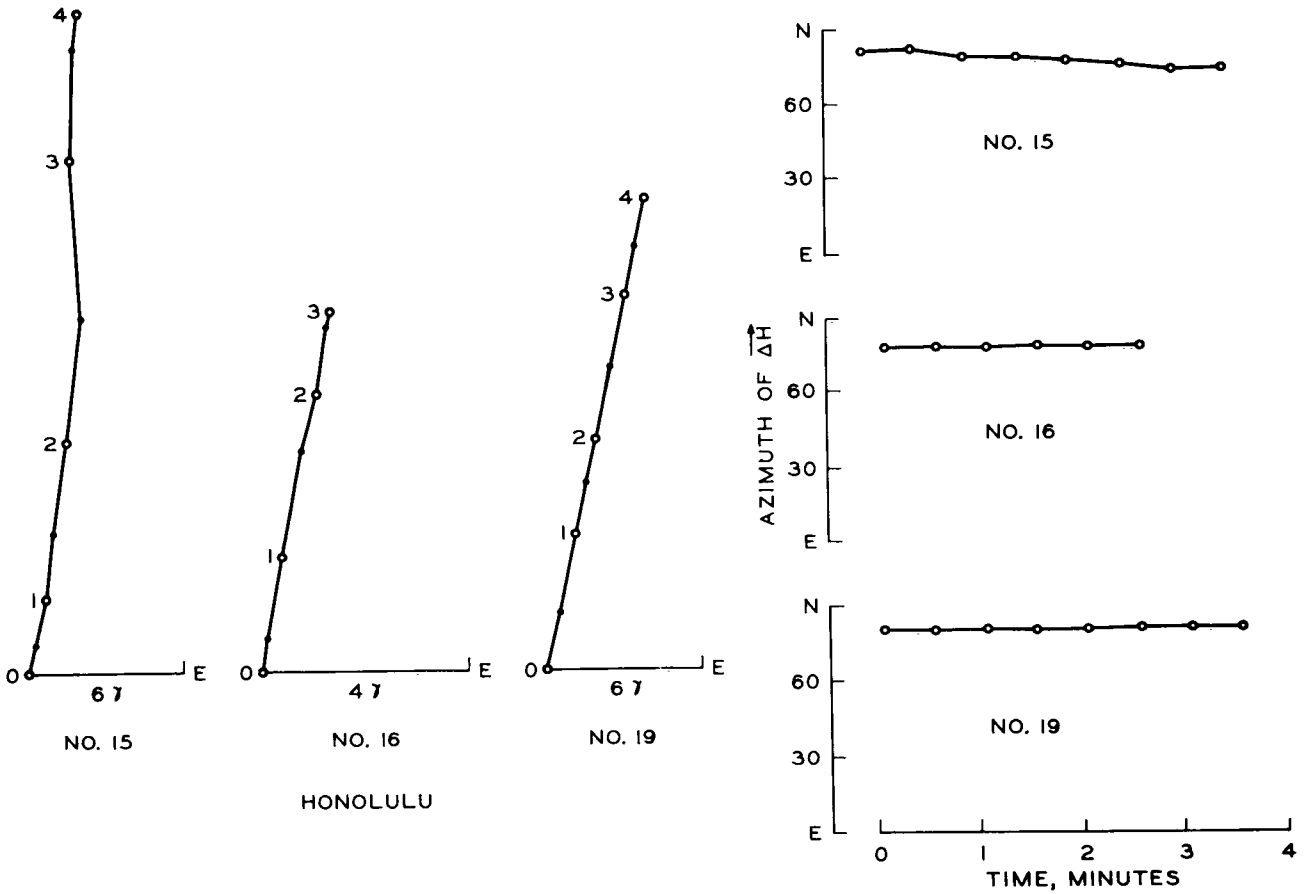

Fig. 5-14. SC vector diagrams at Honolulu with corresponding azimuth of $\underset{\sim}{\Delta H}$ versus time graphs.

Honolulu shown in the right of Figure 5-14 may be contrasted with those for elliptically polarized SC's in Figure 5-13.

All previous attempts to classify SC's have been in terms of the behavior of H with time. Thus Ferraro, Parkinson and Unthank (1951) suggested the four classifications: SC(+), SC(-), SC(+-), SC(-+) to describe the changes in H. Matsushita (1957) proposed the notation Sc, -Sc and Sc- and Akasofu and Chapman (1960) proposed to extend the notation proposed by Ferraro et al. by the addition of one or more signs, as for instance, SC(++) to indicate two successive increases in H. As the hundreds of vector diagrams presented thus far have shown, to ignore the D variations for SC's of even low latitudes is equivalent to ignoring the essential nature of the SC field, namely its polarization. Also a classification and subsequent description of the SC field in terms of the H variations alone has led many workers to attempt to explain such features as the preliminary reversed impulse of an SC(-+) or SC* as a separate phenomenon rather than as merely being due to the simple rotation of $\Delta\underset{\sim}{H}$ vector as can be seen in Figure 1-1.

By studying the synthesized vector diagrams presented in Figures 5-1, 5-2 and 5-3 and the variation in H shown to the left for each vector diagram, it is immediately apparent that almost all of the previous classifications of SC's in terms of the variation of H depend solely on the projection of the variation of $\Delta\underset{\sim}{H}$ on the X' axis. Thus the SC(+) <u>can</u> be caused by an SC whose vector diagram is similar to that shown in Figure 5-1, 2B = A, S; the SC(-+) can result from such vector diagrams as those in Figure 5-3, model II or III, B = A, B = 2A or 2B = A, for initial phases of east or south; the SC(+-) can be seen in H for Figures 5-2 or 5-3 for models II and III, B = A, for initial phase of N; the SC(++) can be seen in Figure 5-2, model III, 2B = A, E or in Figure 5-3, model III, 2B = A, W. Although SC(-)

does not appear, it could easily be produced by decreasing the relative size of the longitudinal component and by making the period of h(t) variation equal to the rotation period in Figure 5-2, models II or III for W initial phase or in Figure 5-3, models II or III for E initial phase.

Since all of the previous classifications of SC's can be explained in terms of the projection of the vector diagram of the total horizontal disturbance vector on the X' axis, it is suggested that a new system of classification for SC's be based on the characteristics manifested in the vector diagram. The most physically significant characteristic of an SC is whether it is due to a combination of a circularly polarized hydromagnetic wave and a longitudinal hydromagnetic wave or simply to the latter alone. The characteristic of the polarization, i.e. elliptical, linear or irregular of the SC vector diagram can be used to descriminate between these two cases. The second most important aspect of an SC, if it is polarized, is whether it is due to an E or 0 wave. This is indicated by the direction of polarization of the vector diagram. The next most important characteristic is the initial phase which, together with the direction of polarization and the ratio B to A, will determine the shape of the vector diagram and the subsequent shape of the H variation. Other physically significant aspects of SC's which are unfortunately very difficult to determine are the ratio B/A of the maximum amplitudes of the two components; the period of rotation of the transverse component, the rise time of the components and the frequency spectrum of the transverse component.

As an illustration of how the direction of polarization and the initial phase of the transverse component determines the shape of the SC vector diagram and thus the variation of the H component we will consider the SC's

classified as SC* or SC(-+) and SC(+-). From models II and III shown in Figures 5-2 and 5-3 it can be seen that SC(-+) will occur as follows:

a) for counterclockwise polarization when the initial phase is west or south (or any phase between W and S).

b) for clockwise polarization when the initial phase is east or south (or any phase between E and S).

Illustrations of SC(-+) for clockwise polarization are given in Figure 1-1 for College, Figure 3-1 for College and Sitka, Figure 5-4, #5 and #6 for Sitka and Healy, Figure 5-5 #3 and #4 for Sitka. For all of these clockwise SC(-+)'s the initial phase is either E or S or between E and S resulting in an SC(-+) as predicted by the vector diagram models.

Illustrations of SC(-+) for counterclockwise polarization are given in Figure 5-5 #1 and #2 for College. In these counterclockwise SC(-+)'s the initial phase is W and SW which both result in SC(-+) as predicted.

Illustrations of SC(+-) are given in Figure 5-4 #1 and #2 for Sitka and Reykjavik and in Figure 5-5 #5 and #6 for Sitka and College. In all of these the initial phase is approximately north which for counterclockwise polarization results in an SC(+-) as predicted by the vector diagram in Figure 5-2, model II or III, B = A, N.

If it were possible to give definite rules for the initial phase of the circularly polarized transverse component as a function of local time, then, following the above discussion, it would be then possible to give the distribution of the various types of SC's with local time. This can be done with moderate success for the morning hemisphere where the 0 wave initial phase obeys the pattern given in Figure 5-8. Thus if we assume that the solar wind direction is parallel to the 2200 - 1000 hour meridian plane,

then from Figure 5-8, SC's that occur around 0200 to 0300 hours should have an initial phase about 30° south of east. According to the model II or III vector diagrams in Figure 5-2 an initial phase south of east should produce a circular or an elliptical vector diagram depending on the ratio B/A. Referring to the vector diagrams in the top of Figure 3-1, we see that for College, Sitka and Honolulu the initial phase is about 30° south of east and that the vector diagrams are elliptical at Honolulu where, because of the low latitude, the transverse component amplitude B is smaller than the longitudinal component amplitude A, the segment of the elliptical vector diagram shown in Figure 3-1 is more like that for 2B = A in Figure 5-2, model III S. The initial phase for the SC at 0431 local time at Fredericksburg in Figure 3-1 is almost east. The vector diagram for this SC is more circular as is predicted by the vector diagrams in Figure 5-2 for model II or III, B = A, E.

Matsushita (1962) has given the distribution of SC(+-) as a function of local time. He shows that they occur over a span of about 8 hours at Point Barrow and College and over a span of a few hours at Cheltenham. The time of maximum occurrence is about 1000 local time. From Figures 5-2 and 5-3 for models II and III for any given ratios of B to A and for Figure 5-1 for model I for B = 2A, if the initial phase is N, an SC(+-) will occur. Now for B = A an SC(+-) will also occur for counterclockwise polarization and E initial phase or for clockwise and W. The phase predicted for the 0 wave in Figure 5-8 is N at 1000 hours of local time and is east of north until 0400 when it is east. Thus unless the longitudinal component were very much larger than the transverse component one would always expect an SC(+-) around 1000 hours in high latitude. There was an indication that the phase of the E wave tends to be west of north in Figure 5-11. This is consistent

with the appearance of SC(+-) from 1000 to 1400 hours according to Figure 5-3 model II, B = A, W or NW. The increase of occurrences of SC(+-) at higher latitudes found by Matsushita (1962) is consitent with the behavior predicted by the vector diagrams for N initial phase model II or III in Figures 5-2 and 5-3. Thus for 2B = A, which would correspond to a larger longitudinal component at lower latitude, the SC(+-) is not as pronounced as it is for B = A which condition prevails in a higher latitude. Thus the variation of frequency of occurrence of SC(+-) with local time and latitude is well explained by the above model for the vector diagrams and the expected phase of the 0 wave around 1000 hours.

The situation as far as the SC(-+) is concerned is not as clear. The vector diagram model does accurately predict that if the SC has a clockwise polarization then the initial phase must be either E or S in order to be an SC(-+) and if the SC has a counterclockwise polarization then in order to be an SC(-+) the initial phase must be W or S. This was shown to be the case in all the examples mentioned above and was also found to hold for all the SC(-+)'s that were analyzed. The distribution of SC(-+)'s found by Ferraro, Parkinson and Unthank (1951), by Nagata (1952) and by Matsushita (1962) showed that they tend to occur most frequently at high latitudes with a maximum frequency between 1200 and 1900 hours. As is predicted by the vector diagrams in Figures 5-2 and 5-3, SC(-+)'s will be most pronounced for a west initial phase for counterclockwise polarization and for an east initial phase for a clockwise polarization. Thus the fact that SC(-+) are very infrequently observed over the morning hemisphere (counterclockwise polarization) is consistent with the initial phase pattern given in Figure 5-8 for the 0 wave in which the initial phase is always east and never west

of the N-S line. Because the initial phase pattern of the E wave is not understood over the evening hemisphere, the occurrence of east initial phase to produce SC(-+) cannot be explained at this point. The shape of the vector diagrams for SC's at Fredericksburg from 0300 to 0600 as shown in Figure 3-2 are very circular compared to the form at all other local times. This gives a further verification of the correctness of the vector diagram models and the predicted 0 wave initial phase pattern. Thus according to Figure 5-8 the initial phase around 0400 hours should be east. According to Figure 5-2, model II or III for B = A (which is consistent with both the moderate latitude of Fredericksburg and this local time) an east initial phase should give a circular vector diagram.

CHAPTER VI

DISCUSSIONS

In Chapter III, on polarization of SC's, data were presented from both statistical studies of the direction of polarization of elliptically polarized SC's and studies of this property for individual SC's. The direction of polarization of elliptically polarized SC's, as viewed downward on the earth's surface, was found to be consistent with the interpretation that the polarized component of the SC field is due to an ordinary hydromagnetic wave in the morning hemisphere from 2200 to 1000 hours, and to an extraordinary hydromagnetic wave in the evening hemisphere. The direction of the polarization of an E wave was shown, in Chapter V, to be clockwise when looking along the direction of the field regardless of the direction of propagation of the wave; whereas the O wave is characterized by counter-clockwise polarization. By referring to Figure 1-2 one can see how the model, as schematically represented in the diagram, would produce O and E wave in the morning and evening hemispheres respectively; and furthermore, how the pattern of polarization of elliptically polarized SC's as determined by this model is completely consistent with the data presented in Tables 3-1 and 3-2.

The observed decrease in the percentage of occurrence of elliptically polarized SC's with decreasing latitude, as well as the independence with change in latitude of the percentage of these elliptically polarized SC's that obey the polarization rules, are both concordant with the model.

The departure of the agreement of the polarization direction at the very high latitudes follows directly from the departure of the earth's field from a dipole configuration. Recent plasma measurements by Mariner II

indicate that a steady solar wind exists in interplanetary space (Neugebauer and Snyder, 1962), and due to this continuous flow of solar plasma, the magnetosphere is confined in a "cavity". Observational evidence for the "cavity surface" has been provided by magnetic measurements made with instruments aboard Pioneer I (Sonett et al., 1960), Pioneer V (Coleman et al., 1960), Explorer X (Heppner et al., 1962), and Explorer XII (Cahill and Amazeen, 1963). The measurement by Explorer X indicated that the cavity surface extends to distances greater than 20 earth radii on the dark side of the earth. On the day side of the earth the cavity surface is near 10 earth radii and as close as 8 earth radii during magnetic storm sudden commencements.

For an unperturbed centered dipole the magnetic field lines crossing the equator at a geocentric distance of 10 earth radii intersect the earth's surface at 72° latitude. Due to the magnetic field produced by the electric current on the boundary surface the field lines will be distorted. Theoretical studies of the shape of the cavity surface have been made by a number of workers (Dungey (1961), Hurley (1961), Midgley and Davis (1962), Slutz (1962), Spreiter and Briggs (1962), and Mead (1962). However, the idealizations and approximations made in these studies make it difficult to determine the distortions of the magnetic field lines that are anchored in the earth near the magnetic poles. Magnetic measurements in the magnetosphere over the polar regions have not been made.

Thus it is not certain whether the magnetic field lines intersecting the earth's surface near the magnetic poles all cross the equator on the dark side of the earth as has been suggested by Johnson (1960), or if some of these lines of force are connected to those of interplanetary magnetic

fields or to the disordered lines of force of the irregular magnetic field that has been observed by Pioneer I, Pioneer V, Explorer X, Explorer XII and Explorer XIV as discussed by Dessler (1962). However, in a recent study of diurnal effects in magnetic conjugacy at very high latitude stations, (Φ = 79.0°; r_e = 26), Wescott and Mather (1963) have found evidence that supports the Johnson (1960) model of the distortion of the earth's field by the solar wind. Thus these authors find an indication that the field lines are interhemispherically connected as in a simple dipole configuration only during the night and that during the day there is no magnetic conjugacy between the stations. If the magnetic field lines originating near the magnetic poles are not interhemispherically connected, the mode, i.e. ordinary or extraordinary, of the transverse SC waves may not agree between high latitude stations in the adjacent northern and southern quadrants. Even if these lines of force are connected on the dark side of the earth at distances greater than 10 earth radii, the magnetic field may be too weak for an efficient coupling of longitudinal and transverse hydromagnetic waves. Thus the break-down of the agreement of the polarization of very high latitude SC's with the polarization rules is to be expected from the present ideas and experimental evidence concerning the distortion of the dipole field by the solar wind at very high latitudes.

For the two SC's listed in Table 3-2, 1050 U.T. January 25, 1958 and 1821 U.T. November 6, 1957, the percentage of agreement of the elliptically polarized SC's is still low (69% and 65% respectively) even after the very high latitude stations have been removed. In cases such as these the lack of agreement of the direction of polarization is not due to random polarizations of SC's at adjacent stations; even in these cases the polarizations

are the same within each of several large areas. This behavior is more compatible with the model than random polarization would be. Thus, for some unknown reason, there seem to be times when the mode excited by the solar wind is different than that expected by the simple model. This may be due to irregularities in the magnetospheric boundary or to the effect of magnetic fields carried by the solar stream.

Wilson (1962), on the basis of the asymmetry between the sun-earth line and the meridian plane separating the zones of opposite polarization of elliptically polarized SC's, suggested that the solar plasma may arrive at the earth from the west of the sun-earth line. This idea was in an attempt to explain many geophysical phenomena which, through their relation to the geomagnetic field, exhibit symmetry about a meridian plane west of the sun-earth line. Thus Davis (1962) has shown that auroral arcs over the polar cap line up with the 1000 to 2200 hour meridian; Hasegawa (1960) gives the foci of the Sq current system at 1100 hours on the day side of the earth; Wilson and Sugiura (1961) give the 1000 to 2200 hour meridian plane for separation of the SC polarization zones.

Wilson (1962) assumed that the solar plasma is guided by the extended solar field (Parker (1961)) and thus arrives at the earth from west of the sun-earth line as shown in Figure 1-2.

There is considerable evidence suggesting that solar particles of higher energies than those causing SC magnetic storms are in fact guided by an extended spiral solar field. Thus, Obayashi and Hakura (1960) and Dvoryashin, Levitskii, and Pankratov (1961), from the analysis of the delay times of polar-cap absorption events, have shown that the 10 to 100-Mev solar particles that cause polar-cap absorption arrive at the earth sooner if they originate in solar flares that are west of the solar central

meridian than they would if they are from solar flares to the east of the central meridian. Reid and Leinbach (1959) have shown that there are more polar-cap absorptions associated with western-side solar flares than those associated with eastern-side flares. They think that these two PCA effects can be explained if it is assumed that the ejected solar particles travel to the earth along the lines of force of the spiral solar field. This path of the particle cloud would result in easier access to the earth for particles from western flares, whereas the solar particles from eastern flares would have to diffuse across the field lines to reach the earth and would thus be delayed in time and would be fewer in number.

In an analysis of cosmic-ray increases caused by high-energy particles from the sun, Carmichael and Steljes (1961) have concluded that the cosmic rays are guided by the field of a magnetic bottle (Gold 1959) that is the extension of a sun-spot magnetic field blown out by solar wind. The distortion of the magnetic bottle by the sun's rotation causes the enclosed field lines to intersect the earth's orbit from west of the sun-earth line. Carmichael and Steljes have observed particles that arrive at the earth from a direction 50° to 60° west of the sun-earth line.

Explorer X magnetic field measurements by Heppner et al. (1963) of the cavity characteristics could be explained if it were assumed that the average solar stream was incident from a direction west of the sun-earth line. Whether or not the solar plasma is moving radially away from the sun or is guided by an extended solar field the velocity of the solar plasma, when observed from a moving earth, will always appear to have a component from the west. Thus, when a Galilean transformation of the velocity of the solar wind (assumed to be radial at 10^3km/sec.) to a system fixed with

respect to the earth (which is moving to the west of the sun-earth line at 30 km/sec. in its orbit) is made, the aberration amount to 1.5 degrees to the west.

According to Parker (1958), the general solar dipole field is drawn out into interplanetary space by the solar wind, so that the projection of a line of force of the extended field on the solar equatorial plane forms an Archimedes spiral that is convex to the west due to the rotation of the sun. At the earth the angle ψ measured west from the sun-earth line to a line of force of the extended solar magnetic field can be found from the ratio of the azimuthal B_ϕ to the radial B_r components of the field. For large distance R, Parker (1958) gives this ratio as $B_\phi/B_r = R\Omega/v \sin\theta$. In the plane of the ecliptic the polar angle $\theta \simeq 90°$, thus ψ is given by $\tan\psi = \frac{R}{V}\Omega$ where R is the sun-earth distance, Ω is the solar angular velocity, and V is the radial velocity of the solar wind that is extending the solar field.

The average delay time between solar flares and magnetic storms gives a velocity of the solar plasma causing the storms of about 10^3km/sec. The angle ψ corresponding to $V = 10^3$km/sec is 23° west of the sun-earth line. In Figure 6-1 the two zones of opposite directions of polarization of SC vector diagrams for SC's at College and Sitka are plotted. Solid or open circles represent clockwise or counterclockwise polarization respectively. The angle between the sun-earth line and the meridian plane separating the two zones of opposite polarization is indicated by ψ. The close agreement between ψ and the angle west of the sun-earth line of the plane of symmetry separating the two polarization zones of SC hydromagnetic waves

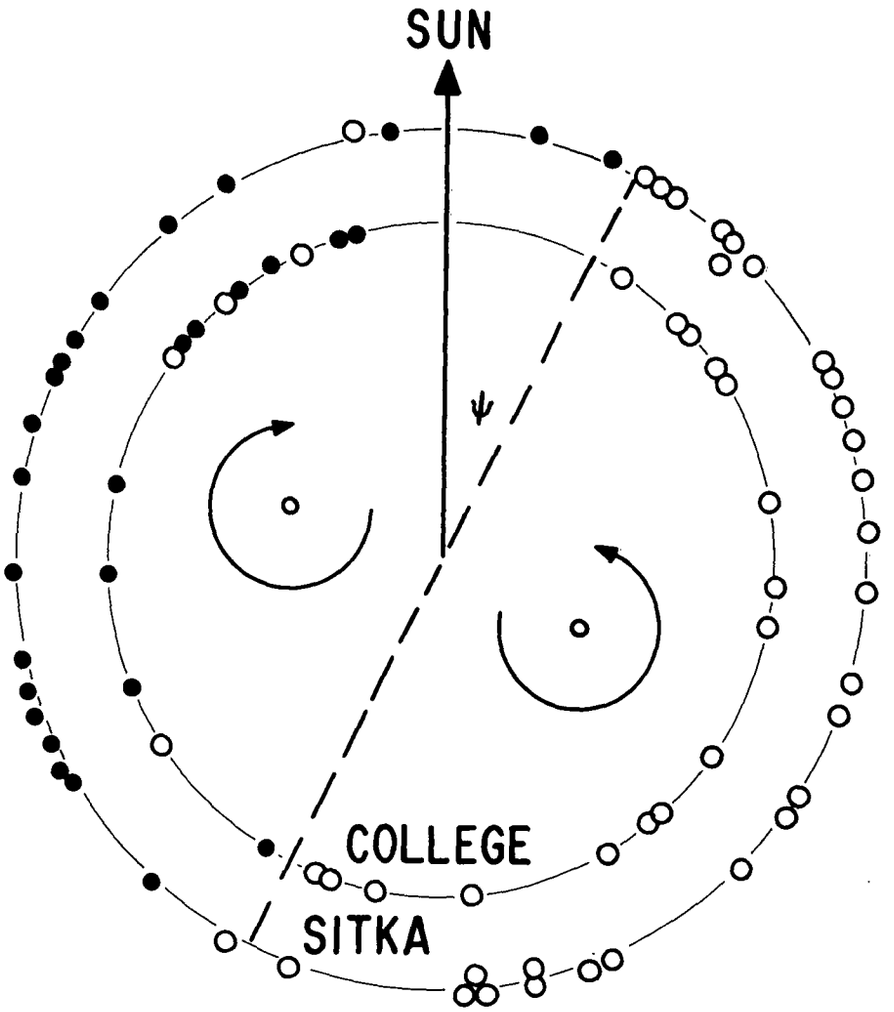

Fig. 6-1 Local time distribution of direction of polarization of SC's at College and Sitka.

seems to indicate that the shock front of the solar plasma stream propagates parallel to the solar field lines.

Another possible source of the asymmetry of the pattern of SC polarization with respect to the sun-earth line lies in the rotation of the earth's field in the interplanetary gas. At the surface the earth's atmosphere obviously rotates with the earth. In the region where the magnetospheric plasma merges with the interplanetary gas there is friction between the plasma and the interplanetary gas which attenuates the rotation of the magnetospheric plasma. Because of the low collision frequency, the viscosity is not kinetic but is electromagnetic in nature as discussed by Parker (1958). Now because the earth's field is frozen into the plasma of the magnetosphere, there will be a westward directed spiral distortion of the fringe of the geomagnetic field where the earth's outer atmosphere ceases to rotate. This spiral distortion of the earth's field will be superimposed on the other distortion due to the flow of the solar wind.

Thus it is suggested that there is a permanent spiral distortion (spiraling to the west when looking down on the north pole of the earth) of the geomagnetic field due to the rotation of the earth's field in the interplanetary gas that may account for the asymmetry with respect to the sun-earth line that is observed in the SC polarization pattern over the earth.

Before any conclusive results can be reached about the origin of SC oscillations, observations will have to be made of many individual SC oscillations simultaneously at a large number of stations. Statistical studies of the type reported in Chapter IV for 29 SC oscillations at College serve only to show the great range of variability of the various characteristics of the SC oscillations; as in the case of the SC itself, the accompanying oscillations are very complex.

SC oscillations were shown to be elliptically polarized and the direction of polarization was found to obey the polarization rules; however, little else of a definite nature, other than that their frequency spectra show harmonic structure, can be said about them. No consistent relation was found between the period or amplitude of the oscillation and the size of the SC shock (as indicated by the increase in H in a low latitude station, namely at Honolulu).

Although two types of spectral sequences were found, as given in Table 4-6, the occurrence of either of these sequences could not be definitely related to any of the other oscillation parameters or to local time. However, a similarity was found between the frequency ratios for the sequences C and D in Table 4-6 (as indicated by $n = 1,3,6$ next to the periods in seconds) and the harmonic frequency ratios calculated by MacDonald (1961) in his Table 1 for $\phi = 60°$. Thus the even series of MacDonald's mode numbers $n = 1,2,4$ corresponds to the frequency ratios of sequence D in Table 4-6 with $n = 1,3,6$ found here for the SC oscillations. Thus sequences C and D may represent "even" harmonic excitation in SC oscillations, while the other sequences A and B may represent "odd" harmonic excitation.

If the distortion of the field line by the solar wind is nearly symmetrical about the dipole equatorial plane with the maximum displacement of the field line occurring in the equatorial plane, then this initial condition would excite oscillations with even harmonics. However, if the distortion of the field line is not symmetrical about the equatorial plane and the maximum distortion occurs off this plane, then a sequence of odd harmonics is likely to be excited. The case of asymmetric distortion of the field line by the solar wind would result if the normal to the shock front

of the solar wind did not lie in the equatorial plane; whereas symmetrical distortion of the field line would occur when this normal is in the equatorial plane.

The angle between the earth's dipole equatorial plane and the ecliptic plane varies with season because of the variation in the inclination of the earth's geographic axis to the ecliptic plane. This angle also varies with universal time because of the earth's dipole axis not being coincident with its rotational axis. If it is assumed that the normal to the solar wind shock front lies in the ecliptic plane then, from the above considerations, it follows that the symmetry of the distortion of the field line will depend on season and universal time in a complicated way. There are not as yet sufficient data to determine the relationship between the type of spectral sequence, i.e. odd or even, and season or universal time.

Calculation was made of the fundamental period for a resonance model that gave good agreement for one of the "fundamental" periods seen most often at College, that is 220 seconds. The 540 second periods observed at Point Barrow and Byrd Station were also consistent with the curve shown in Figure 4-12. However, at Sitka the model predicted a period of 78 seconds, whereas the SC oscillations observed at Sitka seemed to have the same spectra as that found at College. For the SC of 0622 U.T. August 17, 1958, the period of the SC oscillation was found to be about 200 seconds at College and also at Fredericksburg where the model would require a period of only 20 seconds.

The model assumes that the energy is propagated along a field line and yet there is evidence from the direction of the incoming wave for one particular SC oscillation given in Table 4-4, to indicate that the energy is

propagating transverse to the field from the impact zone in the 1000 hour meridian of the magnetosphere boundary. This complex state of affairs cannot be resolved with the available data. However, the general picture of SC oscillations as revealed in the present study is consistent with the following ideas. SC oscillations are produced by the impact of the solar stream on the boundary of the magnetosphere and have a fundamental period and harmonic structure determined by a natural resonance excitation mechansim. There is an optimum r_e range in the magnetosphere for which this excitation takes place (which may be from about 5 to 8 earth radii). When SC oscillations are observed at low latitudes (for which $r_e < 5$) then these oscillations are the result of coupling of the field lines in a wide range of latitude or of "leaking" of the wave from the higher latitude field line. There seems to be some general condition of the magnetosphere that results in giant pulsations as well as SC oscillations.

When the spectrum analysis was made of the SC oscillations at College and Sitka the H component was used. Thus the spectra obtained will include components due to the longitudinal wave in the initial impulse as well as that of the transverse oscillation. The principal change in H due to the longitudinal wave is a monotonic increase that levels off in about one half cycle of the oscillation. However, there may be enough power in this component to give a spectrum that does not accurately represent the harmonic structure of the transverse wave itself.

Simultaneous spectra of all three components H,D and Z for the SC of 0622 U.T. August 17, 1958 at College gave similar spectra for D and Z as shown in Table 4-7. The spectra for H did not include the first maxima or preliminary reversed impulse and is thus slightly different. In most cases

when simultaneous spectra were determined in both D and H for an SC oscillation the spectra were identical as one would expect if they represent the spectra of the two components of a rotating vector projected onto two orthogonal axes.

In the discussion in Chapter V concerning the relative magnitudes of the longitudinal and transverse components of SC hydromagnetic waves, it was assumed that the longitudinal component was approximately uniform over the earth. The projection of this component on to the earth's surface was given by equation 5-9. Parker (1958) shows that there is a uniform increase in the field due to the compression by the solar wind and that this increase can be represented by a field parallel to the dipole axis. The projection of such a perturbation on the earth's surface would be proportional to $\cos \phi$ and would thus not be given by equation 5-9. Thus in very high latitudes nearly all the SC field, as projected on the earth, would be due to the transverse component.

The vertical component of the uniform increase would be proportional to $\sin \phi$ so that at higher latitudes the Z component should show increased tendency for an initial upward or negative change. Superimposed on this, however, would be the vertical component of the transverse wave. Thus the Z component at high latitudes may be either + or - as shown for the SC's in Table 4-3.

An observation due to Nagata (1952), that the ratio of the maximum deflection of a preliminary reversed impulse of an SC to the total range of the SC is greater at higher latitudes is consistent with the vector diagram model for SC given in Chapter V. At higher latitudes the ratio of the transverse to the longitudinal component is larger. Thus, as shown in

Figure 5-2, the preliminary reversed impulse is larger for B = A in model III which corresponds to higher latitude than in the diagram for 2B = A.

The rise time of an SC has been discussed by Dessler et al. (1960) however, one must be careful in defining the rise time of an SC because of the effect of the polarized component on the rise time observed in H as discussed in Chapter V.

Vestine and Kern (1962), Watanabe (1961), and Sano (1962) considered the preliminary reversed impulse as a separate phenomenon, whereas the mechanism presented in Chapter V accounts for all types of SC's without involving any additional mechanism for the preliminary reversed impulse of SC(-+)'s.

The vector diagram form for a given ratio of the transverse to longitudinal waves, is determined by the initial phase of the polarized component. Because the initial phase propagates without rotation with respect to the field line from the source of the perturbation in the equatorial plane; and because the initial phase in the equatorial plane depends on the angle between the solar wind and the plane of the field lines, one would naturally expect that the initial phase of the polarized component and thus the shape of the vector diagram would be a unique function of the local time.

The fact that the initial phase of $\underset{\sim}{b}$ propagates parallel to itself along the field line, as explained in Chapter V, can be seen for the special case of a wave of arbitrary form in an incompressible fluid with infinite conductivity. Alfvén (Cosmical Electrodynamics, p. 87, 1950) gives the following equation to show that any state of motion is displaced with the Alfvén velocity in the direction of the uniform field:

$$(\underset{\sim}{B}_o \cdot \text{grad})\,\underset{\sim}{b} = \sqrt{4\pi\rho}\ \frac{\partial \underset{\sim}{b}}{\partial t} \qquad 6\text{-}1$$

In the past SC's have been interpreted as a simple compression of the field, whereas in many cases, such as the hook forms shown in Figure 5-4 No's 11 and 12, H decreases again after the initial increase. This can be explained in terms of the rotational component of $\underset{\sim}{\Delta H}$. Thus in the synthesized vector diagram shown in Figure 5-1 for 2B = A, S the horizontal component H, to the left of the vector diagram, can be seen to decrease after the initial increase.

In Chapter III hook forms were described in terms of the successive arrival of longitudinal and circularly polarized transverse waves to illustrate how the polarized component obeyed the direction of polarization rules. However, because of coupling of the modes, the SC perturbation is probably due to a coupled wave with both longitudinal and transverse components. Thus there may not be any time delay between the arrivals of the two components. In the synthesized vector diagrams in Figure 5-1 there are forms which closely resemble the hook forms as shown in Figure 5-4 #11 and #12. Thus for model I, 2B = A, S or E initial phase in Figure 5-1, the vector diagrams are almost hook forms. If the longitudinal component were larger the similarity to a hook would be even greater. According to the diagram given in Figure 5-8 for the initial phase of the 0 wave (counter-clockwise in the northern hemisphere from 2200 to 1000 hours), the initial phase will be S or E for the 0 wave around 2200 to 0400 hours. In Table 3-3, giving the polarization and local times of 15 hook (h) forms, all the cases of hook forms for the 0 wave (cc polarization) occurred from 0230 to 0437 hours local time.

The hook form can thus also be explained as a consequence of the particular initial phase of the polarized component of the SC field and the particular ratio of the amplitudes of the two components. Most hook forms are observed at low latitudes where $B > A$; this gives further support to the above argument.

The DS current systems for SC's devised by Sano (1962), Watanabe (1961) and Oguti (1956) based on the precipitation of charged particles into the polar ionosphere do not account for the behavior of the SC field near the geomagnetic poles. The vector diagrams for SC's at Godhavn ($\Phi = 79.^{\circ}8$) and Scott Base ($\Phi = 79.^{\circ}0$), given in Figures 3-4 and 3-5, are of open elliptical and circular polarization and the directions of the polarizations are random. Any DS current system which shows parallel flow over the polar cap, such as that given by Obayashi and Jacobs (1957), cannot account for the rotation of $\underset{\sim}{\Delta H}$ near the pole. The DS current system of Watanabe or of Oguti (1956), which rotates clockwise for SC*, could not explain for frequent counterclockwise rotation of the SC field observed during SC(- +).

The DS current system for SC's proposed by Sano (1962) accounts for the zones of opposite SC direction of polarization by assuming that the foci of the DS_p and DS_m current systems increase in latitude with storm time during the SC. However, the zones of precipitation of the charged particles from the "horns" in the Chapman-Ferraro model shift toward lower latitudes as the current sheet compresses the field farther and farther instead of shifting poleward as required by the mechanism proposed by Sano (1962). Although the current systems shown by Sano (1962) for 4 SC's do give the SC fields for the first few minutes during the preliminary reversed impulse and main impulse, these current systems would have to move southward again

to explain the next few minutes of the SC field variations. For the SC of 0622 U.T. August 17, 1958 the SC field is oscillatory for many cycles. To account for such pulsative SC's the DS current system foci given by Sano (1962) would have to oscillate back and forth.

From all the above considerations it would seem that the currents in the ionosphere which are responsible for the SC field are the currents that result from hydromagnetic waves incident upon the ionosphere from above.

Proof of the existence of both transverse and longitudinal hydromagnetic waves deep in the magnetosphere far above the ionosphere has been obtained by the earth satellite Explorer 6, Judge and Coleman (1962). They found hydromagnetic waves of period 100 to 500 seconds. When the satellite was at 1900 local time, the magnetometer of Explorer 6 observed a circularly polarized transverse hydromagnetic wave. The direction of polarization was clockwise when looking along the field which defines it as an extraordinary wave. As Judge and Coleman (1962) state, the direction of polarization of this transverse wave is consistent with the polarization rules given by Wilson and Sugiura (1961) for SC hydromagnetic waves.

Although this observation of a circularly polarized hydromagnetic wave in the magnetosphere was not of an SC wave, there is a close connection between giant pulsations and SC oscillations as has been discussed in Chapter IV. Sugiura (1963) has found that giant pulsations obey the same polarization rules as those for the elliptically polarized SC's.

CHAPTER VII

CONCLUSIONS

The storm time variations of the total horizontal disturbance vector of the SC field have been investigated by both the statistical approach using many SC's at individual stations and by the specific approach of studying individual SC's at many magnetic observatories, and a new morphology of the SC field has been obtained. The main features of the SC morphology and their relation to the model proposed for the generation of the SC field are summarized below.

1) Polarization of SC field

Vector diagrams of the total horizontal disturbance vector for the first five minutes of SC's of magnetic storms exhibit elliptical polarization at moderate to high latitudes. The direction of polarization of the SC field is determined by the local time and hemisphere in which it is observed. From 2200 to 1000 hours of local time, the polarization is counterclockwise in the northern and clockwise in the southern hemisphere; whereas from 1000 to 2200 hours, the polarization is clockwise in the northern and counterclockwise in the southern hemisphere. This pattern of polarization of the SC field follows directly from the generation of a circularly polarized transverse hydromagnetic wave in the ordinary mode in the morning hemisphere and from the generation of an extraordinary wave in the evening hemisphere. The direction of polarization of the O wave is counterclockwise looking along the direction of the field line while for the E wave it is clockwise. The directions of polarization for O and E waves are independent of the direction of propagation of the wave and thus when the polarization is viewed downward on the earth's surface, the direction of

the 0 wave and E wave polarizations become reversed from the northern to the southern hemisphere. The initial counterclockwise (as viewed along the direction of the field) perturbation of the field lines in the morning hemisphere, to produce an 0 wave, is caused by the blowing back of the equatorial portions of the frozen-in field lines by the SC shock wave. The initial clockwise perturbation in the E mode is generated in the evening hemisphere in a similar manner. The circularly polarized 0 and E waves propagate to the earth to give the elliptically polarized SC field observed in moderate to high latitudes.

2) Phase of the polarized component of SC field

Over the morning hemisphere in the northern hemisphere the initial phase of the circularly polarized component of the SC field rotates from south at 2200, to east 0400, to north at 1000 hours of local time monotonically with local time. This rotation of the initial phase of the 0 wave indicates that the initial perturbation of the field line, where the field line through the station loops across the equatorial plane, is antiparallel to the direction of the propagation of the shock. It is assumed that the solar wind blows parallel to the 1000-2200 hour meridian plane and that the initial perturbation propagates to the earth without any rotation about the field line.

The phase of the E wave over the evening hemisphere is not as regular as that of the 0 wave; however, the variation of the phase of the E wave seems to be given by the reflection of the 0 wave initial phase across the 1000-2200 hour meridian plane. The initial phase of the circularly polarized component in the southern hemisphere can always be determined by reflection across the east-west line of the corresponding initial phase direction in the northern hemisphere.

3) Variation of degree of polarization of SC field with latitude and local time.

If the SC field is resolved into two components; namely, a circularly polarized transverse component and a linearly polarized longitudinal component, then the type of polarization of the SC field can be described in terms of the relative amplitude of the transverse and longitudinal components. The morphology of the SC field is such that: the longitudinal component is greater at low latitudes, the two compoents are equal at moderate latitudes, and the transverse component is greater at high latitudes. Superimposed on this increase in the degree of elliptical polarization of the SC field with increasing latitude is an increase at all latitudes in the size of the transverse component relative to that of the longitudinal component near the 0400 and 1600 local time meridians. This distribution of the transverse SC field component follows from the ducting of the transverse hydromagnetic waves along the field lines to high latitudes and from the fact that a maximum twist of the field lines is produced in the meridians at 0400 and 1600 hours local time, where the direction of propagation of the shock wave is nearly perpendicular to the plane of field lines.

The dominance of the longitudinal component at low latitudes follows from the fact that the longitudinal hydromagnetic wave carries a perturbation parallel to the field in equatorial latitudes.

4) Polarization of the SC field at very high latitudes

Above geomagnetic latitude of about $72.^{\circ}0$, corresponding to an r_e distance of 10 earth radii, the SC field is always circularly polarized but with random direction of polarization. This follows from the fact that the field lines are no longer of simple dipole configuration at very high

latitudes. The latitude at which the SC field polarization no longer follows the pattern described above can be used as a measure of the size and shape of the magnetic cavity.

5) Oscillation of the SC field

The percentage of occurrence of strong oscillation at SC's is a maximum of about 80% of the SC's at auroral zone latitudes and decreases rapidly both north and south of this zone. The field lines from the auroral zone cross the equatorial plane just inside the boundary of the magnetic cavity and thus would experience the full force of the impact of the enhanced solar wind. The power spectra of the oscillations has a harmonic structure. Thus the SC oscillations are thought to be a resonance phenomenon excited in the field by the impact.

6) Local time and latitude variations in the shape of the SC field vector diagram

The shape of SC vector diagrams of $\underset{\sim}{\Delta H}$ and the classification of SC's in terms of the H variation both depend on the initial phase of the circularly polarized component and on the relative amplitudes and time dependency of the transverse and longitudinal components. The frequency of occurrence of the various types of SC vector diagrams, corresponding, for example, to SC(-+) or SC(+-), is thus determined by the variation over the earth of these parameters.

From the vector diagram model it was found that for counterclockwise polarization SC(+-) will always occur if the initial phase is north and that SC(-+) will always occur if the initial phase is west; while for clockwise polarization SC(+-) will always occur if the initial phase is north and SC(-+) will always occur if the initial phase is east. For either polarization hook forms will always occur for south initial phase. The maximum

frequency of occurrence of SC(+-) around 0900 hours local time and the absence of SC(-+) in the morning hours are in agreement with the initial phase of the 0 wave as predicted by the model. The observed initial phases of the SC(-+)'s are all in agreement with the phases predicted by the vector diagram model.

7) SC vector diagrams for magnetically conjugate stations

The shape of the vector diagrams of an SC observed at conjugate stations depends on the initial phase of the circularly polarized component. If the initial phase of this component is N, S, E or W for the SC in the northern hemisphere, then the corresponding conjugate vector diagram for the SC in the southern hemisphere can be found by a simple reflection about the X' axis of a northern hemisphere vector diagram for an initial phase of S, N, W and E respectively.

The rather complete agreement between the observed morphology of the SC field and the characteristics of the SC field predicted by the model as well as the physically tenable nature of the model itself offer strong support to the SC model propsed in this thesis.

APPENDIX I

DATA REDUCTION FOR VECTOR DIAGRAMS

Most of the rapid-run magnetograms of H and D were scaled manually in order to obtain ΔH and ΔD for the calculation of $\Delta X'$ and $\Delta Y'$ from which the vector diagrams were plotted. However, when an Oscar K oscillograph analyzer and reader, manufactured by the Benson-Lehner Corporation, became available the data reduction was done using this machine. The H and D rapid-run magnetograms were mounted on the Oscar K in such a manner that both of these elements were scaled simultaneously. The values of the deviation of H and D from the pre-SC base line values were automatically punched on IBM cards by the Oscar K with one card being used for each time interval. These data cards, along with a card giving the base line and scale values for H and D and the angle $D\text{-}\psi$, were read into an IBM 1620 computer that was programmed to calculate $\Delta X'$, $\Delta Y'$, $|\underset{\sim}{\Delta H}|$ and arctan $\Delta X'/\Delta Y'$ for each time interval. The Fortran program used for obtaining the vector components of $\underset{\sim}{\Delta H}$ is given below.

```
C       VECTOR COMPONENTS FOR C.R. WILSON
C
        PUNCH 103
2       READ 100,SH,SD,THE,B,C
        TH=THE*.01745329
1       READ 101,H,D,  T, DI,I
        IF(I-9999)3,2,3
3       D=B-D
        H=H-C
        DD = D*SD
        DH = H*SH
        Y = DD*COS(TH)+DH* SIN(TH)
        X = DH*COS(TH)-DD*SIN(TH)
        IF(Y)10,11,10
11      THTA = 90.0
        GO TO 12
10      THTA = ATAN(X/Y)
        THTA = THTA*57.29578
12      IF(X)5,6,6
```

```
5       THTA = THTA+180.0
6       R = SQRT(X*X+Y*Y)
        PUNCH 102, T,X,Y, R,DH,DD,THE,DI,THTA
        GO  TO  1
100     FORMAT(5F8.3)
101     FORMAT (4F10.8,I4)
102     FORMAT (F8.6,6F8.3,3XF8.6,2XF8.2)
103     FORMAT(5H TIME,7X1HX,7X1HY,7X1HR,7X2HDH,6X2HDD,3X5HTHETA,13X2HID)
        END
```

APPENDIX II

POWER SPECTRUM ANALYSIS OF SC OSCILLATIONS

The power spectrum of the SC oscillations discussed in Chapter IV were obtained by the use of an IBM 1620 computer and a program developed by Mr. E. J. Gauss of the Geophysical Institute staff. The SC oscillations in H were scaled with the Oscar K at intervals of one millimeter which corresponds to a time interval of about 12 seconds. Five data points per card were used for the input data to the computer. The output of the 1620 computer was in the form of relative power per cycle per second at each frequency listed. The program is written assuming that the data points are scaled at one second intervals. Thus to convert the listed frequencies to the actual period in seconds, it was necessary to divide the scaling time interval in seconds by the listed frequencies. The Fortran program used with the IBM 1620 computer for the power spectrum analysis is given below.

```
C       SPECTRAL III
C       E J GAUSS
        DIMENSION A(31),TM(31),SS(31),SC(31),W(31),Y(31),Z(31)
        DIMENSION V(8)     .
        PRINT 22
   22   FORMAT (//33HPOWER SPECTRAL DENSITY ESTIMATION/)
        PRINT 41
   41   FORMAT (38HGEOPHYSICAL INSTITUTE U OF ALASKA 1962/)
   21   L=9
        READ 5,F1,CA,ILIM,TLIM,KA,LWPC
    5   FORMAT (F10.9,F10.9,I2,F10.7,I3,I3)
         IF (SENSE SWITCH 1) 23,24
   24   XAVE=0.0
        SIGMA=1.0
         GO TO 3
   23   PRINT 28
   28   FORMAT (49HFIRST DATA PASS NORMALIZES, SECOND PASS REQUIRED )
         R=0.0
        C=0.0
        TP=0.0
   25   CONTINUE
        L=L+1
        IF(L-LWPC)101,101,102
```

```
102  L=1
     READ 15,V(1),V(2),V(3),V(4),V(5),V(6),V(7)
 15  FORMAT (F10.9,F10.9,F10.9,F10.9,F10.9,F10.9,F10.9)
101  X=V(L)
     IF (X-100000.) 29,26,26
 29  TP=TP+X
     C=C+1.0
     R=R+X*X
     GO TO 25
 26  XAVE=TP/C
     SIGMA=SQRT((R/C-XAVE*XAVE))
     RSIG=1.0/SIGMA
     PRINT 27,XAVE,SIGMA
 27  FORMAT (5HXAVE=E12.5,8H  SIGMA=E12.5//)
  3  T=0.0
     TPC=4.0*F1/CA
     DO 7 I=1,ILIM
     SS(I)=0.0
     SC(I)=0.0
     A(I)=0.0
     TM(I)=0.0
     W(I)=CA*TPC
     Y(I)=0.0
     Z(I)=0.0
  7  TPC=W(I)
      L=9
     IF (SENSE SWITCH 2) 1,6
  1  PRINT 30
 30  FORMAT (34H  T            FREQ.          COEF./)
  6  CONTINUE
  4  T=T+1.0
     IF (SENSE SWITCH 3) 44,42
 42  L=L+1
     IF (L-LWPC) 301,301,302
302  L=1
     READ 15,V(1),V(2),V(3),V(4),V(5),V(6),V(7)
301  X=V(L)
     IF(X-100000.) 8,11,11
 44  TP=0.0
     DO 43 K=1,KA
     L=L+1
     IF(L-LWPC)201,201,202
202  L=1
     READ 15,V(1),V(2),V(3),V(4),V(5),V(6),V(7)
201  X=V(L)
     IF(X-100000.) 43,11,11
 43  TP=TP+X
     TK=K
     X=X/TK
  8  X=X-XAVE
     X=X*RSIG
     DO 2 J=1,ILIM
```

```
    A(J)=A(J)+W(J)
    TM(J)=TM(J)+W(J)
    IF (TM(J)-TLIM) 9,9,10
10  TP=((SS(J)*SS(J))+(SC(J)*SC(J)))/(TM(J)-W(J))
    TF=W(J)/4.0
    IF (SENSE SWITCH 2) 12,13
12  TPA=TP*W(J)*W(J)
    PRINT 14,T,TF,TPA
14  FORMAT (F5.0,6XF10.3,5XF10.5)
13  Z(J)=Z(J)+TP
    Y(J)=Y(J)+1.0
    SS(J)=0.0
    SC(J)=0.0
    TM(J)=TM(J)-TLIM
 9  IF (A(J)-4.0) 38,38,37
37  A(J)=A(J)-4.0
    GO TO 9
38  IF (A(J)-2.0) 39,39,40
39  SS(J)=SS(J)+X*(1.0-(A(J)-1.0)*(A(J)-1.0))
    GO TO 32
40  SS(J)=SS(J)-X*(1.0-(A(J)-3.0)*(A(J)-3.0))
32  TP=A(J)+1.0
    IF(TP-4.0) 33,33,34
34  TP=TP-4.0
33  IF (TP-2.0) 35,35,36
35  SC(J)=SC(J)+X*(1.0-(TP-1.0)*(TP-1.0))
    GO TO 2
36  SC(J)=SC(J)-X*(1.0-(TP-3.0)*(TP-3.0))
 2  CONTINUE
    GO TO 4
11  PRINT 20,T
20  FORMAT (/2HT=F5.0//25H   FREQ.            COEF.    /)
    DO 16 J=1,ILIM
    IF (Y(J)) 17,18,17
17  TP=Z(J)/Y(J)
    TF=W(J)/4.0
    TP=TP*W(J)*W(J)
    PRINT 19,TF,TP
19  FORMAT (F10.4,5XF10.5)
18  CONTINUE
16  CONTINUE
    PRINT 31
31  FORMAT  (/35HDONE, TO BEGIN A NEW RUN PUSH START/)
     PAUSE
    GO TO 21
    END
```

Table A-1

SC's used in the Analysis with the I.G.Y. Designation of the Stations for which the SC was Scaled

Time U.T.	Date							
0016	29-9-57	C277	C236	B318	B009	A107	A092	A039
		A103	C957	C925	A995	A977		
0022	29-8-60	B318	A092	A103	A977			
0022	29-9-60	A039						
0043	16-2-61	A092						
0044	16-2-61	A149						
0046	7-6-58	C277	C236	B318	A149	A039	C925	A997
		A995	A977					
0046	7-7-58	C957						
0046	22-2-59	A103	A997					
0048	25-6-57	C277	C236	A092	A039	C925	A995	A977
0048	25-9-58	B009						
0109	28-10-58	C957	A977					
0109	28-11-58	C277	C236	B318	B009	A149	A039	C925
		A997	A995					
0125	11-2-58	C236	B318	B009	C277			
0127	10-4-60	B318	A149	A092	A039	A977		
0132	30-4-60	A149	A092	A103	A977			
0137	5-1-59	B318	A092	A039	A103	A997		
0145	27-6-60	B318	A092	A039	A977	A103		
0201	5-1-60	A149						
0230	4-9-60	B318	A149	A092	A039			
0252	13-2-61	A092						
0253	13-2-61	A149						

Time U.T.	Date							
0318	11-2-59	B318	A103	A997				
0403	16-8-59	B318	A149	A039	A103			
0408	25-9-58	C236 C925	B318 A995	B009	A149	A107	A039	A103
0421	8-5-60	B318	A149	A092				
0434	11-5-60	B318	A149					
0447	14-7-60	A149						
0508	6-8-57	C277 A039	C236 C925	B318	B009	A149	A107	A092
0540	24-5-59	B318	A149	A092	A103	A997		
0622	17-8-58	C236	A039	C925	A997	A995		
0650	28-10-58	C277 C925	C236 A997	B318 A995	B009 A977	A149	A039	A103
0656	27-9-61	A092						
0659	5-12-59	B318	A149	A092	A103	A977		
0714	16-7-57	C277 A995	C236 A977	B318	B009	A149	A107	A092
0718	10-1-60	B318	A149	A039				
0748	8-7-58	C277	B009	A039	C957	A995		
0755	11-2-59	A149	A092					
0803	15-7-59	B318	A149	A092	A039			
0842	26-3-59	A149	A092	A039	A997			
0857	2-7-57	C277 C925	C236 A995	B009 B318	A107	A092	A039	C957
0859	25-1-59	A997						
0908	11-6-59	B318	A103	A997				
0925	11-2-58	A995						

Time U.T.	Date							
0931	3-3-58	C277 C957	C236 A997	B318 A995	B009	A149	A107	A103
0931	3-4-58	A977						
0937	19-12-57	C236 A997	B318 A995	B009 C277	A149	A107	A092	C925
1005	30-9-58	C277 A149	C236 A107	B009 C925	C957 A977	A103	A997	B318
1005	21-9-57	B318	A149	A107	C925	A995	A977	
1035	23-4-59	B318	A149	A092	A039	A103	A997	
1040	25-3	B318						
1212	14-3-58	C277 A103	C236 C957	B318 C925	B009 A997	A149 A995	A107 A977	A092
1247	26-4-58	C277 C957	C236 C925	B318 A997	B009 A995	A149 A977	A107	A092
1304	15-11-60	B318						
1345	22-9-57	C277	C236	B009	A149	C925	A977	A107
1347	9-8-57	C236 A977	B009 C925	A107	A092	A039	A103	C957
1348	12-11-60	B318	A149	A092	A039			
1349	12-10-60	A977						
1350	16-5-60	B318						
1409	16-8-60	A149	A092	A039	A977			
1441	19-1-61	A092						
1451	13-4-61	A149						
1452	24-10-60	B318	A149	A977				
1510	14-8-60	A977						
1511	7-4-60	A103						

Time U.T.	Date							
1525	23-12-59	B318	A103					
1540	25-3-58	C277 A995	C236 A977	B009	A107	A092	C957	C925
1557	3-8-57	C277 A103	C236 C957	B009 C925	A149 A977	A107	A092	A039
1615	19-8-60	B318						
1615	16-8-60	A149						
1616	19-8-60	A977						
1635	21-7-58	A039						
1637	21-7-58	C277	A149	A107	C957	A977		
1638	17-7-59	A149						
1642	16-2-58	C277 A997	C236 A995	B318 A977	A107	A103	C957	C925
1652	31-5-58	C236	B318	A039	C957	A977		
1702	14-7-60	B318	A149	A092	A977			
1742	28-6-58	C277 A103	C236 C957	B009 C925	A149 A997	A107 A995	A092	A039
1804	7-12-60	B318	A149					
1812	31-8-57	C277	C236	A149	C957	C925		
1817	17-12-58	C277 A977	C236	B318	A149	A103	C957	C925
1828	14-6-58	C277 A103	C236 C957	B318 C925	B009 A997	A149 A995	A107 A977	A039 A092
1828	9-4-59	B318	A149	A092				
1859	13-1-60	B318	A149	A092	A039	A977		
1909	30-11-60	B318	A149	A039	A103	A977	A092	
1939	29-6-60	A977	A039	A092	A149	B318		
2000	27-4-60	B318	A149	A092	A039	A103		

Time U.T.	Date							
2019	28-5-60	A149	B318					
2020	4-5-59	B318	A149	A997				
2022	15-12-58	C277 A103	C236 C957	B318 C925	B009 A995	A149 A977	A107	A039
2027	17-2-61	A092						
2108	30-9-61	A092						
2159	3-9-59	A149	A103					
2241	21-10-57	B009	A149	C957	C925	A995		
2312	2-4-60	B318	A149	A092	A977			
2319	24-2-59	A149						
2323	24-2-59	A092	A103	A997				
2327	11-5-59	A149	A997					
2351	27-11-59	B318	A149	A092	A039	A103	A977	

Table A-2

List of I.G.Y. Sudden Commencements

No.	GMT	Date	No.	GMT	Date
1	0016	Sept.29, 1957	21	1212	Mar. 14, 1958
2	0042	July 5, 1957	22	1247	Apr. 26, 1958
3	0046	June 7, 1958	23	1300	Sept. 4, 1957
4	0048	June 25, 1957	24	1345	Sept.22, 1957
5	0109	Nov. 28, 1958	25	1347	Aug. 9, 1957
6	0125	Feb. 11, 1958	26	1529	July 31, 1958
7	0315	Oct. 22, 1958	27	1540	Mar. 25, 1958
8	0408	Sept.25, 1958	28	1557	Aug. 3, 1957
9	0508	Aug. 6, 1957	29	1637	July 21, 1958
10	0650	Oct. 28, 1958	30	1642	Feb. 16, 1958
11	0714	July 16, 1957	31	1742	June 28, 1958
12	0748	July 8, 1958	32	1812	Aug. 31, 1957
13	0843	Sept. 3, 1958	33	1817	Dec. 17, 1958
14	0857	July 2, 1957	34	1821	Nov. 6, 1957
15	0930	Sept.16, 1958	35	1828	June 14, 1958
16	0931	Mar. 3, 1958	36	1920	Aug. 29, 1957
17	0937	Dec. 19, 1957	37	2022	Dec. 15, 1958
18	1005	Sept.21, 1957	38	2241	Oct. 21, 1957
19	1005	Sept.30, 1958	39	1652	May 31, 1958
20	1050	Jan. 25, 1958	40	0622	Aug. 17, 1958

REFERENCES

Abe, S., Morphology of SSC and SSC*, J. of Geomag. and Geolect. 10, p. 153, 1959.

Akasofu, S.-I. and S. Chapman, The Sudden Commencement of Geomagnetic Storms, Variana, No. 250, 1960.

Alfvén, H., Existence of Electromagnetic-hydrodynamic Waves, Nature, 150, p. 405, 1942.

Alfvén, H., Cosmical Electrodynamics, Oxford University Press, 1950, p. 87.

Åstrom, E., On Waves in an Ionized Gas, Ark. f. fysik, 2, p. 443, 1950.

Benioff, H., Observations of the Geomagnetic Fluctuations in the Period Range 0.3 to 120 seconds, J. Geophys. Research, 65, p. 1413, 1960.

Berthold, W. A., A. K. Harris, and H. J. Hope, Correlated Micropulsations at Magnetic Sudden Commencements, J. Geophys. Research, 65, p. 613, 1960.

Cahill, L. J., and P. Amageen, The Boundry of the Geomagnetic Field, Dept. of Physics Report, U. of New Hampshire, Durham, N.H., 1962.

Carmichael, H., and J. F. Steljes, Review of Recent High-energy Solar Particle Events Including November 1960, Rept. CRGP-1056, Atomic Energy of Canada Std., Physics Division, Deep River, Ontario, from Proc. Kyoto Conf. Cosmic Radiation and Earth Storm, 1961.

Chapman, S., and V.C.A. Ferraro, A New Theory of Magnetic Storms, Terrestrial Magnetism and Atmospheric Elec., 36, pp. 77-97, 171-186, 1931; 37, pp. 147-156, 421-429, 1932; The Theory of the First Phase of a Geomagnetic Storm, Terrestrial Magnetism and Atmospheric Elec., 45, 245-268, 1940.

Chapman, S., and J. Bartels, Geomagnetism, Oxford Univ. Press, 1940.

Chapman, S., The Electrical Conductivity in the Ionosphere, A Review, II Nuovo Cimmento Supp. No. 4, 4, p. 1385, 1956.

Chapman, S., and H. Sugiura, Arc-lengths Along the Lines of Force of a Magnetic Dipole, J. Geophys. Research, 61, p. 485, 1956.

Coleman, P. J., Jr., C. P. Sonett, D. L. Judge and E. J. Smith, Some Preliminary Results of the Pioneer V Magnetometer Experiment, Journal Geophysical Research, 65, 1856-1857, 1960.

Davis, T. N., The Morphology of Auroral Displays of 1957-1958. 2. Detail Analysis of Alaska Data and Analysis of High-latitude Data, J. Geophys. Research, 67, p. 75, 1962.

Dawson, J. and M. Sugiura, Pearl-Type Micropulsations in the Auroral Zones: Polarization and Magnetic Conjugacy, read at 44th Annual Meeting of American Geophysical Union, April 19, 1963.

Dessler, A. J., The Propagation Velocity of World-wide Sudden Commencements of Magnetic Storms, J. Geophys. Research, 63, p. 405, 1958.

Dessler, A. J. and E. N. Parker, Hydromagnetic Theory of Geomagnetic Storms, J. Geophys. Research, 64, p. 2239, 1959.

Dessler, A. J., W. E. Francis and E. N. Parker, Geomagnetic Storm Sudden-Commencement Rise Times, J. Geophys. Research, 65, p. 2715, 1960.

Dessler, A. J., Further Comments on Stability of Interface between Solar Wind and Geomagnetic Field, Journal Geophysical Research, 67, 4892-4894, 1962.

Dungey, J. W., The Propagation of Alfvén Waves Through the Ionosphere, Pennsylvania State University Sci. Rept., No. 57, 1954.

Dungey, J. W., The Physics of the Ionosphere, Physical Society, London, p. 229, 1955.

Dungey, J.W.,Cosmic Electrodynamics, Cambridge Press, p. 73, 1958.

Dungey, J. W., The Steady State of the Chapman-Ferraro Problem in Two Dimensions, J. Geophys. Research, 66, p. 1043, 1961.

Dungey, J. W., Private Communication, 1962.

Dvoryashin, A. S., L. S. Levitskii, and A. K. Pankratov, Active Solar Regions and their Corpuscular Emission, Soviet Astron., 5, (3), 311-325, 1961.

Fejer, J., Hydromagnetic Wave Propagation in the Ionosphere, Jour. Atmos. Terr. Phys., 18, p. 135, 1959.

Ferraro, V.C.A., W. C. Parkinson, and H. W. Unthank, Sudden Commencements and Sudden Impulses in Geomagnetism, J. Geophys. Research, 56, p. 177, 1951.

Ferraro, V. C. A., Theory of the Sudden Commencement and the First Phase of a Magnetic Storm, Rev. Mod. Phys., 32, p. 934, 1960.

Francis, W. E., and R. Karplus, Hydromagnetic Waves in the Ionosphere, J. Geophys. Research, 65, p. 3593, 1960.

Gold, T., Gas Dynamics of Cosmic Clouds, ed. by H. C. Van de Hulst and J. M. Burgers, North-Holland Publ. Co., Amsterdam, 1955, p. 103.

Gold, Thomas, Plasma and Magnetic Fields in the Solar System, J. Geophys. Research, 64, 1665-1674, 1959.

Hasegawa, M., On the Position of the Focus of the Geomagnetic Sq Current System, J. Geophys. Research, 65, p. 1437, 1960.

Heppner, J. P., N. F. Ness, C. S. Scearce, and T. L. Skillman, Explorer X Magnetic Field Measurements, J. Geophys. Research, 68, p. 1, 1963.

Hurley, J., Interaction of a Streaming Plasma with the Magnetic Field of a Two Dimensional Dipole Phys. of Fluids, 4, p. 854, 1961.

Jackson, W., World-side Simultaneous Magnetic Fluctuations and their Relation to Sudden Commencements, Jour. Atmos. Terr. Phys., 2, p. 160, 1952.

Johnson, F. S., The Gross Character of the Geomagnetic Field in the Solar Wind, J. Geophys. Research, 65, p. 3049, 1960.

Judge, D. L., and P. J. Coleman Jr., Observations of Low-frequency Hydromagnetic Waves in the Distant Geomagnetic Field: Explorer 6, J. Geophys. Research, 67, p. 5071, 1962.

Kahalas, S., Magnetohydrodynamic Wave Propagation in the Ionosphere, Phys. of Fluids, 3, p. 372, 1960.

Kato, Y., and T. Saito, On the Damped Type Rapid Pulsation Accompanying SSC, Science Reports, Tohoku University, Geophys., 9, p. 99, 1958.

Kato, Y., Investigation of the Geomagnetic Rapid Pulsation, Science Reports, Tohoku University, Geophys., 11, p. 1, 1959.

Lehnert, B., Magneto-hydrodynamic Waves in the Ionosphere and their Application to Giant Pulsations, Tellus, 8, p. 241, 1956.

MacDonald, G., Spectrum of Hydromagnetic Waves in the Exosphere, J. Geophys. Research, 66, p. 3639, 1961.

Maeda, H., On the Geomagnetic Sq Field, Journal of Geomag. and Geolect. 10, p. 66, 1959.

Matsushita, S., On Sudden Commencements of Magnetic Storms at High Latitudes, J. Geophys. Research, 62, p. 162, 1957.

Matsushita, S., Studies on Sudden Commencements of Geomagnetic Storms using I.G.Y. Data from United States Stations, J. Geophys. Research, 65, p. 1423, 1960.

Matsushita, S., On Geomagnetic Sudden Commencements, Sudden Impulses, and Storm Duration, J. Geophys. Research, 67, p. 3753, 1962.

Mead, G. D., Paper Presented at the Second Western National Meeting of American Geophysical Union, December 27-29, 1962.

Midgeley, J. E., and L. Davis Jr., Computation of the Bounding Surface of a Dipole Field in a Plasma by a Moment Technique, J. Geophys. Research, 67, p. 499, 1962.

Nagata, T., Distribution of SC* of Magnetic Storms, Rep. Ionosphere Res. Japan, 6, 13, 1952.

Nagata, T., and S. Abe, Notes on the Distribution of SC* in High Latitudes, Rep. Ionospheric Research, Japan, 9, p. 39, 1955.

Neugebauer, M., and C. W. Snyder, Paper Presented at the Symposium on Results of the Venus Probe, Mariner II, The Second Western National Meeting of American Geophysical Union, Stanford, December 27-29, 1962.

Newton, H. W., Sudden Commencements in the Greenwich Magnetic Records (1879-1944) and Related Sunspot Data, Mon. Not. Roy. Astron. Soc., Geophys. Suppl. 5, p. 159, 1948.

Nishida, A., World Wide Changes in the Geomagnetic Field, Ph. D. Thesis, University of British Columbia, 1962.

Obayashi, Totsujo, and Yukio Hakura, Propagation of Solar Cosmic Rays through Interplanetary Magnetic Field, J. Geophys. Research, 65, 3143-3148, 1960.

Obayashi, T., Geomagnetic Pulsations and the Earth's Outer Atmosphere, Ann. de Geophys., 14, p. 464, 1958.

Obayashi, T., and A. J. Jacobs, Sudden Commencements of Magnetic Storms and Atmospheric Dynamo Action, J. Geophys. Research, 62, p. 589, 1957.

Oguti, T., Notes on the Morphology of SC, Rep. Ionosphere Res., Japan, 10, p. 81, 1956.

Parker, E. N., Interaction of the Solar Wind with the Geomagnetic Field, Phys. of Fluids, 1, p. 171, 1958.

Parker, E. N., Dynamics of the Interplanetary Gas and Magnetic Fields, Astrophys. Journal, 128, 664-676, 1958.

Parker, E. N., Sudden Expansion of the Corona Following a Large Solar Flare and the Attendant Magnetic Field and Cosmic-ray Effects, Astrophys. Journal, 133, p. 1014, 1961.

Parker, E. N., Dynamics of the Geomagnetic Storm, Space Science Reviews, 1, p. 62, 1962.

Piddington, J., Electromagnetic Field Equations for a Moving Medium with Hall Conductivity, Monthly Notices, Roy. Astron. Society, 114, p. 638, 1954.

Piddington, J., Hydromagnetic Waves in Ionized Gas, Monthly Notices, Roy. Astron. Society, 115, p. 671, 1955.

Piddington, J., The Transmission of Geomagnetic Disturbances through the Atmosphere and Interplanetary Space, J. Geophys. Roy. Astron. Society, 2, p. 173, 1959.

Piddington, J., A Theory of Polar Geomagnetic Storms, J. Geophys. Roy. Astron. Society, 3, p. 314, 1960.

Reid, G., and H. Leinbach, Low-energy Cosmic-ray Events Associated with Solar Flares, J. Geophys. Research, 64, 1801-1805, 1959.

Sano, Y., Morphological Studies on Sudden Commencements of Magnetic Storms using the Rapid-run Magnetograms during the I.G.Y., Jour. of Geomag. and Geoelect., 14, p. 1, 1962.

Singer, S. F., A New Model of Magnetic Storms and Aurora, Trans. Aner. Geophys. Union, 38, p. 175, 1957.

Slutz, R. J., The Shape of the Geomagnetic Field Boundry under Uniform External Pressure, J. Geophys. Research, 67, p. 505, 1962.

Smith, R. L., Properties of the Outer Ionosphere Deduced from Nose Whistlers, Journal Geophysical Research, 66, p. 3709, 1961.

Sonett, C. P., E. J. Smith and A. R. Sims, Space Research, edited by H. Kallman-Byl, North-Holland Publ. Co., Amsterdam, 1960, pp. 921-937.

Spreiter, J. R., and B. R. Briggs, Theoretical Determination of the Form of the Boundary of the Solar Corpuscular Stream Produced by Interaction with the Magnetic Dipole Field of the Earth, J. Geophys. Research, 67, p. 37, 1962.

Sugiura, M., Evidence of Low Frequency Hydromagnetic Waves in the Exosphere, J. Geophys. Research, 66, p. 4087, 1961.

Sugiura, M., Private Communication, 1962 and 1963.

Vestine, E. H., The Immediate Source of the Field of Magnetic Storms, J. Geophys. Research, 58, p. 560, 1953.

Vestine, E. H., and J. W. Kern, Cause of the Preliminary Reverse Impulse of Storms, J. Geophys. Research, 67, p. 2181, 1962.

von Kenschitzki, C. H., and E. J. Stegelmann, The Propagation of Alfvén Waves in the Earth's Magnetosphere, paper presented at A.G.U. meeting Jan. 31 to Feb. 2, Tucson, Arizona, 1962.

Watanabe, T., Studies on P.S.C. After the Ashour-Price's Model for the Ionospheric Shielding Effect, Science Reports, Tohoku University, Geophys. 8, p. 9, 1956.

Watanabe, T., Geomagnetic Bays and Storm Sudden Commencements in High Latitudes, Science Reports, Tohoku University, Geophys. 13, p. 62, 1961.

Wescott, E., and K. Mather, Diurnal Effects in Magnetic Conjugacy at Very High Latitudes, Nature, 197, p. 1259, 1963.

Wilson, C. R. and M. Sugiura, Hydromagnetic Interpretation of Sudden Commencements of Magnetic Storms, J. Geophys. Research, 66, p. 4097, 1961.

Wilson, C. R., Sudden Commencement Hydromagnetic Waves and the Enhanced Solar Wind Direction, J. Geophys. Research, 67, p. 2054, 1962.

AF Cambridge Research Laboratories, Bedford, Mass. UNCLASSIFIED

HYDROMAGNETIC INTERPRETATION OF SUDDEN COMMENCEMENTS OF GEOMAGNETIC STORMS, by C.R. Wilson, May 1963. 161 pp.

AFCRL-63-605 Unclassified report I. Wilson, C.R.

A new hydromagnetic model for the sudden commencement (SC) of a magnetic storm is presented. The model is based on a new morphology of the SC field in which the polarization of the field is interpreted in terms of circularly polarized transverse and linearly polarized longitudinal hydromagnetic (HM) waves. The variation of the types of SC's with local time and latitude is explained in terms of the initial phase and direction of polarization of the circularly polarized HM wave and the relative amplitude of the linearly polarized HM wave.

AF Cambridge Research Laboratories, Bedford, Mass. UNCLASSIFIED

HYDROMAGNETIC INTERPRETATION OF SUDDEN COMMENCEMENTS OF GEOMAGNETIC STORMS, by C. R. Wilson, May 1963. 161 pp.

AFCRL-63-605 Unclassified report I. Wilson, C.R.

A new hydromagnetic model for the sudden commencement (SC) of a magnetic storm is presented. The model is based on a new morphology of the SC field in which the polarization of the field is interpreted in terms of circularly polarized transverse and linearly polarized longitudinal hydromagnetic (HM) waves. The variation of the types of SC's with local time and latitude is explained in terms of the initial phase and direction of polarization of the circularly polarized HM wave and the relative amplitude of the linearly polarized HM wave.

AF Cambridge Research Laboratories, Bedford, Mass. UNCLASSIFIED

HYDROMAGNETIC INTERPRETATION OF SUDDEN COMMENCEMENTS OF GEOMAGNETIC STORMS, by C.R. Wilson, May 1963. 161 pp.

AFCRL-63-605 Unclassified report I. Wilson, C.R.

A new hydromagnetic model for the sudden commencement (SC) of a magnetic storm is presented. The model is based on a new morphology of the SC field in which the polarization of the field is interpreted in terms of circularly polarized transverse and linearly polarized longitudinal hydromagnetic (HM) waves. The variation of the types of SC's with local time and latitude is explained in terms of the initial phase and direction of polarization of the circularly polarized HM wave and the relative amplitude of the linearly polarized HM wave.

AF Cambridge Research Laboratories, Bedford, Mass. UNCLASSIFIED

HYDROMAGNETIC INTERPRETATION OF SUDDEN COMMENCEMENTS OF GEOMAGNETIC STORMS, by C.R. Wilson, May 1963. 161 pp.

AFCRL-63-605 Unclassified report I. Wilson, C.R.

A new hydromagnetic model for the sudden commencement (SC) of a magnetic storm is presented. The model is based on a new morphology of the SC field in which the polarization of the field is interpreted in terms of circularly polarized transverse and linearly polarized longitudinal hydromagnetic (HM) waves. The variation of the types of SC's with local time and latitude is explained in terms of the initial phase and direction of polarization of the circularly polarized HM wave and the relative amplitude of the linearly polarized HM wave.